"The important thing is to not stop questioning.
Curiosity has its own reason for existing."
-Albert Einstein

Members of the jury

Prof. dr. S. Hendrix, Universiteit Hasselt, Diepenbeek, Belgium, chairman
Prof. dr. N. Hellings, Universiteit Hasselt, Diepenbeek, Belgium, promotor
Prof. dr. JP. Noben, Universiteit Hasselt, Diepenbeek, Belgium, copromotor

Prof. dr. M. De Baets, Universiteit Maastricht, Maastricht, The Nederlands
Prof. dr. R. Hintzen, Erasmus Medical Centre, Rotterdam, The Nederlands
Prof. dr. P. Leprince, Universiteit Luik, Luik, Belgium

Prof. dr. P. Stinissen, Universiteit Hasselt, Diepenbeek, Belgium
Prof. dr. J. Hendriks, Universiteit Hasselt, Diepenbeek, Belgium
Prof. dr. B. Brône, Universiteit Hasselt, Diepenbeek, Belgium

Table of Contents

List of Figures

List of Tables

List of Abbreviations

2D-GE: Two-dimensional gel electrophoresis
2D-DIGE: Two-dimensional difference in-gel electrophoresis
4-AP: 4-aminopyridine
ABAT: GABA transaminase
ACh: Acetylcholine
AChR: Acetylcholine receptor
AGT: Angiotensin
ALB: Serum albumin
ALDH5A1: Succinate-semialdehyde dehydrogenase
ANOVA: Analysis of variance
APC: Antigen presenting cell
APC: Allophycocyanin
APP: Ameloid precursor protein
BBB: Blood brain barrier
BK: Large conductance potassium channel
CaIII: Carbonic anhydrase III
CAPG: Macrophage capping protein
CCL: Chemokine (C-C motif) ligand
CD: Cluster of differentiation
CFA: Complede Freunds adjuvant
CHAPS: 3-((3-cholamidopropyl) dimethylammonio)-1-propanesulfonate
CIS: Clinically isolated syndrome
CNP: 2',3'-cyclic-nucleotide 3'-phoshodiesterase
CMV: Cytomegalovirus
CNS: Central nervous system
CRMP2: Collapsin response-mediated protein 2
CSF: Cerebrospinal fluid
CXC: Chemokine (C-X-C motif)
CXCL: CXC ligand
CXCR: CXC receptor
DAB: 3,3'-diaminobenzidine
DAVID: Database for Annotation, Visualization and Integrated Discovery
DC: Dendritic cell
DiI: 1,14-dioctadecyl-3,3,3',3'-tetramethylindocarbocyanine perchlorate
DLG4: Post-synaptic density protein 95
DMF: Dimethylformamide
DMSO: Dimethylsulfoxide
DPYSL2: Dihydropyrimidinase-related protein 2
DTT: Dithiothreitol
EAE: Experimental autoimmune encephalomyelitis
EAMG: Experimental autoimmune MG
EBV: Epstein-Barr virus
EDA: Extended data analysis
EDTA: Ethylenediaminetetraacetic acid
EGTA: Egtazic acid
ELISA: Enzyme-linked immunosorbent assay
ESI: Electrospray ionization
FACS: Fluorescence activated cell sorter
FBS: Fetal bovine serum
FITC: Fluorescein isothiocyanate
FT-ICR: Fourier transform ion cyclotron resonance
GABA: Gamma aminobutyric acid
GAPDH: Glyceraldehyde 3-phosphate dehydrogenase
GDNF: Glial-derived neurotrophic factor
GFAP: Glial fibrillary acidic protein
GLUD1: Glutamate dehydrogenase 1

GM-CSF: Granulocyte-macrophage colony-stimulating factor
GSK3β: Glycogen synthase kinase 3 beta
GWAS: Genome wide association study
HC: Healthy control
HET: Heterozygous
HLA: Human leukocyte antigen
HPLC: High pressure liquid chromatography
IEF: Isoelectric focussing
IFN-β: Interferon bèta
IFN-γ: Interferon-gamma
IgG: Immunoglobuline G
IHC: Immunohistochemistry
IK: Intermediate conductance potassium channel
IL: Interleukin
IPA: Ingenuity pathway analysis
IPG: Immobilised pH gradient
iTRAQ: Isobaric tag for relative and absolute quantification
Kca: Calcium-activated potassium channel
KCNMA1: Potassium large-conductance calcium-activated channel M alpha
KD: Knock down
KO: Knock out
Kv: Voltage-gated potassium channel
LCQ: Liquid chromatography quadrupole
LFB: Luxol fast blue
LIF: Leukemia inhibitory factor
LKE: Lanthionine ketamine ester
LPS: Lypopolysacharide
Lrp4: Low-density lipoprotein receptor-related protein 4
MBP: Myelin basic protein
MFI: Mean fluorescence intensity
MG: Myastenia gravis
MHC: Major histocompatibility Complex
MMP: Matrix metalloproteinase
MS: Multiple sclerosis
MuSK: Muscle specific kinase
MW: Molecular weight
m/z: Mass to charge value
NaPyr: Sodium pyruvate
NEAA: Non-essential aminoacids
NF-κβ: Nuclear factor kappa bèta
NgR1: Nogo-66 receptor
NIND: Non-inflammatory neurological disease
NMJ: Neuromuscular junction
NO: Nitric oxide
OIND: Other inflammatory neurological disease
OLN: Oligodendrocyte
OND: Other neurological disease
OPC: Oligodendrocyte precursor cell
PBMC: Peripheral blood mononuclear cells
PBS: Phosphate buffered saline
PCA: Principal component analysis
PDIA: Protein disulfide-isomerase A3
PE: Phycoerythrin
PEC: Peritoneal exudate cell
PerCP: Peridinin chlorophyllprotein
PFA: Paraformaldehyde
PLP: Proteolipid protein
PMSF: Phenylmethane sulfonyl fluoride
PPAR: Peroxisome proliferator-activated receptor

PPMS: Primary progressive MS
PTM: Posttranslational modification
Q-TOF: Quadrupole time-of-flight
RAS: Renin-angiotensin system
ROS: Reactive oxygen species
RPMI: Roswell Park Memorial Institute
RRMS: Relapsing-remitting MS
RuBPS: Ruthenium (II) tris (bathophenantroline disulfonate)
SAS: Statistic analysis software
SDS: Sodium dodecyl sulphate
SDS-PAGE: SDS-polyacrylamide gel electrophoresis
SEM: Standard error of the mean
Sema3A: Semaphorin 3A
SERCA: Sarco/endoplasmic reticulum Ca^{2+}-ATPase
SILAC: Stable isotope labelling by amino acids in cell culture
SK: Small conductance potassium channel
SOM: Self organizing maps
SPMS: Secondary progressive MS
SRM: Selected reaction monitoring
TA: Tibialis anterior
Th: T helper
THOP1: Thimet oligopeptidase
Thr: Threonine
TLR: Toll-like receptor
TMEV: Theiler's murine encephalomyelitis virus
TMT: Tandem mass tag
TNFα: Tumor necrosis factor alpha
TP53: Tumor protein 53
Treg: Regulatory T cell
UBiLim: University biobank Limburg
WB: Western blot
WT: Wild type

1

INTRODUCTION AND AIMS

1.1 Multiple sclerosis

Multiple sclerosis (MS) is an autoimmune, neurodegenerative disease of the central nervous system of which the exact cause and working mechanism is not known yet. Over the last decade, researchers did make some important discoveries concerning the disease pathways (1-4). Many of these findings enabled the development of new treatment strategies (5, 6).

1.1.1 Pathology and clinical features

In Europe, the prevalence of MS is approximately 1 in 1000 people (MS international federation), women being 3 times more affected than men. This discrepancy in prevalence of MS between women and men has been linked to the differences in hormonal levels (7). Striking adolescents, the peak of clinical onset is approximately around 30 years of age. Common symptoms of MS are blurred vision, changes in sensitivity, ranging from complete loss of sensitivity in a certain region of the body, tingling or pain. Furthermore, muscle strength is affected, making movement, exercise and even basic tasks difficult. Other symptoms include fatigue, bladder dysfunction and cognitive impairment (8).

Demyelination and degeneration of axons in inflammatory brain lesions results in a decreased neuronal signaling, leading to the variety of symptoms mentioned above (9). While MS lesions are mostly seen around ventricles, optical nerves, and in the spinal cord, the position in the central nervous system (CNS) white matter varies from patient to patient. Also, evidence of gray matter lesions is accumulating, adding to the wide variety in lesion position and clinical symptoms (10, 11).

Clinically isolated syndrome (CIS), the occurrence of a first episode of neurological symptoms caused by inflammation and/or demyelination in the CNS, precedes MS in 80-85 % of the cases (12-14). This disorder is closely related to MS as lesions are alike. MS diagnosis is based on the McDonald criteria (15, 16). These include the dissemination of lesions in time and space, the presence of oligoclonal bands in the cerebrospinal fluid (CSF) and the exclusion of other autoimmune diseases or infections (10). Several clinical disease types of MS exist, the most frequent

one being relapsing-remitting MS (RRMS), which affects 80% of MS patients. RRMS is recognised by alterations between relapses, in which disease symptoms occur, and remissions, periods of recovery. In the early phase of this disease course, complete recovery from all symptoms occurs, while over time permanent damage remains. Approximately 1 to 2 relapses occur per year. This period of relapses and remissions is often followed by a secondary progressive phase (SPMS), a clinical disease course were symptoms gradually deteriorate, and recovery does not take place. The progressive phase of MS is generally seen as more neurodegenerative compared to the RRMS phase, where inflammation is the key player (17). A minority of MS patients have primary progressive MS (PPMS), were aggrevation of symptoms starts right away (9, 17-19). This heterogeneity of disease types and symptoms makes it even harder to understand this devastating disease.

Current treatment options for MS patients are not curative, but disease-modifying. First-line treatments include interferon-β (IFN-β), glatiramer acetate and teriflunomide which are immunomodulators. These drugs reduce the relapse-rate in approximately 30% of RRMS patients (20). Second-line treatments are available for non-responders and patients that experience too much side effects of first-line therapy. Overall, these drugs are more effective in limiting relapse-rate, but have more severe side-effects. These therapies, such as Natalizumab and Fingolimod inhibit the migration of T and B cells into the CNS, thereby limiting CNS inflammation. Furthermore, symptomatic treatment during relapses is also important. Limiting inflammatory relapse-rate by immunosuppression or -modulation is valuable for RRMS patients, but there is a lack of effective treatments for progressive MS patients, in which neurodegeneration is more prominent than inflammation (6). Recently ocrelizumab, a B-cell depleting monoclonal antibody, was approved as a first treatment for progressive MS (21). Ongoing research for better treatment of progressive MS focuses on limiting

neurodegeneration and enhancing remyelination. Stem cell therapies are also considered (22).

1.1.2 Etiology

While the exact cause of MS is unclear, genetic, environmental and immunological factors have been linked to MS. Genome-wide association studies (GWAS) revealed several risk-alleles in MS. No single polymorphism can explain the etiology of MS, and only about one quarter of MS etiology can be explained by our current knowledge of MS susceptibility-loci. The most important risk-locus is the major histocompatibility complex (MHC) region, with the class II human leukocyte antigen (HLA) DRB1*1501 allele as most important one, leading to a three times increased risk for MS. Also genes outside of this risk-region have been associated with MS, such as IL7RA and IL2RA. Overall the majority of risk genes are associated with T cell mediated immunity (23-25).
Apart from genetics, environmental factors influence MS susceptibility. Geographical influences such as sunlight and exposure to microorganisms have been linked to MS. Migration before puberty alters the risk of getting MS to the risk associated with the new geographical area. Month of birth, diet and smoking are environmental factors that seem to be important in MS development. Furthermore, infections such as Epstein Barr virus (EBV) have been associated with MS (26-32). These genetic and environmental factors result in a decreased tolerance for self-antigens and thus may lead to the development of MS.

1.1.3 Pathogenesis

Over the last decades, a vast amount of knowledge about the MS disease pathogenesis has been uncovered (1-3, 5, 6, 23). Overall MS is seen as an autoimmune disease in which T cells are primed to recognize myelin proteins such as myelin basic protein (MBP) and myelin proteolipid protein (PLP). Autoimmunity could arise from a less efficient negative selection of T cells during maturation in the thymus. CNS-reactive T cells are present in blood of healthy controls (HC) and MS-patients. These autoreactive T cells are in a more activated state in MS-

patients, indicating that these T cells could be responsible for myelin breakdown in the CNS (8).

How these autoreactive T cells get activated is still debated. Peripheral activation and expansion of autoreactive T cells could arise from molecular mimicry based on viral infections such as EBV or cytomegalovirus (CMV) (33, 34). Molecular mimicry refers to the activation of autoreactive T cells by antigens of pathogens that structurally are similar to the self-antigens. These antigens are being presented on HLA molecules, creating the link to both environmental and genetic risk factors (34-36).

Activation of autoimmune T cells could also occur through bacterial or viral superantigens, capable of activating T cells in an MHC dependent manner, regardless of their antigen specificity (10, 34). The activation of autoreactive T cells in the periphery is commonly called the "Outside-In" model, where CNS reactivity originates outside of the CNS (9, 37).

Another option is the "Inside-Out" model, where neuronal degeneration and/or demyelination of the axons occur as a first insult (9, 37). Due to this damage, oligodendrocyte (OLN) proteins are presented to microglia for clearance. Peptides of the OLN debris could then be presented on the microglia /macrophages to activate myelin-specific T cells. Peripheral T cells could enter the non-inflamed brain through the choroid plexus and meningeal arteries for immunosurveillance, and subsequently get exposed to the myelin-presenting microglia (38) and attrack and activate other immune cells. Debate is still ongoing regarding these two models that could possibly explain the activation of peripheral myelin-specific T cells (6).

Apart from the fact that the myelin-specific T cells in MS patients are in a more activated state, regulatory T cells (Treg) of MS patients are functionally impaired. Treg normally control the size of an immune response and have proven to be less potent in controlling autoreactive T cells in MS (39, 40). Once the autoimmune myelin-specific T cells are activated, they can enter the CNS via the perivascular space (38). In the perivascular space, antigen presenting cells (APCs) are present that reactivate these autoimmune T cells, leading to the production of cytokines such as tumor necrosis factor alpha (TNFα) and interferon gamma (IFNγ) (41). These cytokines are responsible for an upregulation of MHC II molecules on astrocytes and microglia, and the increased expression of adhesion molecules on

the blood brain barrier (BBB). These events lead to the amplification of myelin-specific T cells as well as B cells and macrophages, and allow the migration of these cells into the parenchyma (10, 42), where they play a role in MS lesion development.

The T cell subtypes that are most abundant in MS lesions are cytotoxic T cells and T helper 17 cells (Th17), named for their production of the cytokine interleukine 17 (IL-17) (43). Th17 cells are helper T cells that secrete IL-17, IL-6, IL-22 and granulocyte-macrophage colony-stimulating factor (GM-CSF). The secretion of GM-CSF by these Th17 cells creates a positive feedback loop, as GM-CSF promotes IL-23 production by APC. This IL-23 secretion in turn is responsible for the differentiation of Th17 cells. Th17 cells add to MS lesion formation by disruption of BBB tight junctions, mainly through the secretion of IL-22 and IL-17. This allows for other cell types to easily migrate into the perivascular space (44). These cells are separated from the parenchyma by the glia limitans, the barrier formed by the end feed of astrocytes that surrounds the perivascular space (38).

The second T cell subtype that is highly associated with MS lesions is the cytotoxic T cell or $CD8^+$ T cell. They are found in great quantities in MS lesions. In healthy individuals, they are responsible for killing damaged, virally infected or cancer cells. When entering the CNS, these $CD8^+$ T cells can induce myelin damage by secreting cytokines (IFN-γ and TNF-α). Furthermore, they secrete perforin and granzyme B, two cytotoxins involved in cell death by creating a pore in the cell membrane or through caspase activation respectively (11, 17, 45).

Macrophages and other APC in the perivascular space secrete matrix metalloproteinases (MMP) 2 and 9. These MMPs disrupt the astrocyte end feed, allowing the entry of immune cells into the brain parenchyma. Once in the CNS, macrophages damage myelin by the secretion of pro-inflammatory cytokines, such as TNF-α, IL-1 and IL-6. By means of an oxidative burst, these macrophages induce free radicals that further damage the tissue. Also, glutamate is released in large quantities, which leads to the production of nitric oxide (NO), reactive oxygen species (ROS) and an influx of calcium into the cells, resulting in glutamate excitotoxicity (38, 41, 45-47).

Proof for the involvement of B-cells in MS is mostly given by the presence of oligoclonal bands in the CSF of MS patients. These oligoclonal bands are present in the CSF of more than 90% of MS patients and represent intrathecal antibody

production. For many years, this feature has been one of the criteria to help diagnose MS. B-cells play a part in lesion development by the production of cytokines and autoantibodies (48). These antibodies bind to myelin, directing innate immune cells and complement to induce damage. The antibody-specificity of these antibodies remains largely unknown, although progress has been made in recent years (1, 48-50). As T cells, B-cells and macrophages damage the CNS and make the CNS parenchyma more accessible, epitope spreading can occur. This means that a wider variety of myelin epitopes is being processed by APC, and presented on their surface (10). An overview of the involved cells in MS lesion development is shown in figure 1.1 (42).

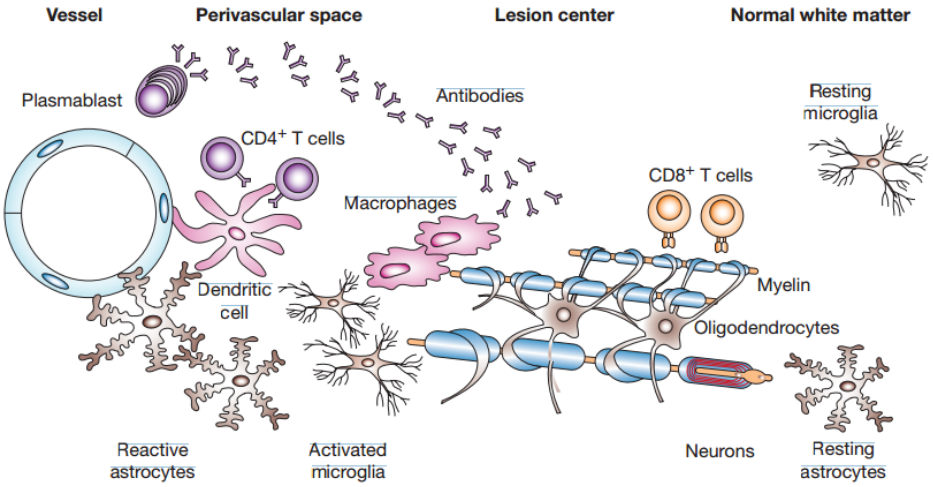

Figure 1.1. Immunopathogenesis of MS. A schematic overview of the immunopathology in the MS lesion. A variety of immune and CNS cell types are involved in lesion development. In the lesion center, cytotoxic T cells are most prominent, together with activated microglia and infiltrating macrophages. B-cells and CD4+ T cells are mostly found in the perivascular space.
Reprinted with permission from Hemmer B. et al. Nature Clin Pract Neurol. 2006 Apr;2(4):201-11.

In the early stages of RRMS, remyelination of axons occurs, which could explain the recovery of clinical symptoms. Newly formed myelin sheets can be found at the edges of lesions, or even throughout the whole lesion. These remyelinated lesions are called shadow plaques (17). They can be distinguished from normal white matter since the newly formed myelin sheets are thinner and have a reduced density. Myelin is formed by differentiation of infiltrating oligodendrocyte

precursor cells (OPC). In later stages of RRMS and especially in progressive MS, remyelination is rare. Remyelination failure results from a reduced repopulation of the lesions with OPCs, presence of inhibitory factors or a lack of stimulatory factors for OPC activation (25, 45). It was shown that acute inflammation stimulates remyelination, which highlights the possible positive effects of T cells, macrophages and antibodies (17, 45, 51).

While the cell types identified to be involved in MS enable us to understand the processes that play a role in MS pathogenesis, the causes and exact working mechanisms remain uncertain. Moreover, MS pathology is not uniform since different disease courses are known, probably resulting from an interplay of genetic, environmental and/or immune factors. Therefore, further research is needed in this matter to facilitate the development of dedicated therapies for both RRMS and progressive MS patients.

1.1.4 Animal models

Currently no animal model represents the combination of all features of MS. However, several good animal models exist that represent pathological processes of MS including inflammation, de- and remyelination. Two of the most common animal models for MS are experimental autoimmune encephalomyelitis (EAE) and the cuprizone induced demyelination model.

In various EAE models the inflammatory processes are represented (52). EAE is induced by active immunisation with myelin protein peptides or by passive transfer of autoreactive T cells. This is achieved in several species including primate models. Depending on the animal strain and autoantigen epitope, monophasic acute, relapsing-remitting or chronic EAE occurs. Recently, spontaneous transgenic EAE models have been developed.

The cuprizone model represents the de- and remyelination processes that occur during MS. Cuprizone, a neurotoxin, is a copper chelator that induces oligodendrocyte degeneration. Extensive demyelination is found in the corpus callosum, cerebellar peduncles, internal capsule and anterior commisure (53). Demyelination is induced in mice when 0.2% cuprizone is added to the diet. Acute demyelination is seen after 4-6 weeks. When cuprizone is removed from the diet, spontaneous remyelination occurs. When cuprizone is kept in the diet for 12

weeks, chronic demyelination is established, and spontaneous remyelination is limited.

Another model for de- and remyelination is the lysolecithin model, where lysolecithin is stereotactically injected in the white matter tracks of the CNS (54, 55). This toxin is particularly harmful for myelin as it dissolves membranes which results in oligodendrocyte cell death. Demyelination occurs only hours after injection and lasts for approximately 7 days after which remyelination occurs.

A neurotrophic viral infection model for MS is also available, Theiler's murine encephalomyelitis virus (TMEV). This is a single stranded RNA virus that causes a chronic-progressive inflammatory demyelinating disease in mice (56). In this model, axonal damage occurs which induces inflammatory demyelination.

1.2 Myastenia gravis

Myasthenia gravis (MG) is an autoimmune disease that is characterized by muscle weakness and fatigability. It is one of the best characterised antibody-mediated autoimmune diseases. MG has a prevalence of 150-300 in 1 000 000. In most cases the disease is successfully treated with symptomatic and immunomodulatory drugs and a thymectomy (57). Initial steps triggering humoral immunity in MG are thought to take place inside the thymic tissue (57). Thymic epithelial cells are capable of expressing muscle-like epitopes that are presented to T cells together with co-stimulatory molecules. This immune response can than spill to components of the neuromuscular junction (NMJ) sharing these epitopes.The autoantibodies in MG are primarily directed to membrane associated proteins of the neuromuscular junction (NMJ). In 85% of cases acetylcholine receptor (AChR) antibodies are found (58, 59). These autoantibodies cause extensive damage at the NMJ, mainly by activation of the complement system and by antigenic modulation of the AChR (60). This autoimmune attack leads to a reduction of AChRs, and blocking of the signaling pathway (57, 61, 62), which further contributes to the severity of symptoms.

Antibodies to muscle specific kinase (MuSK) occur in 10% of cases (58, 59). MuSK is an AChR related membrane protein involved in the formation of the NMJ. These autoantibodies result in a reduced postsynaptic AChR density. Another autoantigen is low-density lipoprotein receptor-related protein 4 (Lrp4). Lrp4 autoantibodies are found in ~2% of cases (58, 59). These autoantibodies disrupt the interaction between Lrp4 and agrin, an interaction responsible for NMJ formation, maintenance and regeneration. The disruption of this interaction inhibits neuromuscular transmission (57).

1.3 Proteomics

Genomics and transcriptomics involve the large scale study of genes and mRNA (a representation of genes that are expressed and the template for protein synthesis) respectively. Proteomics is the term used to describe large-scale studies of proteins present in cells, tissues, biofluids or organisms. Protein abundance, structure, function and the interactions between them can be monitored. Proteins are important in all processes in the cell. They are responsible for cell and tissue structure, cell cycle and DNA replication, for signaling and cell adhesion, but they are also the enzymes needed for cellular metabolism and energy production.

The open approach of proteomic studies, like other –omics technologies, allows for the identification of proteins involved in disease mechanisms without prior knowledge of the involved molecular mechanisms. This is a great advantage compared to the candidate approach as it is likely to gain better insights into disease mechanisms or identify novel biomarkers. Proteomic studies are highly valuable in addition to genomics and transcriptomics, since the proteome is highly variable and not always correctly represented by mRNA levels (63, 64). Over time protein expression is subject to change due to differences in translation efficiency and mRNA and protein turnover (65). Furthermore, proteomics also allows the study of post-translational modifications (PTM) such as phosphorylation, ubiquitination or methylation. These PTM are essential for protein function and activity (63, 66). Because proteins, in contrast to DNA or mRNA, are present in body fluids, they are easily accessible and thus ideal biomarker material.

Unlike in earlier years, emphasis is now on quantitative proteomic techniques, and non-quantitative proteomic techniques are reserved for descriptive studies, general identification of all proteins present in a sample. Quantitative proteomic techniques determine the relative amount of protein present in a sample compared to control samples. Changes in abundance can indicate changes in expression of these proteins, but could also represent an altered rate of degradation or changes in post-translational changes. Furthermore, even if there are changes in expression, these do not necessarily correspond to an altered

functionality. Quantitative techniques are subdivided into gel-free and gel-based techniques.

1.3.1 Gel-free proteomics

Gel-free proteomics is a bottem-up approach for the identification of peptides present in a sample. This is accomplished by mass spectrometry often preceded by fractionation to reduce sample complexity. Mass spectrometry enables protein identification by generating a peptide fragmentation profile (or mass-to-charge value list, m/z) dependent on the underlying sequence, like a barcode. This fragmentation profile is compared to protein databases by means of a search engine (Mascot™, Sequest™). Given a preset probability (Mascot) or cross-correlation value (Sequest) a peptide will become top-ranked in case a theoretical barcode matches the experimental derived barcode. Protein identifications relying on a minimum of three top-ranked peptides are considered as confident.

Two main strategies have been introduced to integrate protein quantification and mass spectrometry identification: with and without the use of labels. Two labeling methods are currently widely used, namely isobaric tag for relative and absolute quantification (iTRAQ™) and tandem mass tags (TMT™). For both, peptides are labeled after protein digestion. Samples with different labels are then pooled and fractionated before identification. The labels produce a reporter ion that appears in the spectrum and allows relative quantification. Eight different iTRAQ labels and ten TMT labels are currently available (67-70). To compare protein content of cells in culture, stable isotope labeling by amino acids in cell culture (SILAC) can be used (71).

Quantification is also possible without the use of labels. Two main quantification strategies are based on these correlations: peptide signal intensity measurement (normalised peak height or area under the peak) and spectral counting (number of acquired fragment spectra) (72). To measure peptide signal intensity, high mass accuracy and high resolution mass spectrometers are needed such as orbitrap, quadrupole time-of-flight (Q-TOF) or fourier transform ion cyclotron resonance (FT-ICR).

Absolute quantification of selected target proteins can be achieved in the selected reaction monitoring mode (SRM) of the mass spectrometer. This is based on the isotope dilution principle: known amount(s) of an isotopically labeled peptide(s)

are added to the sample and signal abundance can be compared (73). This is a targeted approach, mainly reserved for biomarker validation rather than for the discovery phase.

1.3.2 Gel-based proteomics

Compared to peptide quantity in gel-free methods, gel-based proteomic techniques provide information about the whole protein quantity, mass, isoelectric point and protein isoforms (74). Quantitative gel-based techniques identify protein spots that differ between samples. Mass spectrometry is needed to identify the proteins present in these differential spots. A state-of-the-art technique to eliminate inter-gel variability is two-dimensional difference in-gel electrophoresis (2D-DIGE). This approach was first described by Ünlü et al. in 1997 (75) and allows for the comparison of two or more samples through the use of different fluorescent labels.

Three different CyDye™ fluor dyes are available, Cy2, Cy3 and Cy5, allowing the co-electrophoresis of up to three samples on the same gel. These dyes are photostable, water soluble, pH insensitive over a wide range and give minimal crosstalk (75). For the comparison of more than 3 samples, multiple gels need to be used. A pooled sample consisting of equal amounts of every sample in the study, needs to be included as an internal standard on all gels to correct for gel to gel variability (76). Normalization of spot volume is based on this internal standard as the loss of proteins during gel-entry is the same for all samples on one gel. The internal standard further enables a reliable matching of spot patterns across different gels.

Bias due to preferential labeling and differences in gel-associated artifacts are minimised by including a dye-swap within the experimental groups and ensuring that samples from each biological group are divided over the different gels. (77). Disadvantage of this technique is the limited separation of both high and low molecular weight proteins (74, 78).

1.4 Proteomics & multiple sclerosis

As proteomic techniques emerged, great interest for their application in unraveling MS disease pathways arose. However, choosing a relevant sample-type is not straight-forward and dependent on the aim of the study. The sample-type that contains most information on neuroinflammatory mechanisms is the CNS itself. As CNS samples are often only available post mortem, they are not a good representation of active disease processes. Furthermore, conservation of proteins in post mortem tissue remains difficult to monitor. As an alternative, CSF samples can be used. This is the sample type most closely linked to the inflamed CNS. CSF sampling requires an invasive collection procedure and the volume is limited. Also, CSF samples are taken to a lesser extent nowadays.

For studying the systemic autoimmune response, blood, serum or peripheral blood mononuclear cells (PBMC) are valuable samples types. These are the most readily available sample types, and further allows comparison with samples from healthy controls. More than 99% of the total protein concentration in blood is formed by about 20 abundant proteins including albumin and immunoglobulins. Depletion of these high abundant proteins is therefore necessary but risky, as co-precipitation of low abundant disease relevant proteins can occur. (79).

Several non-quantitative gel-based and gel-free studies were performed to help unravel the MS disease pathogenesis and identify disease related biomarkers. Cell types involved in MS pathogenesis and several proteins specific to CSF of MS patients were identified. These first proteomic studies of MS used CSF or EAE brain samples. The strengths and limitations of these non-quantitative MS proteomic papers were reviewed by Elkabes, S. et al. (74).

One non-quantitative study that stands out due to methodology and sample type is that of May H. Han (3). A Nature article comparing samples collected with laser-capture microdissection from acute, chronic-active and chronic MS lesions. With 158, 416 and 236 proteins unique to the respective lesion types, this study resulted in a whole list of proteins that are thought to be involved in lesion formation and progression. This is one of the first articles that not only reported a list of protein identifications, but also validated some of the markers. E.g. tissue

factor was identified as a protein unique to chronic active lesions, indicating the importance of the coagulation pathway in these lesions.

An overview of the quantitative proteomics studies conducted in MS research is presented in Table 1.1. An example of a gel-based 2D-DIGE study compares CSF of RRMS to that of non-neural disease controls and CIS. Proteins were identified that changed in expression between pools of CSF. These proteins provide an insight into MS specific molecular disease mechanisms. Comparison between CIS and RRMS in turn elucidates initial pathways involved in MS disease initiation (80).

Another example of a gel-free approach compares CSF samples of RRMS to that of PPMS. Both forms of MS are very different, and thus different molecular pathways could play a role. Several differential proteins were identified, some of which were validated using an enzyme-linked imuno sorbent assay (ELISA) or Western blot (WB). Although there was a great overlap between samples, these differences can clarify disease mechanisms that are important for the respective disease types, and help unravel differences between disease types and treatment options (81).

Regarding the identifications made by quantitative proteomics studies performed so far, most of these are related to neurodegeneration (82). Examples are (neuro)filaments, glial fibrillary acidic protein (GFAP) and evidence of homeostatic dysregulation. The few inflammatory proteins found are for example albumin, complement proteins, prostaglandins and immunoglobulins. Differentially expressed proteins mostly link to biological processes such as protein metabolism, immune responses and cellular communication and signaling (79).

Table1.1: Overview quantitative proteomics studies in MS research

	methodology	tissue	comparison (n)	# Ids*	validation		reference
					proteins	method	
Gel-based	2D-DIGE	CSF	RRMS (12: pool) vs. HC(12: pool)	11	Apoliporpotein A1	WB	(80)
			CIS(12: pool) vs. HC(12: pool)	13			
	2D-DIGE	CSF	CIS-CIS (8: pool) vs. CIS-MS (8: pool)	19	Fetuin-A	ELISA	(83)
	2D-DIGE	spinal cord	EAE (pool) vs. HC (pool)	11	GFAP	WB, IHC, ELISA	(84)
	2D-DIGE	OLN	LIF-treated (3) vs. Control (3)	11			(85)
	2D-DIGE	CSF	RRMS (10: pool) vs. OIND (10: pool)	13	Vitamin D binding protein	ELISA	(86)
	2D-DIGE	CSF	MS (10: pool) vs. OIND (10: pool)	43	cystatin C	ELISA	(87)
	2D-DIGE	CSF	SPMS (10: pool) vs. OIND (10: pool)	8	Vitamin D binding protein	IHC, WB, EAE	(88)
	2D-DIGE	plasma	IFNβ responders (3) vs.non-responders (3)	3			(89)
Gel-free	iTRAQ	spinal cord	EAE (2) vs. HC (2)	41	PA28	IHC, WB	(90)
					I2PP2A	WB	
					ApoE	WB	
					Vimentin	WB	
					CaMKIIα	WB	
					Moesin	WB	
	iTRAQ	spinal cord	EAE (2) vs. HC (2) (differentially cleaved proteins)	7	α2 macroglobulin	WB	(91)
	iTRAQ	spinal cord	EAE: formalin-fixed parafin -embedded (2) vs. fresh frozen (2)	5			(92)
	Q-TOF	CSF	MS (10: pool) vs. OIND (10: pool)	68	cystatin C	ELISA	(87)
	FT-ICR	CSF	MS (45) vs. OND (25)	24			(93)
			CIS (40) vs. OND (53)	6			
			MS vs. OIND	9			
			CIS vs. OIND	19			
			MS vs. CIS	5			
			OND vs. OIND	26			
	FT-ICR	CSF	PPMS (10) vs. HC (10)	29	Vitamin D binding protein	WB, ELISA	(81)
			RRMS (11) vs. HC	24	Jagged 1	WB, ELISA	
			PPMS vs. RRMS	7			
	Orbitrap & QTOF	CSF	EAE (13/11&14/9) vs. HC (15&14/13) (d10 & d14)	44	Afamin	SRM	(94)
	orbitrap	CSF	EAE: responders (5) vs. non-responders (5) minocycline	14	Complement C3	SRM	(95)
			EAE: untreated (8) vs. Non-responders (5)	20	Carboxypeptidase B2	SRM	

Table 1.1 continued

	methodology	tissue	comparison (n)	# IDs	validation		reference
					proteins	method	
Gel-free	orbitrap	CSF	pre-Nabalizumab (17) vs. 1 year post treatment (17)	5	Igμ chain C region	SRM	(96)
					haptoglobin	SRM	
					chitinase 3-like protein 1	SRM, ELISA	
	orbitrap	CSF	CIS (47) vs. control (45)	36	amyloid-like protein 1	ELISA	(97)
	iTRAQ	CSF	CIS-CIS (30: 5 pools) vs. CIS-MS (30: 5 pools)	23	ceruloplasmin	ELISA	(98)
					Vitamin D binding protein	ELISA	
					chitinase 3-like protein 1	ELISA	
	iTRAQ	brain	formalin-fixed autopsy tissue; ≠ comparisons (3)	257			(99)
	iTRAQ	CSF	CIS - MS (5) vs. OIND (5)	3	Alpha-1-antichymotrypsin	SRM	(100)
			CIS (5) vs. OIND	4	Leucine-rich alpha-2-glycoprotein	SRM	
			CIS - MS vs. CIS	0			
	iTRAQ	CSF	RRMS (6) vs. OND (12) and OIND (6)	7	Chitinase 3-like protein 1	MRM	(101)
					secretogranin-1	MRM	
					cerebellin-1	MRM	
					neuroserpin	MRM	
					cell surface glycoprotein MUC18	MRM	
					testican-2	MRM	
					glutamate receptor 4	MRM	
	TMT	CSF	RRMS (21) vs. OND (21), 3 pools of 7 matched samples	484			(102)
	TMT	brain	longitudinal EAE progression (8 x 20 samples)	1032	synapsin-1	serum ELISA	(103)
					Alpha-II-spectrin	serum ELISA	
	TMT	CSF	RRMS (21) vs. control (21), 3 pools of 7 matched samples	22	Chitinase 3-like protein 1/2	ELISA, IHC	(104)
	iTRAQ	serum	benign (7) vs. aggressive (7) MS	11			(105)
	TMT	CSF	RRMS (21) vs. OND (21), 3 pools of 7 matched samples	484			(106)
	orbitrap	CSF	case (MS & CIS, 11) vs. control (15)	26			(107)

OND: other neurological diseases, OIND: other inflammatory neurological diseases, NIND: non-inflammatory neurological diseases
#IDs: number of proteins statistically different between study populations

Due to the bottom up approach, large amounts of data are created in these studies. Processing these data and finding the information wanted or needed is laborious and not straight forward. Often more data are created than possible to validate and follow up. The aim of a proteomics study can be to describe all proteins present in a sample, in which case a list of identified proteins is a straightforward result. However, in most studies the aim is the discovery of biological pathways, disease mechanisms or biomarkers. Validation and further research of the proteins on the target list is thus necessary and indispensable for answering the research questions. Network analysis using programmes such as Ingenuity Pathway Analysis (IPA) or Database for Annotation, Visualization and Integrated Discovery (DAVID) can help to get a more structured view on the large amount of data generated.

A list of all proteins identified in the first 10 years of quantitative proteomics in MS was published by Farias et al. (79). They conclude that there are to date no unique MS biomarkers identified by means of proteomics techniques. Instead, candidates have been proposed and knowledge of MS biopathology was gained. Published reports are numerous but without certainty, as validation studies are needed in many cases. Large-scale proteomic studies of PTM and protein-protein interactions are still missing. An attempt for large scale validation of potential biomarkers was made by Jia et al. (108). Twenty-six potential CSF biomarkers for SPMS were selected based on discovery results and literature. Using SRM proteomics, protein abundance in CSF samples (SPMS, HC and NIND) was compared for these 26 candidates. Five biomarkers were associated with diagnosis.

1.4.1 MS Proteomics at BIOMED

Several peer-reviewed proteomic papers have been published by our group to identify MS disease related proteins and evaluate the pro and cons of different proteomic approaches. These articles use both non-quantitative and quantitative techniques, gel-free and gel-based methods to identify global protein presence or

differences in protein content in bodily fluids or cell cultures. A short summary is provided here.

To create a database of proteins present in the CSF of MS patients, samples of 4 RRMS patients and 1 PPMS patient were separated with two-dimensional gelelectrophoresis (2-DE). Sixty-five of the 300 protein spots were identified, 18 of which had never been detected in CSF before (109).

Adding to the previous intent to identify proteins present in the CSF of MS patients, a gel-free approach combining 2 different separation techniques was used to identify proteins present in a pool of CSF of 8 MS patients. This was compared to a pool of CSF of 6 cancer patients as controls. Two-dimensional liquid chromatography separation was compared to direct identification using gas-phase fractionation. Both separation techniques were valuable, and complemented each other. In total, 148 proteins were identified of which 24 exclusively in the CSF of the controls and 44 exclusively in the CSF of MS patients. Sixty of these proteins were identified in the CSF for the first time. The presence of one of these proteins, cystatin A, was validated in CSF and serum of individual patients and controls by ELISA (110).

In another approach, a quantitative gel-based 2D-DIGE was performed to identify proteins that are affected by treatment of oligodendrocytes with leukemia inhibitory factor (LIF). This is a neuropoietic cytokine that promotes oligodendrocyte survival *in vitro* and in the animal model of MS, EAE (2, 111). This study was performed to gain insights into the cellular processes that explain the protective effect of LIF. LIF was shown to induce a shift in protein profile towards a prosurvival execution program (85).

The aims of proteomic studies range from the identification of proteins present in bodily samples to create a protein catalogue, to the comparison of different experimental samples to identify new insights in molecular disease mechanisms or for instance treatment effects. Of note, it is not only important to publish lists of proteins identified, but also to validate results and determine the function of these proteins in the disease process.

1.5 Aims

Most of the knowledge currently available on MS disease processes was obtained in studies using a candidate approach. Proteomics studies start from a more open view, allowing the identification of proteins and disease processes that have not been considered so far. These proteomics studies are unbiased and provide a more complete image of the processes that are studied. Here we conducted a 2D-DIGE study, the only available quantitative gel-based proteomics technique. Gel-based studies have the advantage of providing information on different protein isoforms and post-translational modifications in addition to the identification of differential regulation. This information is essential for the further validation of protein function in disease.

1.5.1 Proteomic identification of novel players involved in autoimmune disease

Current MS proteomic studies have mostly focused on human CSF samples to identify proteins involved in neuroinflammation. Still, the brain itself holds the most relevant information regarding CNS related disease mechanisms. Longitudinal changes in protein expression in the brain can help to unravel molecular mechanisms involved in disease progression. Since MS brain tissue is mostly available post mortem, and of patients with longstanding disease, we have chosen the EAE animal model instead. In **chapter 3** the brain proteome of EAE animals is studied at different time points along the disease course. Hereto, the protein expression profile of brainstem is determined before onset of EAE, at the peak of clinical symptoms and after recovery. Healthy brainstem samples are included as a control. Ingenuity pathway analysis (IPA) is performed to find relationships, common functions and pathways of relevance in our data.

Profiling proteomic changes in target tissue over time is not only of use for MS, but also for other (autoimmune) diseases such as myasthenia gravis (MG). Although this is one of the best characterized antibody–mediated autoimmune diseases, changes in muscle protein content over time have not been studied. Knowing the alterations in protein levels in response to autoimmune attack could

help in the development of symptomatic treatments. In **chapter 2**, we determine temporal changes in protein expression at the neuromuscular junction using the animal model of MG, experimental autoimmune myasthenia gravis (EAMG) This study was set up in collaboration with the Division of Neuroscience at Maastricht University.

1.5.2 Functional validation of CRMP2 and KCNMA1 in MS/EAE

The validation and further characterisation of two targets of interest obtained in our EAE proteomics study is our next aim in the search for mechanisms involved in lesion formation. One of the proteins we found to be differentially expressed over time during acute EAE is collapsin response-mediated protein 2 (CRMP2). This protein is part of the collapsin-response mediator protein family and important for brain development, neuronal guidance, neurite-axon differentiation and growth-cone collapse. CRMP2 was reported to be involved in MS pathogenesis at the neuronal level. More specifically, CRMP2 is a downstream molecule of Nogo-A, a signalling molecule involved in neurodegeneration during MS (112). In T cells, CRMP2 is a key element in migration towards chemokines during viral infections (113). Since T cell migration is an important step in MS lesion formation, we analysed the expression levels of CRMP2 in T cells and other immune cell subsets relevant to MS disease **(chapter 4)**.

Another important target of our 2D-DIGE study (chapter 3) is potassium large-conductance calcium-activated channel Mα (KCNMA1). This potassium channel was not identified as differentially abundant in our 2D-DIGE study, but is a central molecule in one of the major networks formed by our differential proteins. KCNMA1 is a calcium-activated potassium channel that is widely expressed. Activation of this channel opens the potassium pore and leads to the efflux of potassium from the cell. This results in membrane hyperpolarisation, and thus decreased cell excitability. Functionally, KCNMA1 is involved in the regulation of smooth muscle tone and neuronal excitability (114). Blocking of potassium channels has been described to be beneficial in EAE, with an effect on disease score and delay of disease onset (115). The mode of action of KCNMA1 blockage on EAE has not been described yet, but the fact that other potassium channels

seem to be important, indicates that research evaluating the role of KCNMA1 in the disease processes of EAE/MS is necessary. In **chapter 5** efforts are made to elucidate the role of KCNMA1 in macrophage functions important in MS pathogenesis.

In **chapter 6**, we integrate our findings and discuss the added value of proteomics research and network analyses. Furthermore, the functional role of selected targets CRMP2 and KCNMA1 in MS disease pathology is evaluated.

2

IDENTIFICATION OF PROTEINS INVOLVED IN MYASTHENIA GRAVIS

Based on:

Proteomic analysis of rat tibialis antirior muscles at different stages of experimental autoimmune myasthenia gravis.

Annelies Vanheel[b,1], Alejandro M. Gomez[a,1], Mario Losen[a], Peter C. Molenaar[a], Marc H. De Baets[a,b], Jean-Paul Noben[b], Niels Hellings[b], Pilar Martinez-Martinez[a]

Journal of Neuroimmunology 2013 Aug 15;261(1-2):141-5.

[a]Division Neuroscience, School for mental Health and Neuroscience, Maastricht University, 6200 MD Maastricht, The Netherlands

[b]Biomedical Research Institute, Hasselt University and Transnationale Universiteit Limburg, School of Life Scieces, 3500 Hasselt, Belgium

[1]These authors contributed equally to this work. Both authors conceived the experiments, AV designed, performed and analyzed the 2D-DIGE study, AMG performed and analyzed the WB. Both authors wrote the paper, input on the proteomics part was from AV, input on MG disease mechanisms was from AMG.

ABSTRACT

Myasthenia gravis (MG) is an autoimmune disease in which autoantibodies, most commonly directed against the acetylcholine receptor (AChR), impair neuromuscular transmission and cause muscle weakness. In this study, we utilised two-dimensional difference in-gel electrophoresis (2D-DIGE) to analyze the muscle's proteomic profile at different stages of experimental autoimmune myasthenia gravis (EAMG). We identified twenty-two differentially expressed proteins, mainly related to metabolic and stress-response pathways. Interestingly, these identified proteins have also been associated with other contraction-impairing muscle pathologies (e.g. denervation and atrophy), suggesting a similar response of the muscle to such conditions.

2.1 Introduction

Myasthenia gravis (MG) is one of the best characterised antibody-mediated autoimmune diseases, and its symptoms include muscle weakness and fatigability. The autoantibodies in MG are primarily directed to proteins of the neuromuscular junction (NMJ), such as the acetylcholine receptor (AChR-MG, 85% cases), muscle specific kinase (MuSK-MG, 10% cases) and low-density lipoprotein receptor-related protein 4 (Lrp4-MG, ~2% cases) (58, 59). In AChR-MG, autoantibodies cause extensive damage at the NMJ, mainly by activation of the complement system and by antigenic modulation of the AChR (60). This autoimmune attack leads to a reduction of AChRs, but also other AChR-related proteins (61, 62), which further contributes to the severity of symptoms. Consequently, such AChR-related proteins could represent novel targets for symptomatic treatments. However, the precise number and identity of muscle proteins affected by the autoimmune attack in MG remains largely unknown.

In recent years, the advent of the two-dimensional difference in-gel electrophoresis (2D-DIGE) technology has allowed a more sensitive and accurate quantification of differential protein expression and/or protein modifications affecting size and charge in biological samples (116). In this study, we used the experimental autoimmune myasthenia gravis model (EAMG) rat model and 2D-DIGE to evaluate the muscle's proteomic profile at different disease stages of EAMG.

2.2 Materials and methods

2.2.1. Animals, induction of EAMG and tissue preparation

7-week-old female Lewis rats were obtained from Charles River laboratories (Cologne, Germany). Chronic EAMG was induced by immunization with AChRs purified from *T. californica,* the severity of EAMG symptoms was assessed three times a week with the paw-grip test for muscle weakness as described (117). Animals were sacrificed between 5 and 8 weeks after immunization according to their disease score, to have a representative number of muscles from each score (0, no weakness; 0/1, mild weakness after testing; 1, weakness after testing; 2, clinical signs of EAMG present before testing; 3, severe clinical signs of EAMG, moribund). Animals were perfused to obtain blood-free tibialis anterior muscle [5 mM EDTA in PBS pH 7.2, containing Complete Protease Inhibitor Cocktail (Roche, Almere, the Netherlands)]. Muscles were processed to remove their connective membranes and tendons, frozen in liquid nitrogen and subsequently stored at -80°C. All experiments were done with permission from the Committee on Animal Welfare of Maastricht University, according to Dutch governmental rules.

2.2.2. Protein Extraction

Proteins were extracted as described (118). Briefly, muscle samples were lyophilised, crushed (GentleMACS, Miltenyi Biotec, Leiden, the Netherlands) and proteins solubilised before ultracentrifugation. Samples were then desalted and the buffer was exchanged to labeling buffer (7 M urea, 2 M thiourea, 4% w/v CHAPS in 30 mM Tris HCl pH 8.5) using Amicon Ultra filters (Millipore, 3 kDa cut-off). Protein concentration was determined using the 2D Quant kit (GE Healthcare, Diegem, Belgium) and aliquots were stored at -80°C. For Western blotting experiments, additional muscles from animals of a previous study (117) were homogenised with a Mini BeadBeater (Biospec Products, Bartlesville, OK) in lysis buffer (30 mM triethanolamine, 50 mM NaCl, 5 mM EDTA, 5 mM EGTA, 50 mM NaF, 1 mM Na-orthovanadate, 1 mM benzamidine, 1 mM Na-tetrathionate, 1 mM

PMSF, pH 9.5) containing HALT Protease Inhibitor Cocktail (Thermo Scientific, Rockford, IL) and Triton X-100 (1%).

2.2.3. 2D-DIGE

Minimal labeling with N-hydroxysuccinimidyl-ester dyes Cy2, Cy3 and Cy5 (GE healthcare, Diegem, Belgium) and 2D-GE were performed as described (119). CyDye-labeled 2D-DIGE gels were scanned on the Ettan DIGE imager (GE healthcare, Diegem, Belgium). Gel images from all three CyDyes were loaded into DeCyder 7.0 software (GE healthcare) and analysed. Statistical significance was calculated using analysis of variance (ANOVA) and multiple comparison test. Spots present in 85% of the gel images, and with $p \leq 0.05$ were considered for further analysis.

2.2.4. Spotpicking, protein digestion and identification

For spot picking (ProPicII, Isogen Life Science, PW De Meern, the Netherlands) a 12.5% acrylamide gel was loaded with 200 µg of an unlabeled internal standard and 50 µg of the Cy2 labeled internal standard. In-gel digestion using trypsin (Promega, Leiden, the Netherlands) (120) was performed followed by protein identification by mass spectrometry (119).

2.2.5. Western blotting

To validate the results obtained by 2D-DIGE, we performed Western blotting both with muscle extracts used for the 2D-DIGE analysis and muscle extracts from control and EAMG animals characterised in a previous study (117). Protein extracts were separated by SDS polyacrilamide gel electrophoresis (SDS-PAGE) and membranes were incubated with either rabbit anti-β-enolase (W-25, Santa Cruz Biotechnology, CA; 1:800) or goat anti-CAIII (E-19, Santa Cruz Biotechnology, CA; 1:800), and mouse anti-GAPDH (10R-G109a, Fitzgerald, MA; 1:5000000). Secondary antibodies were donkey anti-mouse IgG IRDye 680, goat anti-rabbit IgG IRDye 800 and donkey anti-goat IgG IRDye 800 (926-32222, 926-32211 and 926-32214 respectively; LI-COR Biosciences, NE), diluted 1:10000. Membranes were imaged with Odyssey Infrared Imaging System (LI-COR

Biosciences, Lincoln, NE) and bands were quantified with Image J software (mean intensity), normalizing for GAPDH mean intensity. Protein levels were compared between groups with a unpaired *t*-test using GraphPad Prism 4 software.

2.3 Results

A 2D-DIGE proteomics experiment was performed to identify proteins that are affected at various disease stages of EAMG. Proteins were extracted from blood-free tibialis anterior muscles from each of the experimental groups (control, clinical scores 0, 0-1, 1, 2, 3; $n = 4$). A 2D spotmap with an average of 3342 protein spots per sample was obtained and analysed in the DeCyder 7.0 software. Twenty-six protein spots with significantly different fluorescence intensities, at least between two of the experimental groups, were identified (1w-ANOVA, $p \leq 0.05$) (Supplemental fig. S2.1). Unequivocal protein identification by mass spectrometry was achieved for seventeen of the selected spots. There were spots containing more than one protein due to co-migration, so a total of twenty-seven proteins were identified. In this study, a maximum of three proteins per spot were found. Two proteins, serum albumin and pyruvate kinase were present in three spots, leading to the identification of twenty two unique proteins in EAMG TA muscle (Table 2.1).

As expected, most identified proteins detected by 2D-DIGE were cytoplasmic, probably due to the bias of detecting soluble proteins using this technique. We observed changes by 2D-DIGE in: β-enolase and carbonic anhydrase III (CAIII) (Fig. 2.1 A, B), and quantified their protein levels in control and EAMG animals by Western blotting. Protein levels of β-enolase were significantly reduced in EAMG muscles compared with controls ($n = 6$ for both groups, $p < 0.05$), with an average reduction of approximately 25% (Fig. 2.1C). CAIII protein levels were increased in all EAMG stages when quantified by immunoblotting (data not shown). Interestingly, only severely affected animals (score 3) had significantly higher levels of CAIII protein compared with controls. In such muscles, average levels of CAIII were increased by approximately 35% compared with control muscles ($p < 0.01$; $n = 5$ for score 3 EAMG and $n = 10$ for control) (Fig. 2.1D).

Table 2.1: Protein identification. Muscle proteome was analysed, differential protein spots were picked and in-gel digestion was performed. Proteins were identified by mass spectrometry. For each spot: the 1way-ANOVA value, spot relative fluorescence intensity, protein identification, and protein accession numbers are presented.

Spotnumber	1w-ANOVA	Relative fluorescence intensity	Protein identification	Protein accession numbers				
147	0,0233	decreased	Pyruvate kinase isozymes M1/M2	IPI00231929				
			Serotransferrin	IPI00679202				
			Aconitate hydratase, mitochondrial	IPI00421539	IPI00950672			
195	0,0255	depends on the experimental group	Myosin-4	IPI00476111	IPI00948572			
			mitochondrial inner membrane protein	IPI00364895	IPI00566985	IPI00777695	IPI00948331	
214	0,015	decreased	mitochondrial inner membrane protein	IPI00364895	IPI00566985	IPI00948331		
265	0,00177	decreased	Serum albumin	IPI00191737				
295	0,0318	decreased	Dihydrolipoyllysine-residue acetyltransferase complex, mitochondrial component of pyruvate dehydrogenase	IPI00231714				
			Serum albumin	IPI00191737				
305	0,000398	decreased	Serum albumin	IPI00191737				
377	0,0131	decreased	60 kDa heat shock protein, mitochondrial	IPI00339148				
488	0,0406	decreased	Dihydrolipoyllysine-residue succinyltransferase component of 2-oxoglutarate dehydrogenase complex, mitochondrial	IPI00551702	IPI00948493			
523	0,0373	depends on the experimental group	Pyruvate kinase isozymes M1/M2	IPI00231929				
577	0,0241	decreased	Beta-enolase	IPI00231631				
			Cytochrome b-c1 complex subunit 1, mitochondrial	IPI00471577				
716	0,0195	decreased	Creatine kinase M-type	IPI00211053				
			Aspartate aminotransferase, cytoplasmic	IPI00421513				
			Fructose-bisphosphate aldolase A	IPI00231734	IPI00951991			
749	0,0188	decreased	Protein S100-A11	IPI00554148	IPI00766347			
			Annexin A1	IPI00231615	IPI00777179			
935	0,0124	decreased	Malate dehydrogenase, cytoplasmic	IPI00198717				
971	0,00166	decreased	Voltage-dependent anion-selective channel protein 2	IPI00198327	IPI00206268			
			myozenin-1	IPI00199718				
1078	0,00636	increased	Carbonic anhydrase 3	IPI00230788				
1173	0,0242	increased	Glutathione S-transferase Yb-3	IPI00230942	IPI00411230	IPI00778425	IPI00870234	
			Triosephosphate isomerase	IPI00231767				
1196	0,0199	decreased	Pyruvate kinase isozymes M1/M2	IPI00231929	IPI00339197	IPI00454375	IPI00561880	IPI00764193
				IPI00777829	IPI00948028	IPI00957976	IPI00968449	

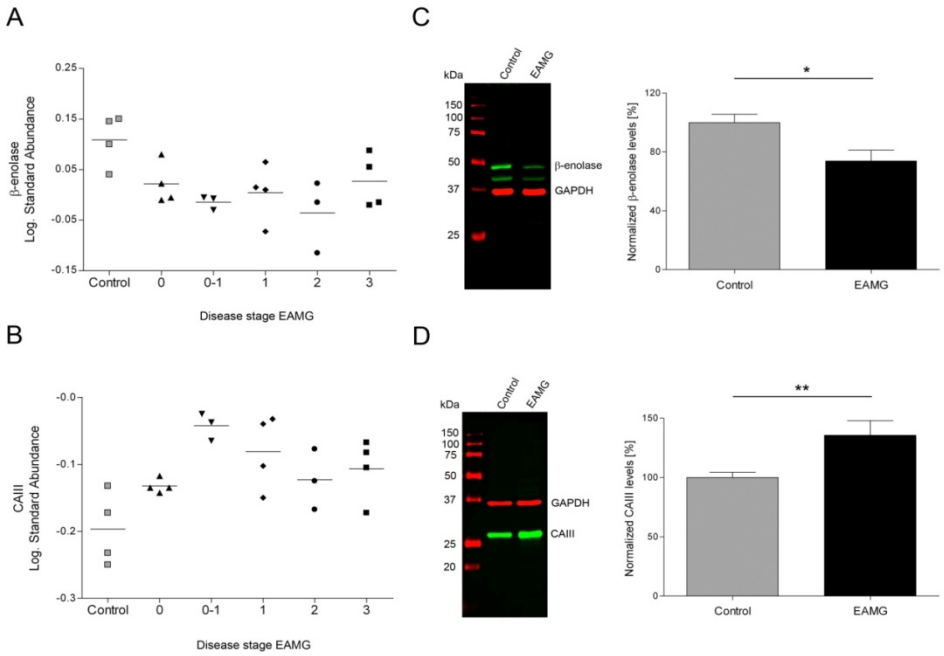

Figure 2.1: β-enolase and CAIII protein levels in tibialis anterior muscles of EAMG and control rats. Both a reduction of β-enolase **(A)** and an increase of CAIII **(B**) levels were detected by 2D-DIGE in all EAMG disease stages**.** Reduction in β-enolase protein levels were corroborated by Western blotting (**C).** A significant reduction in muscle homogenates from EAMG animals compared with controls (* $p < 0.05$, $n = 6$ per condition) was observed. CAIII protein levels measured by Western blotting (**D**) were significantly increased in muscle homogenates from severely affected EAMG animals compared with controls (** $p < 0.01$; score 3 EAMG, $n = 5$, control $n = 10$). β-enolase (C upper green band) / CAIII intensity (D green band) were normalised with GAPDH intensity (red band).

2.4 Discussion

We analysed the muscle proteome at different EAMG disease stages by 2D-DIGE and identified twenty two differentially expressed proteins. The majority of these identified proteins are involved in metabolic pathways (glycolysis and the citric-acid cycle), while others are related to cellular-stress responses (e.g. glutathione S-transferase Yb3, 60 KDa heat shock protein), or are contractile proteins (myosin-4 and myozenin-1). Overall, we observed a reduction of the glycolytic capacity and the expression of fast-twitch myosin isoforms in EAMG tibialis anterior muscles, which is suggestive of a switch from fast- to slow-twitch fibers. Similar proteomic profiles were previously described in conditions that impair muscle contraction, such as denervation (121, 122), inclusion body myositis (123), immobilization (124) and aging (125). In such studies, relatively few differentially expressed proteins were identified (between 17 and 73), most of them also related to cellular-stress responses and to changes in the type of muscle fibers. Therefore, it appears that the most evident protein alterations in EAMG are a consequence of the impaired muscle-nerve signaling and, possibly, of the atrophy (or loss) of fast-twitch fibers; as it was previously demonstrated in muscle biopsies from MG patients (126-128). In this connection it might be relevant that enhancing the response of fast-twitch muscle cells with a selective troponin activator improves muscle strength in EAMG (129).

Most of the proteins found in our study are not specific for MG, since they are also affected in other pathological (and physiological) conditions of the muscle. Nonetheless, β-enolase and CAIII have been associated with muscle regeneration and autoimmunity respectively. β-enolase is a muscle-specific metabolic enzyme very sensible to physiological stimuli (130), with an important role in developing and regenerating muscles (131). Moreover, its deficiency leads to severe myalgias, muscle weakness and fatigability in affected individuals (132). CAIII is a muscle specific enzyme that catalyzes the hydration of carbon dioxide and can protect the cell from oxidative damage (133). It has been described as an auto-antigen in several autoimmune diseases , e.g. rheumatoid arthritis and systemic lupus erythematosus (134) and its expression is reduced in pectoralis muscle biopses of MG patients (135). The discrepancy in CAIII expression between our experiment (increased) and MG biopses (decreased) is probably explained by

differences in the experimental design. In this regard, timing seems essential because it has been reported that CAIII levels are reduced immediately after denervation, but they subsequently increase over basal levels six days after the procedure (122).

We could not identify any changes in well-known NMJ-related proteins between EAMG and control muscles (136, 137). This is possibly a result of the under-representation of membrane proteins that is characteristic of 2D-gel proteomics. Membrane proteins are considerably less abundant than cytoplasmic proteins and, since they usually have several hydrophobic domains, they are poorly soluble in the aqueous buffers required for isoelectric focusing (138, 139). Moreover, there is high inter-individual variation within the EAMG model, which also limits the robustness of 2D-DIGE for detecting differentially expressed proteins, especially those present at low quantities.

At present, the response of muscle fibers to the autoimmune attack in MG remains poorly understood. This study describes alterations in cytoplasmic proteins that are not intuitively considered to be involved in the pathogenesis of MG and suggests that AChR-MG shares similar intracellular disease mechanisms with other muscle pathologies.

2.5 Supplemental figures

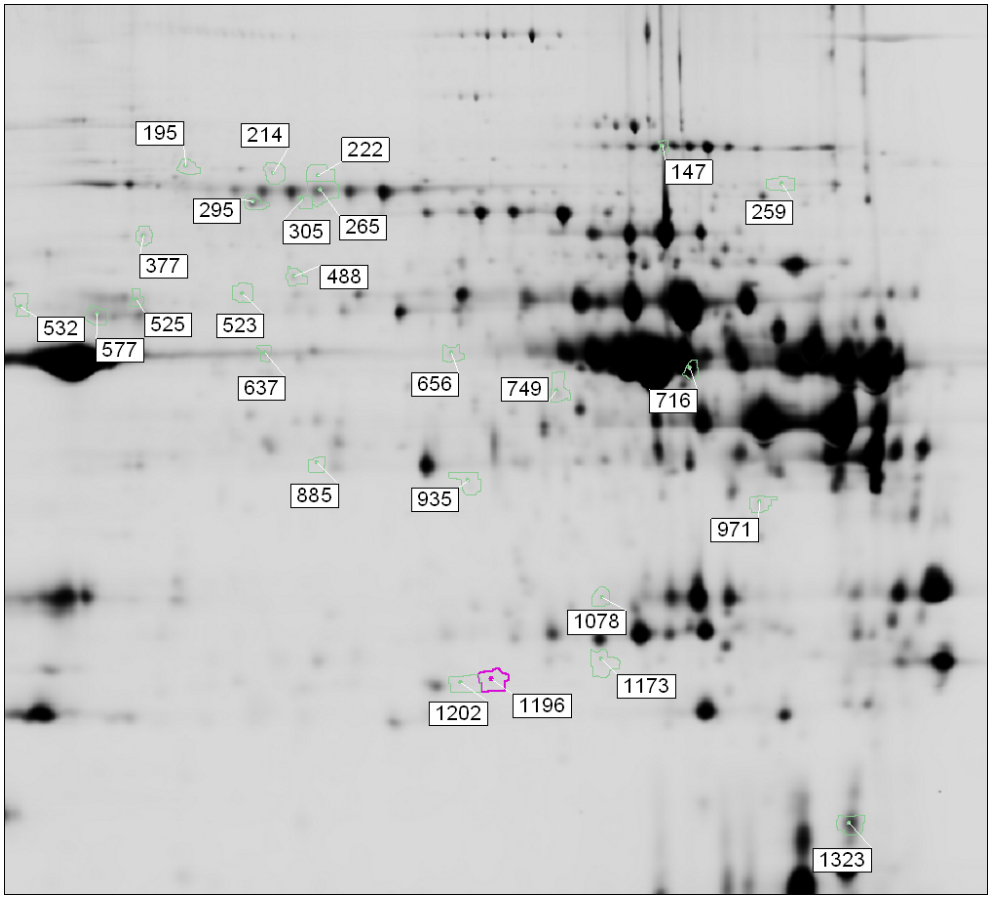

Figure S2.1. 2D-DIGE gel image. The twenty-six protein spots that are differentially expressed in EAMG are shown (1w-ANOVA, $p \leq 0.05$). Seventeen of these spots were successfully identified by mass spectrometry (significant MASCOT and SEQUEST scores).

3

IDENTIFICATION OF PROTEIN NETWORKS INVOLVED IN MULTIPLE SCLEROSIS

Based on:

Identification of Protein Networks Involved in the Disease Course of Experimental Autoimmune Encephalomyelitis, an Animal Model of Multiple Sclerosis.

Annelies Vanheel[1*], Ruth Daniels[1*], Stéphane Plaisance[2], Kurt Baeten[1], Jerome JA. Hendriks[1], Pierre Leprince[3], Debora Dumont[1], Johan Robben[4], Bert Brône[1], Piet Stinissen[1], Jean-Paul Noben[1] and Niels Hellings[1]

PLoS ONE 2012; 7(4):e35544

[1]Biomedical Research Institute, Hasselt University and Transnationale Universiteit Limburg, School of Life Sciences, Hasselt, Belgium

[2]VIB – Bioinformatics Training and Service Facility (BITS), Gent, Belgium

[3] GIGA-Neuroscience, University of Liège, Liège, Belgium

[4]Biochemistry, Molecular and Structural Biology, Katholieke Universiteit Leuven, Heverlee, Belgium

*These authors contributed equally to this work. RD conceived and performed the animal experiments. Both authors performed and analyzed the 2D-DIGE study. AV performed and analyzed the IHC, WB and myelin phagocytosis assays. Both authors wrote the paper.

ABSTRACT

A more detailed insight into disease mechanisms of multiple sclerosis (MS) is crucial for the development of new and more effective therapies. MS is a chronic inflammatory autoimmune disease of the central nervous system. The aim of this study is to identify novel disease associated proteins involved in the development of inflammatory brain lesions, to help unravel underlying disease processes. Brainstem proteins were obtained from rats with MBP induced acute experimental autoimmune encephalomyelitis (EAE), a well characterised disease model of MS. Samples were collected at different time points: just before onset of symptoms, at the top of the disease and following recovery. To analyze changes in the brainstem proteome during the disease course, a quantitative proteomics study was performed using two-dimensional difference in-gel electrophoresis (2D-DIGE) followed by mass spectrometry. We identified 75 unique proteins in 92 spots with a significant abundance difference between the experimental groups. To find disease-related networks, these regulated proteins were mapped to existing biological networks by Ingenuity Pathway Analysis (IPA). The analysis revealed that 70% of these proteins have been described to take part in neurological disease. Furthermore, some focus networks were created by IPA. These networks suggest an integrated regulation of the identified proteins with the addition of some putative regulators. Post-synaptic density protein 95 (DLG4), a key player in neuronal signalling and calcium-activated potassium channel alpha 1 (KCNMA1), involved in neurotransmitter release, are 2 putative regulators connecting 64% of the identified proteins. Functional blocking of the KCNMA1 in macrophages was able to alter myelin phagocytosis, a disease mechanism highly involved in EAE and MS pathology. Quantitative analysis of differentially expressed brainstem proteins in an animal model of MS is a first step to identify disease-associated proteins and networks that warrant further research to study their actual contribution to disease pathology.

3.1 Introduction

MS is an inflammatory autoimmune disease of the central nervous system (CNS) in which genetic, environmental and immunological factors are involved (27, 140). The disease is characterised by blood brain barrier (BBB) breakdown, demyelination, oligodendrocyte apoptosis, progressive axonal damage and reactive astrogliosis (141-143). These pathological hallmarks are present in the multifocal inflammatory lesions of the CNS, primarily localised in the white matter. The infiltration of autoreactive T cells, B cells and macrophages, and the production of pro-inflammatory cytokines are known to take part in the formation of inflammatory CNS lesions (17, 142, 144-146). Still, the exact cause and underlying molecular mechanisms remain poorly understood, but are crucial in the search for new therapeutic options. A proteomics approach was chosen to get more insight in the molecular processes of MS.

Proteomics studies are valuable to get an overview of protein expression in cells, tissues or organisms. These protein expression profiles can provide indications towards molecular mechanisms involved in normal and disease processes. In the past, gel-based proteome studies of brain (147) and cerebrospinal fluid (CSF) (148-151) were carried out by comparison of intensities of (silver) stained gel spots, a procedure that may suffer from experimental variability and poor reproducibility. Only adequate quantitative approaches will allow the analysis of disease processes over time in the brain or CSF during neuroinflammation. Two-dimensional fluorescence difference gel electrophoresis (2D-DIGE) is a very sensitive gel-based proteomics technique that is unique through the utilization of fluorescently labelled samples on the same gel, and the application of an internal standard for intra- and inter-gel comparisons and normalization.

In MS research, some quantitative proteomics studies have already been completed (90, 152, 153). Looking at 2D-DIGE experiments, mostly biomarker studies on human CSF were performed (80, 83, 86, 87, 154). In one proteomics study in MS research, a comparison between multiple plaque-types was performed to obtain new therapeutic targets (3), although not by 2D-DIGE. Post-mortem MS samples are often a snapshot of longstanding disease. However, a well characterised homogeneous animal model, experimental autoimmune encephalomyelitis (EAE), is available and can be used to obtain samples of the

inflammatory lesions. Only 2 experiments were published in which CNS tissue of EAE animals was used for a 2D-DIGE study (84, 155). In these studies protein expression was compared between two experimental groups. To get a better understanding of the pathomechanisms in MS and EAE, we decided to use experimental groups at different time points during the disease.

Here we report disease stage-specific variations in brain protein expression found in samples from different time points during acute EAE, a well characterised animal model of MS. The brainstem of this model was selected to focus on CNS inflammatory pathways involved in the lesion development and regulation of EAE, as it was shown that disease related macrophage infiltration at the onset of acute Lewis rat EAE was mainly localised to the caudal part of the brainstem (156). We performed a 2D-DIGE study to quantitatively compare protein levels at different disease stages. Samples were obtained before onset of the symptoms, at the top of the disease and after recovery. This allows us to create graphs of brain protein levels over time. We were able to identify 75 unique proteins present in 92 differential gel spots. All of these proteins were analysed with Ingenuity Pathway Analysis (IPA) software to disclose connections between these proteins, and thus define pathways that could be involved in the molecular mechanisms of MS.

3.2 Materials and methods

3.2.1 Sample collection

EAE was induced in 7 week-old female Lewis-rats by subcutaneous immunization with myelin basic protein (MBP) in Complete Freunds Adjuvant (CFA)(156). Animals were weighted and scored daily according to the following scale 0, no neurological abnormalities; 0.5, partial loss of tail tonus; 1, complete loss of tail tonus; 2, hind limb paresis; 3, hind limb paralysis; 4, moribund; 5, death. Before disease onset (9 dpi), at the top (14 dpi) and after recovery (18 dpi) three animals were sacrificed and transcardially perfused to obtain blood-free brain stems (5mM EDTA in PBS pH 7.2 with Complete Protease Inhibitor (Roche)). Control animals (n=3) were injected with CFA only and sacrificed at 15 dpi. After isolation, all tissues were frozen in liquid nitrogen and subsequently stored at -80°C. This study was in strict accordance with the EU legislation, Directive 86/609/EEC. The protocol was approved by, and carried out in strict agreement with the recommendations of, the local Ethical Committee for Animal Experiments of Hasselt University (permit number: 201023).

3.2.2 Protein extraction

Proteins were extracted as described by Sizova et al.(118). Briefly, brainstems were lyophilised, crushed (Kontes tissue grinder) and proteins extracted before ultracentrifugation. Samples were then desalted and the buffer was exchanged to labeling buffer (7M urea, 2M thiourea, 4% w/v CHAPS in 30mM Tris HCl pH 8.5) using ultrafree®-MC PLCC centrifugal filter units (Millipore, cut-off 5 kDa). Protein concentration was determined using the 2D Quant kit (Amersham Biosciences) and aliquots were stored at -80°C.

3.2.3 Labeling

Minimal labeling with N-hydroxysuccinimidyl-ester dyes Cy2, Cy3 and Cy5 (GE healthcare) was performed as described by the manufacturer (Ettan™ DIGE Basic course, GE healthcare) with some minor adaptations. Labeling of 50 µg of proteins

was accomplished with 300 pmol of Cy3 or Cy5 in dimethylformamide (DMF, Acros organics). The pooled internal standard, containing identical protein amounts from all samples, was labeled with Cy2. To avoid dye specific labeling artifacts, there was a dye swap in each group (three samples from any condition were never labeled all with Cy3 or Cy5).

3.2.4 2D-GE

For isoelectric focusing (IEF), a 3-10NL IPG strip of 24 cm (GE Healthcare) was rehydrated for 8 hours. IEF runs (IPGphor 3, GE Healthcare) and preparation of second dimension SDS-PAGE gels was done according to the manufacturer's Ettan™ DIGE Basic course (GE healthcare). Strip equilibration was carried out with equilibration buffer I and II (6M urea, 2% SDS, 50 mM Tris pH8.8, 0.02% bromophenol blue and 30% glycerol) containing 1% DTT or 4.5% iodoacetamide respectively. After equilibration, strips were mounted onto the SDS-PAGE gels (12.5%), and run for 2 hours at 5mA/gel and overnight at 25mA/gel in the Ettan DALTsix electrophoresis system (GE healthcare). 2x SDS electrophoresis buffer was used in the lower buffer chamber and 3x SDS electrophoresis buffer in the upper buffer chamber.

3.2.5 2D-DIGE analysis

CyDye-labeled 2D-DIGE gels were scanned on the Ettan DIGE imager (GE healthcare). Gel images from all three CyDyes were loaded into DeCyder 7.0 software (GE healthcare) and analysed. Statistical significance was calculated using Student's t test and analysis of variance (ANOVA) to compare the variation in abundance within a group to the magnitude of change between groups. Spots present in 85% of the gel images, and with a statistically significant ANOVA ($p \leq 0.05$) were considered for further analysis. Unsupervised principal component analysis (PCA) was performed using the DeCyder extended data analysis (EDA) module.

3.2.6 Spotpicking and protein digestion

For spot picking (Ettan SpotPicker, GE healthcare) a preparative gel was made containing 200 µg of an unlabeled sample and 50µg of the labeled internal standard. Bind-silane (GE healthcare) and reference stickers were applied on the glass plate containing spacers before pouring the gel, thereby ensuring the accuracy of robotic protein excision. In-gel digestion using trypsin (Promega) was performed manually as described by Shevchenko (120).

3.2.7 Mass spectrometric analysis and protein identification

The mass spectrometer was calibrated and tuned as described in LCQ 'Operator's Manual' Revision B July 1996. Instrumental ion optics were further optimised for analysis of doubly charged peptide ions by direct infusion (1µl/minute) of synthetic peptide 'IFGKGTTLSVSSNIQ' at 10 pmol/µl in 0.1 M acetic acid ($[M+2H]^{2+}$ = 776.42). Tryptic digests were dried *in vacuo*, solubilised in 20 µl 0.1 M acetic acid in water containing cortisol (4 pg/µl) as an internal standard and analysed in data-dependent mode by nanoflow HPLC/ESI(+)-MS/MS (109). Stability of the chromatographic process and ESI efficiency were monitored using cortisol base peak m/z 361.2. Bovine serum albumin (10 fmole BSA on-column) was used for analytical system control. LCQ Xcalibur v2.0 SR2 raw files and spectra were selected from within Proteome Discoverer 1.0.0.43 (Thermo Electron) with following settings: minimal peak count, 50; total intensity threshold, 4000; and S/N, 6. Peak lists were searched with Sequest v1.0.43 and Mascot v2.2.0.2 against the EMBL-EBI International Protein Index database for rat (v3.69; 39578 entries) and for mouse (v3.69; 56737 entries) both with following settings: fragment tolerance, 1.00 Da (monoisotopic); parent tolerance, 3.0 Da (monoisotopic); fixed modifications, carbamidomethylation of cystein; variable modifications, oxidation of methionin; max missed cleavages, 2. Outcome of both search engines was validated with Scaffold v.3.00.03 (Proteome Software) with minimum peptide and protein probability set to 95% and 99.9% respectively. The

protein identifications thus returned by Scaffold for each gel spot were manually validated considering spectral quality.
HASH in TRANCHE representing our data:
nq+91eLffYILUDgesGy6Hx/mmDF6a7hPyvCMAdFcKwBUafN2Dr6DUlM0HaKPWb5XYiVh/nbmTKuRAL+sxbLFD4FyzTwAAAAAAAAEcQ==

3.2.8 Immunohistochemistry

Tissue sections (10 µm, Leica CM1900 UV microtome) of the spinal cord were used for IHC. Macrophages were detected with the ED-1 staining (mouse anti-rat CD68, AbD serotec) as a primary antibody (1/200, 2 hours). Myelin protein 2', 3'-cyclic nucleotide 3'-phosphodiesterase (CNP) was detected using mouse anti-CNP (Millipore) as a primary antibody (1/200, overnight). Biotinylated polyclonal rabbit anti-mouse IgG (Dako) was selected as secondary AB (1/400, 1 hour). 10% rabbit serum was chosen for blocking and 3,3'-diaminobenzidine (DAB) for staining. Hematoxylin was used as a counterstaining. For the analysis of the staining (Nikon ECLIPSE 80i microscope, NIS elements software, 20x objective), 3 ED-1 stained tissue sections were scanned for positive staining regions. These regions were defined as inflammatory plaques, and pictures were taken of these areas. Macrophage infiltration was defined as the percentage of positive area in these pictures. For the CNP staining, 3 slices adjacent to the 3 slices stained for macrophages were used. CNP was measured in the area corresponding to the inflammatory plaques in the ED-1 stained slices. Statistical analysis of the difference in macrophage infiltration and CNP expression between the experimental groups was done using Dunn's multiple comparison test (GraphPad Prism4).

3.2.9 Western blotting

7.5 µg of the brainstem protein extract was separated by 1D SDS-PAGE. After blotting to a nitrocellulose membrane, total protein staining was done by means of ruthenium (II) tris (bathophenantroline disulfonate)(RuBPS) staining (Rubilab) as previously described (157). A subsequent immunostaining was performed with mouse anti-CNP (Millipore, 1/2500 for 1 hour), rabbit anti-DLG4 (Millipore, 1/1000

for 2 hours) and rabbit anti-KCNMA1 (Millipore, 1/1000 for 2 hours) as primary antibodies. Goat anti-mouse/rabbit Alexa fluor 647 (Invitrogen) were used as a secondary antibody (1/5000, 2 hours). The fluorescent signal was measured with the Ettan DIGE scanner and imagequant TL software was used for processing (GE healthcare). The immunostaining intensities were normalised for unequal protein load (fluorescent total protein stain). The peak volume was used for quantification.

3.2.10 Network analysis

Mapping of proteins identified by mass spectrometry onto existing networks and pathways was accomplished using Ingenuity Pathway Analysis software (Ingenuity® Systems, www.ingenuity.com). The data set containing protein identities was uploaded into the software. Networks of the identified proteins containing the molecular relationships between genes/gene products were generated algorithmically using the Ingenuity Pathway knowledge base (IPA-KB). Nodes represent genes or gene products and are displayed using various shapes that represent the functional class of the gene product. Nodes are connected by edges (lines) which represent different biological relationships that were in the IPA-KB at the time of creation. In addition, in order to evaluate the overlap of the current work with MS, lists of biological markers were obtained from the IPA-KB as well as from a competitor product GeneGO Metasearch (GeneGo, St. Joseph, MI, USA) and are used for comparison to our data.
Ingenuity Pathway Analysis has been designed to work with human, mouse and rat models. However, in order to support the discussion of MS in human, we decided to use human gene-names in this work. Therefore, all graphs presented in this report contain human nomenclature.

3.2.11 Myelin phagocytosis assay

Rat macrophages (NR8383 cell line) were cultured in RPMI 1640 medium (Invitrogen) enriched with 10% fetal calf serum (Hyclone, Erenbodegen, Belgium), 50 U/ml penicillin and 50 U/ml streptomycin (Invitrogen). Macrophages were activated with 100 ng/ml lipopolysaccharide (LPS, Sigma) for 18 hours. Next, 100µg/ml DiI-labeled myelin, isolated and labeled as described previously (158)

and paxilline (Sigma) were added for 90 minutes. For paxillin treatment a concentration of 300nM was used to obtain a total blockage of the KCNMA1 channel (159). Flow cytometry was used to assess the degree of myelin internalization.

3.3 Results

3.3.1 EAE brain proteome analysis by 2D-DIGE/mass spectrometry

For the analysis of protein abundance at different stages of inflammatory lesion development, the brainstem of a lewis rat acute EAE animal model was selected. This animal model of MS represents the inflammatory processes during the onset of a relapse and has a predictable disease progression. Furthermore, this model allows sufficient tissue isolation for protein isolation. Macrophage infiltration at onset of symptoms was mainly localized to the brainstem in this model (156). Detergent-soluble protein extracts were isolated for a quantitative 2D-DIGE study to identify differential proteins in the brainstem of EAE-animals and controls at different stages of the disease. Controls were CFA injected, whereas acute EAE was induced by immunization with myelin basic protein (MBP) (Figure 3.1). The EAE animals were divided into three groups: before onset, at the top, and following recovery of the disease.

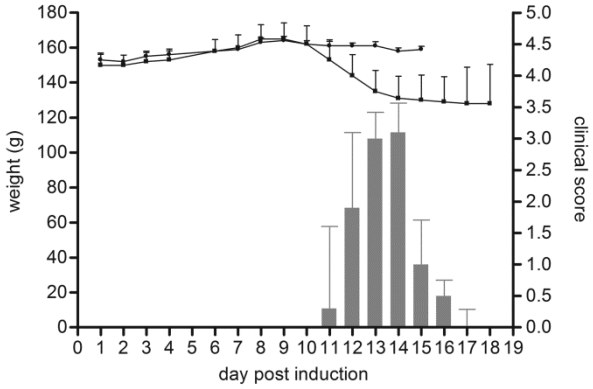

Figure 3.1. Clinical scores and weight changes of EAE and control animals. EAE was induced by injection of MBP in CFA (bars and squares). Control animals were CFA injected (dots). The controls showed no clinical symptoms. Each value represents the mean ± standard deviation of n animals: control day1-15, n=3; EAE day1-9, n=9; day10-14, n=6 and day15-18, n=3.

We identified proteins in 92 differential gelspots (ANOVA ≤0.05) with DeCyder 7.0 gel analysis software and nano-LC-mass spectrometry (Figure 3.2). Sixty-nine of the 92 differential protein spots were even more stringently regulated (ANOVA ≤ 0.01, bold in Table S3.1). A total of 130 proteins were identified in these 92 spots, since multiple proteins can be present in one gelspot (Table 3.1). Furthermore, 24 of these proteins were present in multiple (2-10) spots. Overall, 75 unique proteins were identified.

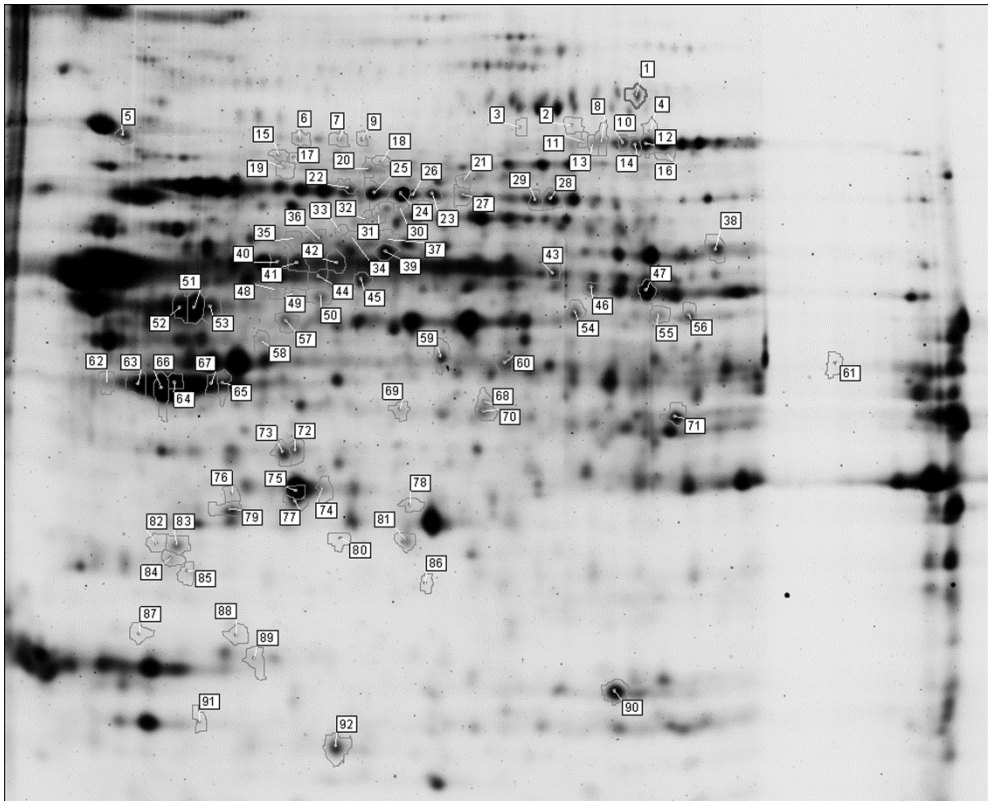

Figure 3.2. 2D-DIGE gel image. The 92 spots presented have a shift in abundance over the four experimental conditions (control, disease onset, top, and recovery) (ANOVA ≤ 0.05). Spots were picked from preparative 2D-gels and proteins identified by nano-LC-ESI-mass spectrometry. The proteins were identified with significant MASCOT and SEQUEST scores. Spots are numbered as in Table S3.1.

Table 3.1. Identification of differentially expressed protein spots (A≤0.05)

# protein identifications/spot	# identified spots	# proteins
1	63	63
2	22	44
3	5	15
4	2	8
Total	92 identified spots	130 identified proteins

To get a better view on the expression profile of these spots along the disease course, a cluster analysis was performed. Using self organizing maps (SOM) analysis, spots that have the same expression patterns during the disease are grouped together (Figure 3.3). The average ratio and T-test, for the six possible comparisons between the four conditions included in this study, provided detailed information on the time course of the proteome changes induced in the inflamed brain (Table S3.2). The difference in fluorescence intensity, as reported in the DeCyder software, indicates a change in expression, turnover and/or protein modification.

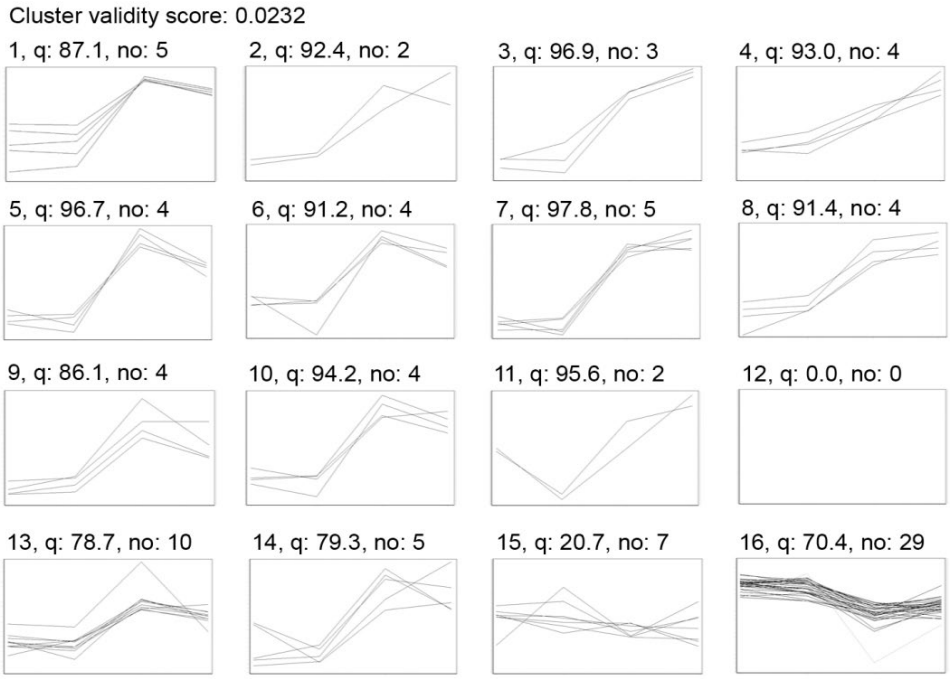

Figure 3.3. SOM analysis. A SOM analysis was performed to group spots with a similar expression pattern, in this way clustering the spots that are regulated in the same way. Sixteen clusters were obtained, one (12) containing no spots. The X-axis chronologically displays the experimental groups (C-O-T-R) while the Y-axis displays the log standardised abundance (scale is not identical for the different clusters). The cluster number, quality value (q) and number of spots present in the cluster (no) are indicated above the graphs.

3.3.2 Identity and validity of differential proteins

BBB disruption, astrocyte activation and macrophage infiltration are processes known to occur in MS and acute EAE. We focused on proteins related to these disease processes to verify the experimental setup and analyses. Indeed, serum albumin (ALB, e.g. spot 874), glial fibrillary acidic protein (GFAP, e.g. spot 1397) and macrophage-capping protein (CAPG, spot 1906) represent these pathological hallmarks and are all upregulated at the top of the disease (Figure 3.4).

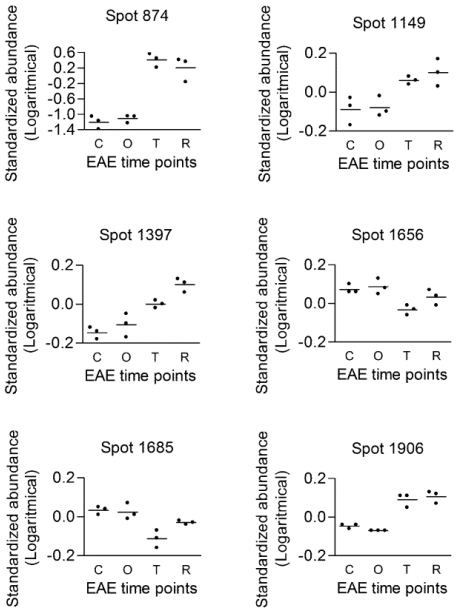

Figure 3.4. Protein expression patterns over the disease course. 2D-DIGE expression profiles: ALB (spot 874), PDIA3 (spot 1149), GFAP (spot 1397), CNP (spot 1656 and 1685) and CAPG (spot 1906). The log standard abundance (the relative abundance change normalised to signals in internal standard specific for each spot) is indicated for control, onset, top and recovery samples (C-O-T-R).

An ED-1 macrophage staining on spinal cord slices verified the infiltration of macrophages in the CNS (Figure 3.5A). In contrast to the absence of macrophages in controls and just prior to disease onset, macrophage infiltration was significantly increased at the top of the disease (Figure 3.5B), a similar pattern as seen for CAPG. Identification of differential proteins that represent processes actively involved in the disease, verifies our experimental design and the ability to pick up disease-related proteins.

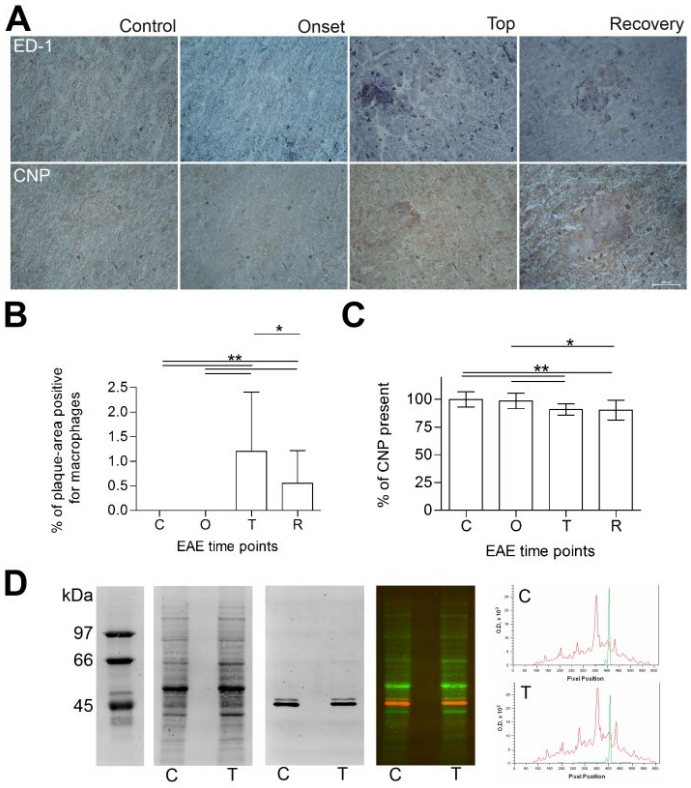

Figure 3.5. Validation of the 2D-DIGE results. Immunohistochemistry was performed to demonstrate the presence of macrophages and CNP. Macrophage (ED-1) and CNP immunostaining of rat spinal cords (same animals as for 2D-DIGE) from control, and EAE rats before disease onset, top and recovery are shown in panel A. These IHC stainings were quantified (Panel B and C), and expression levels compared by Dunn's multiple comparison test (GraphPad Prism4). The error bars indicate standard deviations of measurements performed at least in triplicate. *: significant difference, $p<0.01$ and **: significant difference, $p<0.001$. In Panel D, a quantitative 1D CNP immunoblot of EAE brainstem homogenate from control and disease top is shown. An overview of the fluorescent total protein staining, anti-CNP immunostaining, the fluorescent overlay of both (red and green overlay), and finally a representation of the fluorescent signals as processed with ImageQuant TL software (GE Healthcare). The red curve corresponds with the total protein content and the green curve with the CNP fluorescence. Both a representative control animal (c) and one at the disease top (t) are presented.

The expression pattern of 2',3'-cyclic-nucleotide 3'-phosphodiesterase (CNP), an abundant myelin protein, was significantly decreased in the inflamed brain (Figure 3.4, spot 1656 and 1685). This could be indicative for myelin loss. We confirmed this CNP decrease with immunohistochemistry (IHC) and western blot (WB) (Figure 3.5). IHC was performed and quantified at the site of inflammation. CNP was significantly decreased at the top of the disease and after recovery (Figure 3.5C). Furthermore, a fluorescent quantitative anti-CNP WB revealed two bands, consistent with CNP1 (46 kDa) and CNP2 (48 kDa). Both CNP1 and CNP2 were significantly decreased at top of the disease compared to control animals (fold change -1.54±0.03 and -1.40±0.05 respectively). In conclusion, with two independent techniques, we were able to confirm the 2D-DIGE expression data for CNP.

3.3.3 Principal component analysis and Ingenuity Pathway Analysis

Principal component analysis (PCA) is an unsupervised multivariate method used to analyze the variability between experimental groups. A dimension reduction is applied previous to classification, reducing the possibly correlated variables (differential spots) to a set of uncorrelated variables. In this way a principal component represents a linear combination of the differential spots. Each sample (spotmap) is represented in the PCA plot with respect to the principal components. A PCA was performed on our dataset and shows clustering of the samples according to the disease stage. A clear separation between the early disease stage (before onset of the disease) and the late disease stages (top and recovery) is evident (Figure 3.6). Furthermore, samples from the top of the disease are separated from recovery samples. In contrast, the control and onset samples were not separated; implicating that differences in brain protein expression were not sufficient for separation between these two conditions.

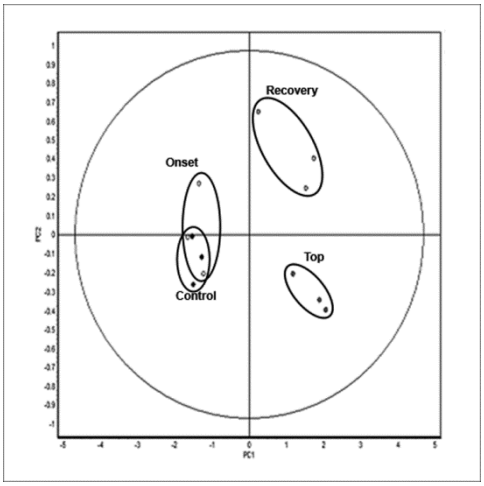

Figure 3.6. Unsupervised multivariate analysis discriminating between early and late groups. PCA reduces the dimensionality of a multidimensional analysis and displays the two principle components that can distinguish between the two largest sources of variation within the dataset (92 spots, ANOVA ≤ 0.05). Principle component analysis clustering the 12 individual spotmaps into the four conditions by two principle components: PC1, which distinguishes 90% of the variance, and PC2 distinguishes an additional 3.8% of the variance.

Human homologues of the 75 unique proteins identified here were subsequently analysed with IPA, a software tool capable of mapping proteins onto existing networks and pathways. Cellular compartments as designated by IPA (gene ontology based) indicated that the majority of identified proteins (76%) were cytoplasmic in origin (Figure 3.7).

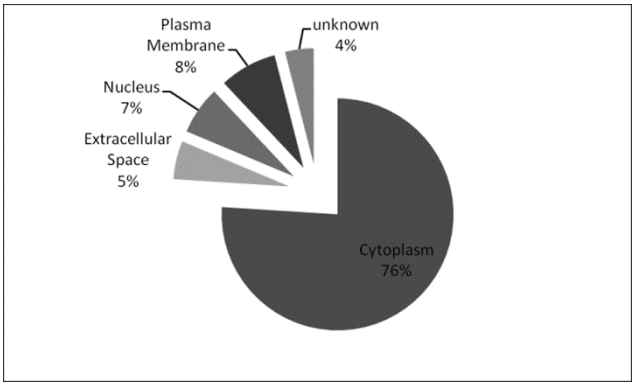

Figure 3.7. GO-Compartments. The 75 unique proteins (ANOVA ≤ 0.05) were categorised according to the subcellular compartment (extracellular space, plasma membrane, cytoplasm, nucleus, and unknown). Information was collected from Gene ontology by IPA. Percentages are presented.

Mapping of our proteins onto biological pathways and disease networks demonstrated that 16 proteins were linked to nervous system development and function (p-value: 2.47E-05 – 4.50E-02), and that 53 of the 75 proteins were associated with neurological disease (p-value: 1.35E-15 – 4.50E-02). Post synaptic density protein 95 (DLG4) and amyloid precursor protein (APP) appear to be central points in the IPA networks identified here, but they were not detected in the 2D-DIGE study.

Another possibility in the IPA software was the comparison of the 75 unique proteins to a list of MS-related proteins present in the IPA knowledge base. As expected due to technical restrictions, only one of these mostly membrane-associated MS-related proteins was also identified in our 2D-DIGE study, protein disulfide-isomerase A3 (PDIA3, spot 1149) (Figure 3.4). However, fifty-eight of our differential proteins were linked to these MS-related proteins, mostly by downstream biochemical pathways (data not shown). Angiotensin (AGT) and calcium-activated potassium channel alpha 1 (KCNMA1) were MS-related proteins from the IPA knowledgebase with a strong relation to our data. Together with DLG4 and APP, they were selected for building focus networks of our dataset. These networks suggest an integrated regulation of the identified proteins with the addition of some putative regulators. They are a model for the effects of these four proteins on our dataset (Figure 3.8 and Table S3.3). Forty-eight proteins (64%) of the 2D-DIGE dataset were directly linked to DLG4 and/or KCNMA1. Forty-two (56%) were linked to AGT and 40 (53.3%) to APP. In the AGT network another important potential regulator of our dataset was identified, being tumor protein p53 (TP53).

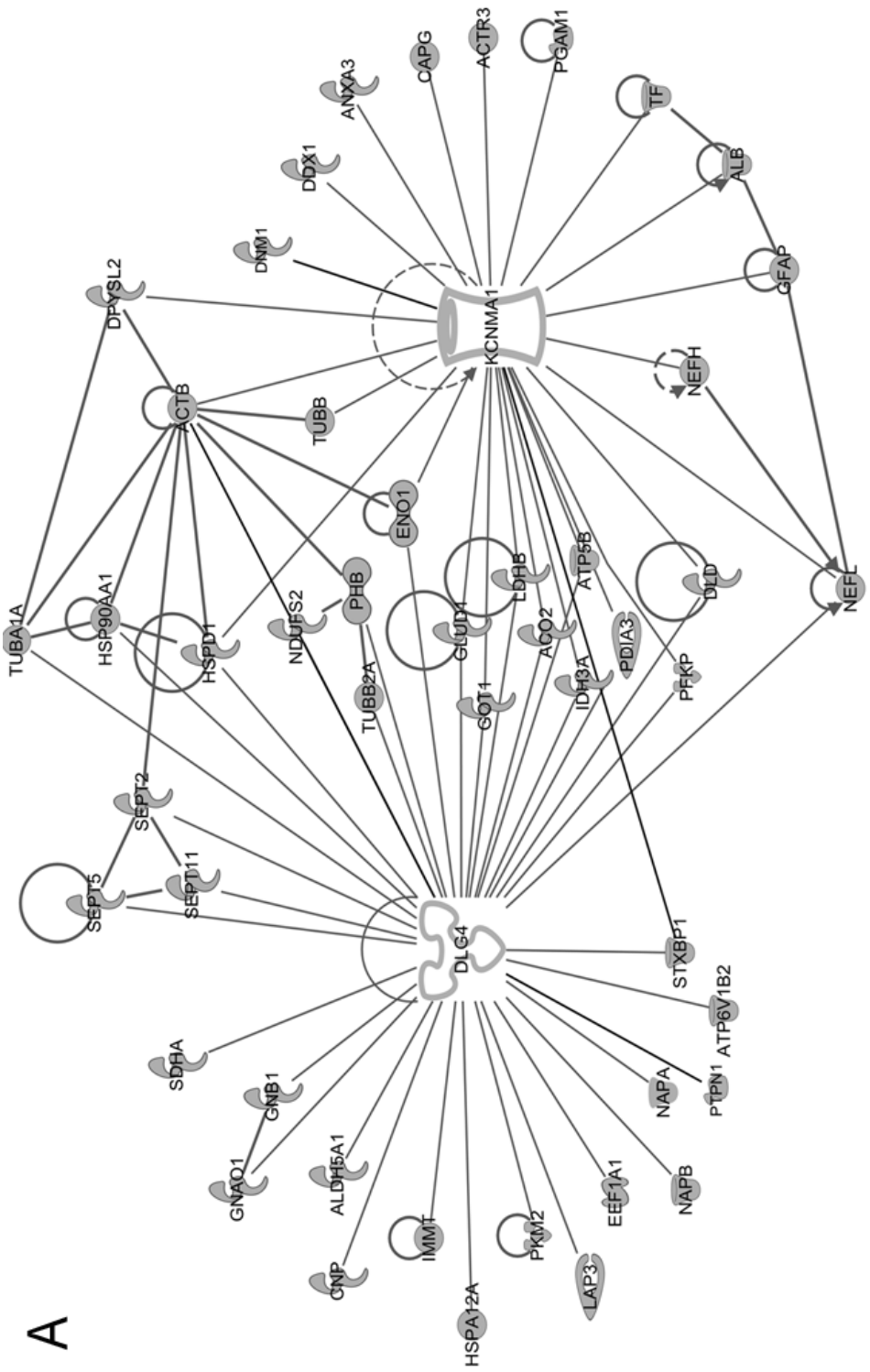
A
KCNMA1
ACTB
TUBB
ENO1
PHB
HSPD1
HSP90AA1
TUBA1A
NDUFS2
TUBB2A
GLUD1
GOT1
LDHB
ACO2
IDH3A
ATP5B
PDIA3
DLD
PFKP
NEFL
NEFH
GFAP
ALB
TF
PGAM1
ACTR3
CAPG
ANXA3
DDX1
DNM1
DPYSL2
SEPT2
SEPT11
SEPT5
DLG4
STXBP1
ATP6V1B2
PTPN1
NAPA
NAPB
EEF1A1
LAP3
PKM2
IMMT
HSPA12A
GNB1
GNAO1
ALDH5A1
GNB
SDHA

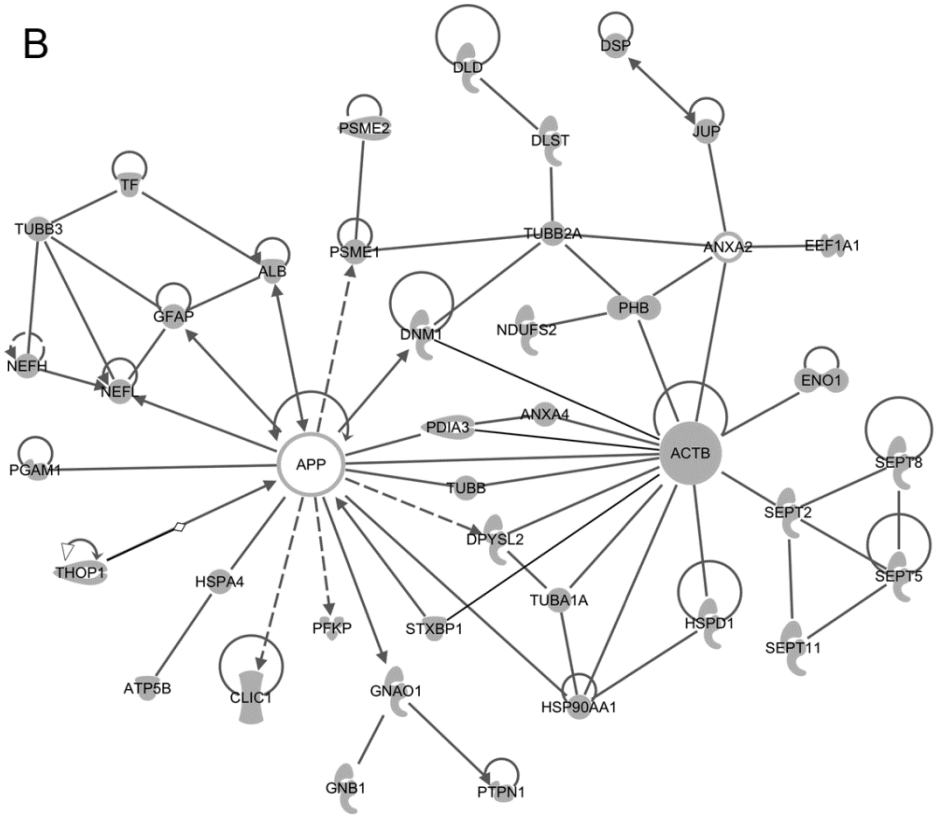
B
DLD
DSP
PSME2
DLST
JUP
TF
TUBB3
PSME1
TUBB2A
ANXA2
EEF1A1
ALB
GFAP
DNM1
NDUFS2
PHB
NEFH
NEFL
ENO1
PDIA3
ANXA4
PGAM1
APP
ACTB
SEPT8
TUBB
SEPT2
DPYSL2
THOP1
SEPT5
HSPA4
TUBA1A
HSPD1
PFKP
STXBP1
SEPT11
ATP5B
CLIC1
GNAO1
HSP90AA1
GNB1
PTPN1

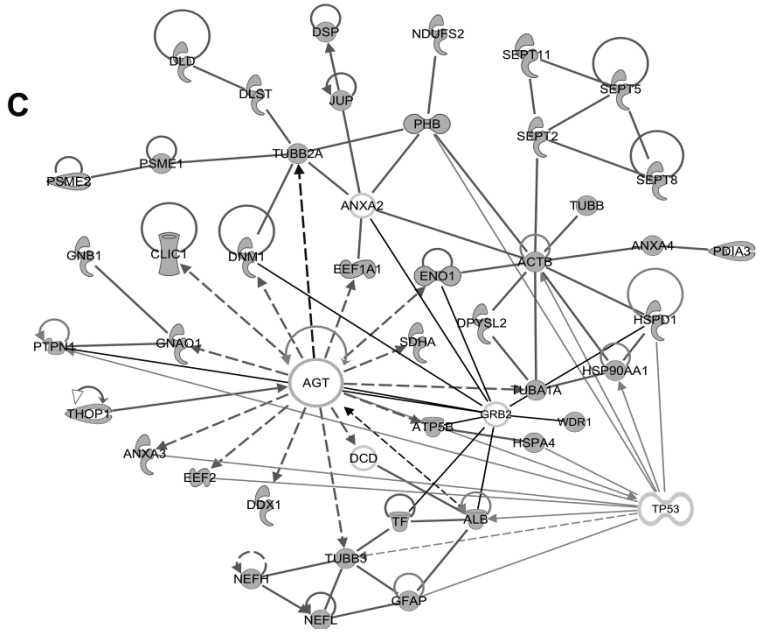
C
DSP
NDUFS2
DLD
SEPT11
DLST
JUP
SEPT5
PHB
SEPT2
PSME2
PSME1
TUBB2A
SEPT8
ANXA2
TUBB
GNB1
CLIC1
DNM1
ANXA4
PDIA3
EEF1A1
ENO1
ACTB
HSPD1
DPYSL2
PTPN1
GNAO1
SDHA
HSP90AA1
AGT
TUBA1A
THOP1
GRB2
ATP5B
WDR1
HSPA4
ANXA3
DCD
EEF2
TP53
DDX1
TF
ALB
TUBB3
NEFH
GFAP
NEFL

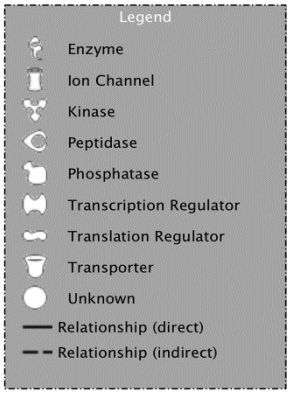

Figure 3.8. Ingenuity pathway analysis networks build with focus proteins. The DLG4-KCNMA1 network (Panel A), APP-ACTB network (Panel B) and AGT-TP53 network (Panel C) are represented. These networks were obtained using the IPA-KB by linking proteins from the data-set (75 unique proteins) to the focus proteins. Nodes containing proteins identified in the dataset have a grey fill.

We confirmed the presence of DLG4 and KCNMA1 in our brain samples performing a quantitative fluorescent immunoblotting (Figure 3.9). By using a combination of a total protein staining and an immunostaining on western blot, it is possible to correct for differences in total protein loading. Fluorescent stains allow for peak detection and quantification. For both DLG4 and KCNMA1, presence of the protein in our samples could be established, but no expression differences were detected between disease stages. This in part explains why these proteins were not picked up in our 2D-DIGE analyses. Even though they are not differentially expressed, their presence in the centre of the IPA networks suggests a role for DLG4 and KCNMA1 as central regulators in the molecular mechanisms of disease progression. KCNMA1 is a calcium-activated potassium channel with a direct connection to CAPG, a protein involved in actin-based cell motility and thus important for macrophage functions such as migration and myelin phagocytosis, processes known to be highly involved in MS and EAE pathology (17). We demonstrated that blocking of KCNMA1 using paxilline significantly reduced myelin phagocytosis by LPS activated macrophages (-17.79 ± 10.67%, $p<0.01$, Figure 3.10). This nicely illustrates that the central regulators reported here indeed have a functional role in the disease process.

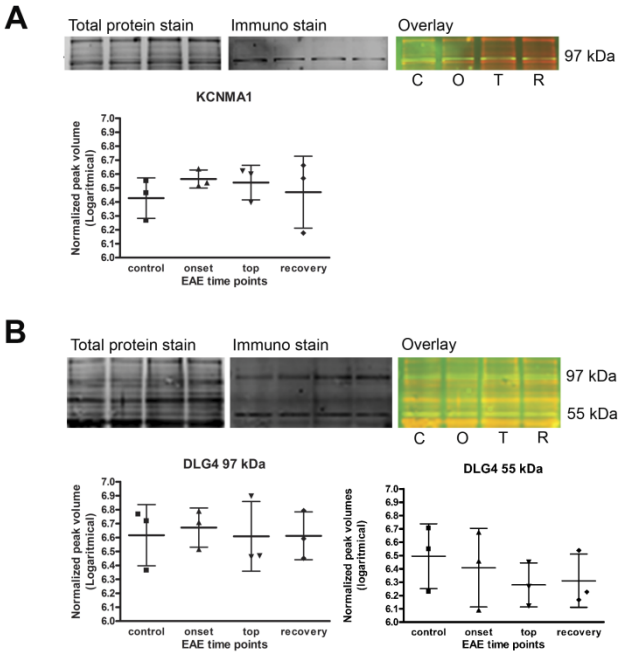

Figure 3.9. Western blot analysis of DLG4 and KCNMA1. A quantitative fluorescent western blot was performed to analyze the presence and expression levels of KCNMA1 (Panel A) and DLG4 (Panel B). By means of peak detection, the normalised peak volumes were used for quantification. No significant difference was found in expression levels, but both proteins were detected in the samples of the 2D-DIGE experiment. All animals were included in the WB analysis; control (C), onset (O), top (T) and recovery (R).

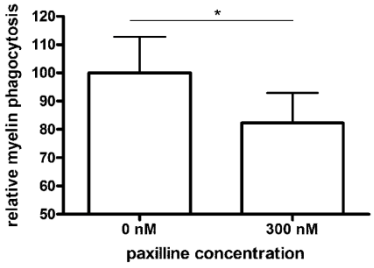

Figure 3.10. Myelin phagocytosis assay. The influence of paxilline, a KCNMA1 channel blocker, on myelin phagocytosis was studied to evaluate the possible biological involvement of this protein in EAE and/or MS related disease processes. After macrophage activation, myelin and paxilline were added and phagocytosis was measured by flow cytometry.

3.4 Discussion

We identified proteins present in 92 differential spots of the inflamed brain of EAE animals by means of a comparative 2D-DIGE proteomics analysis. Changes in the abundance of these 92 spots can discriminate between early (before onset) and late (top and recovery) disease stages by PCA of their values in the sample spotmaps. Seventy-five unique proteins were identified in these 92 differential spots by means of mass spectrometry. Some of these proteins represent known disease processes such as BBB disruption (ALB), astrocyte activation (GFAP) and macrophage infiltration (CAPG). Others are not yet linked to MS, and warrant further research. An in-depth network evaluation was performed for all 75 unique proteins.

Seventy percent of our identifications (53/75 proteins) are part of the biological pathway of neurological disease. One such example is the decrease in GABA transaminase (ABAT, spot 1437 and 1439), succinate-semialdehyde dehydrogenase (ALDH5A1, spot 1428) and mitochondrial glutamate dehydrogenase 1 (GLUD1, spot 1316 and 1331). Both ABAT and ALDH5A1 are enzymes responsible for the degradation of GABA, the principal inhibitory neurotransmitter of the CNS that is also involved in inflammation (160). When these enzymes decrease, GABA levels will increase. GLUD1 is an enzyme responsible for the interconversion of glutamate and alpha-ketoglutarate. A decrease in GLUD1 may result in an increase of glutamate, a neurotransmitter reported to be involved in MS excitotoxicity (146) and the precursor of GABA. Overall, these proteome changes indicate an increase of GABA at the top of the disease. Dysregulation of the GABA pathway in MS brains has been described in several studies and the implications of these findings have been tested in EAE (5, 160).

Four central network-nodes were suggested by IPA. DLG4 and APP are nodes from the IPA networks of our data, while KCNMA1 and AGT are MS-related proteins in the IPA knowledge base, with a strong relationship to our data. APP is an integral membrane protein that is concentrated at neuronal synapses. It can be synthesised by microglia, not only in response to direct nerve injury but also in immune-mediated disease such as EAE (161). A role for APP in immune and repair mechanisms of the CNS is suggested (161). A second network is build around

AGT, a protein produced by astrocytes in the brain (162). It is part of the renin-angiotensin system (RAS) that affects the immune response in general and the neuroinflammatory processes in the context of EAE (163). TP53, a well-known tumor suppressor that responds to cellular stress and can induce apoptosis and changes in metabolism is also present as a regulator in this network. TP53 was recently described to be an important 'network-hub' that interacts with a lot of genes associated with MS, indicating a role for this protein in the disease, namely the expansion of autoimmune cell clones (164). Sixty-four percent of our data are connected to DLG4 and/or KCNMA1, which highlights their possible role in EAE/MS. DLG4 is a membrane-associated protein implicated in the clustering of receptors, ion channels and associated signaling molecules in the post-synaptic membrane. It is a key player in neuronal signaling. KCNMA1 is an IPA MS-related protein involved in neurotransmitter release. The channel activity increases during hypoxia and decreases in response to reactive oxygen species (ROS)(165). Mitochondrial ion channels play an important role in cellular events such as apoptosis (caused by increased mitochondrial membrane permeability), exocytosis and synaptic transmission and are believed to contribute to cytoprotection (165). Both DLG4 and KCNMA1 are key regulation proteins of mitochondrial enzyme complexes involved in the cellular response to oxidative stress, a process that is also described in EAE/MS (166). We were able to detect DLG4 and KCNMA1 in our samples, but they were not differential between the experimental groups. This could indicate that the activation of these molecules does not influence their expression. The alterations in their downstream molecules however suggest that these pathways are activated during the different disease stages and thus involved in disease mechanisms. Indeed, DLG4 immunoreactivity in both gray and white matter of EAE spinal cord tissue was reciprocally associated with damage of postsynaptic structures and directly associated with disease activity. When EAE animals were in remission, DLG4 expression partly restored, further emphasizing the actual involvement of the DLG4 pathway in disease (167). For KCNMA1, the direct link between KCNMA1 and macrophage CAPG in the IPA network indicates KCNMA1 involvement in actin-based cell motility in these cells. Furthermore, local changes in intracellular calcium are associated with cytoskeletal reorganization needed for phagocytosis, these changes in calcium levels could change potassium efflux by KCNMA1, a calcium activated potassium

channel (168). This potassium efflux could hyperpolarize the cell and thus increase the driving force for calcium entry, linking KCNMA1 to cell motility and phagocytosis. Here we showed that blocking of KCNMA1 in macrophages decreased the ability of macrophages to phagocytose myelin, a pathological hallmark of MS and EAE lesions. The above documented functional role of DLG4 and KCNMA1 in EAE indicates that these networks could be biologically important for MS pathology and warrants further research.

Previously a quantitative iTRAQ study was reported comparing EAE spinal cord proteome between EAE and control animals (90). Six proteins were identified in common with our study (ALB, ANXA3, LAP3, PDIA3, PMSE2 and TF). These 6 proteins show an increased abundance during the disease in the iTRAQ study as well as in our study. Han et al. (3) performed a proteomic study on MS tissue, comparing different MS lesion types. They reported a total of 2302 proteins related to MS plaques of which 158, 416 and 236 proteins were unique to acute plaques, chronic active plaques and chronic plaques respectively. Sixty-four of the 75 unique proteins in our study were also reported in the study of Han et al., all but one (DSP is only present in chronic active lesions) are common for the different lesion types. The 11 unique proteins of our study are ACTB, ACTR3, ANXA3, EEF1A1, GNB1, Ifi47, LOC674678, PTPN1, STXBP1, TUBA1A and TUBB1. We believe that all 75 proteins reported here warrant further evaluation, as the data of Han et al. in contrast to our data are not quantitative and non of our 75 proteins were functionally evaluated.

The analysis of the brainstem proteome during EAE identified significant differences in the levels of proteins involved in mitochondrial energy production, apoptosis, antioxidant activity, cytoskeleton regulation and the immune system. The in depth network analysis by IPA as described here adds a major value to 2D-DIGE studies and the combination of both technologies is a prerequisite to find common regulators that extend even the limitations of the proteomics technology. Some proteins may play central roles through functional regulation without being differentially expressed. Still, IPA analysis helps to reveal pathways involved in the disease process and thereby also potentially involved proteins that were not

picked up directly by 2D-DIGE analysis. This strategy helps generate new hypotheses and to select unknown targets in pathways with relevance to MS.

In conclusion, the brain proteome study as presented here identified biological events involved in neuroinflammation that may be important during EAE, and also in MS. IPA analysis provides network information on the differentially expressed proteins in the 2D-DIGE study and enables the detection of proteins that cannot be picked up by a gel-based technology due to the technical restrictions favoring soluble, mostly cytoplasmic proteins (169, 170). The focus on disease-related networks in this work enables us to select several relevant topics in MS for further validation studies in animal models and MS patients and possibly allows the selection of targets for therapy.

3.5 Supplemental tables

Table S3.1. Protein identifications. Differential protein spots were picked and in-gel digestion was performed. Proteins were identified by mass spectrometry. ANOVA ≤0.05, **ANOVA ≤O.01**

Table S3.2. Cluster analysis. A cluster analysis was performed to get a better view on the expression profile of these spots along the disease course. The average ratio and T-test, for the six possible comparisons between the four conditions included in this study, provides detailed information on the time course of the proteome changes induced in the inflamed brain.

Table S3.3. IPA networks. In this table an overview is presented of all 75 unique proteins and their presence in the IPA networks as presented in Figure 3.8.

Table S3.1. Protein identifications (ANOVA ≤ 0.01 bold)

gel ID figure 3.2	master number	Protein name	IPA symbol	# peptides identified	1-ANOVA
1	**0377**	**Elongation factor 2**	**EEF2**	**5**	**0.00494**
2	**0499**	**ATP synthase subunit beta, mitochondrial**	**ATP5B**	**3**	**0.00313**
3	0516	Tyrosine-protein phosphatase non-receptor type 1	PTPN1	2	0.0277
4	**0521**	**ATP-dependent RNA helicase DDX1**	**DDX1**	**2**	**0.00636**
5	0545	Heat shock protein HSP 90-alpha	HSP90AA1	2	0.044
6	**0558**	**Dynamin-1**	**DNM1**	**4**	**0.00106**
7	**0560**	**Dynamin-1**	**DNM1**	**10**	**0.000783**
8	**0562**	**Aconitate hydratase, mitochondrial precursor**	**ACO2**	**2**	**0.000557**
		Serotransferrin	**TF**	**5**	
9	**0566**	**Serotransferrin**	**TF**	**5**	**0.00954**
10	**0581**	**Aconitate hydratase, mitochondrial precursor**	**ACO2**	**2**	**0.000884**
		Serotransferrin	**TF**	**6**	
11	**0588**	**Aconitate hydratase, mitochondrial precursor**	**ACO2**	**2**	**0.0019**
		60 kDa heat shock protein, mitochondrial precursor	**HSPD1**	**2**	
		Pyruvate kinase isozymes M1/M2	**PKM2**	**2**	
		Tubulin beta-5 chain	**TUBB**	**2**	
12	**0599**	**Aconitate hydratase, mitochondrial precursor**	**ACO2**	**11**	**0.00226**
		6-phosphofructokinase type C	**PFKP**	**4**	
		Serotransferrin	**TF**	**18**	

gel ID figure 3.2	master number	Protein name	IPA symbol	# peptides identified	1-ANOVA
13	**0606**	**6-phosphofructokinase type C**	**PFKP**	**6**	**0.00887**
14	**0619**	**Aconitate hydratase, mitochondrial precursor**	**ACO2**	**6**	**0.00453**
		6-phosphofructokinase type C	**PFKP**	**6**	
15	**0674**	**heat shock 70 kDa protein 4**	**HSP4A**	**6**	**0.00286**
16	**0676**	**similar to desmoplakin**	**DSP**	**4**	**0.00059**
17	**0683**	**Thimet oligopeptidase**	**THOP1**	**3**	**0.00929**
18	**0700**	**heat shock 70kDa protein 12A**	**HSPA12A**	**3**	**0.00811**
19	**0742**	**Mitofilin**	**IMMT**	**2**	**0.00425**
20	**0761**	**elongation factor-1 alpha 1**	**EEF1A1**	**2**	**0.00283**
		similar to Glycyl-tRNA synthetase	**GARS**	**4**	
		Histone H4	**LOC674678**	**4**	
21	**0814**	**Heat shock protein 75 kDa, mitochondrial precursor**	**TRAP1**	**2**	**0.00243**
22	0855	Serum albumin	ALB	17	0.0128
23	**0871**	**Serum albumin**	**ALB**	**4**	**0.00162**
24	**0874**	**Serum albumin**	**ALB**	**24**	**0.0000141**
25	**0876**	**Serum albumin**	**ALB**	**17**	**0.0000289**
26	**0877**	**Serum albumin**	**ALB**	**4**	**0.00613**
27	0882	Serum albumin	ALB	3	0.024
		Succinate dehydrogenase [ubiquinone] flavoprotein subunit, mitochondrial	SDHA	9	

gel ID figure 3.2	master number	Protein name	IPA symbol	# peptides identified	1-ANOVA
28	0902	Syntaxin-binding protein 1	STXBP1	9	0.0192
		WD repeat-containing protein 1	WDR1	2	
29	0912	WD repeat-containing protein 1	WDR1	5	0.0104
30	0951	Serum albumin	ALB	11	0.0174
		Dihydropyrimidinase-related protein 2	DPYSL2	2	
		Selenium-binding protein 1	SELENBP1	2	
31	**0972**	**Dihydropyrimidinase-related protein 2**	**DPYSL2**	**12**	**0.00351**
		Leukotriene A4 hydrolase	**LTA4H**	**2**	
32	0990	Dihydropyrimidinase-related protein 2	DPYSL2	2	0.0476
33	**1063**	**alanyl-tRNA synthetase**	**AARS**	**3**	**0.00776**
		Dihydropyrimidinase-related protein 2	**DPYSL2**	**3**	
		Dihydropyrimidinase-related protein 3	**DPYSL3**	**2**	
34	**1088**	**Dihydropyrimidinase-related protein 2**	**DPYSL2**	**3**	**0.00951**
		Dihydropyrimidinase-related protein 3	**DPYSL3**	**2**	
35	**1089**	**Dihydropyrimidinase-related protein 2**	**DPYSL2**	**4**	**0.000767**
36	**1090**	**Serum albumin**	**ALB**	**6**	**0.000137**
		Dihydropyrimidinase-related protein 2	**DPYSL2**	**3**	
37	**1092**	**Dihydropyrimidinase-related protein 3**	**DPYSL3**	**7**	**0.00814**
38	**1135**	**Isoform M2 of Pyruvate kinase isozymes M1/M2**	**PKM2**	**16**	**0.000318**

gel ID figure 3.2	master number	Protein name	IPA symbol	# peptides identified	1-ANOVA
39	**1149**	**Protein disulfide-isomerase A3**	**PDIA3**	**6**	**0.00597**
		Tubulin alpha-1A chain	**TUBB1**	**2**	
40	**1188**	**Dihydropyrimidinase-related protein 2**	**DPYSL2**	**7**	**0.00788**
		Tubulin alpha-1A chain	**TUBB1**	**3**	
41	1190	Dihydropyrimidinase-related protein 2	DPYSL2	6	0.012
42	1198	Tubulin beta-3 chain	TUBB3	2	0.0201
43	**1242**	**Cytosol aminopeptidase**	**LAP3**	**15**	**0.00527**
44	1276	Tubulin alpha-1A chain	TUBA1A	2	0.0209
		Tubulin beta-2A chain	TUBB2A	12	
45	**1297**	**Septin-8**	**SEPT8**	**4**	**0.00818**
		Tubulin beta-2A chain	**TUBB2A**	**10**	
46	**1316**	**dihydrolipoamide dehydrogenase**	**DLD**	**3**	**0.00642**
		Glutamate dehydrogenase 1, mitochondrial	**GLUD1**	**10**	
47	**1331**	**Glutamate dehydrogenase 1, mitochondrial**	**GLUD1**	**16**	**0.00261**
48	**1338**	**V-type proton ATPase subunit B, brain isoform**	**ATP6V1B2**	**3**	**0.00184**
49	**1357**	**Tubulin alpha-1A chain**	**TUBA1A**	**2**	**0.00451**
50	1358	Dihydrolipoyllysine-residue succinyltransferase component of 2-oxoglutarate dehydrogenase complex, mitochondrial	DLST	4	0.0471
51	**1397**	**Glial fibrillary acidic protein**	**GFAP**	**6**	**0.00025**

gel ID figure 3.2	master number	Protein name	IPA symbol	# peptides identified	1-ANOVA
52	**1407**	**Glial fibrillary acidic protein**	**GFAP**	**20**	**0.00125**
		Neurofilament light polypeptide	**NEFL**	**2**	
53	1408	Glial fibrillary acidic protein	GFAP	12	0.0191
54	**1428**	**Succinate-semialdehyde dehydrogenase, mitochondrial**	**ALDH5A1**	**13**	**0.00761**
		Septin-11	**SEPT11**	**4**	
55	1437	4-aminobutyrate aminotransferase, mitochondrial	ABAT	5	0.0142
56	**1439**	**4-aminobutyrate aminotransferase, mitochondrial**	**ABAT**	**5**	**0.000524**
57	**1464**	**Actin-related protein 3**	**ACTR3**	**8**	**0.00171**
		Neurofilament heavy polypeptide	**NEFH**	**2**	
58	1556	Interferon gamma inducible protein 47	IFI47	6	0.018
59	1638	Glial fibrillary acidic protein	GFAP	3	0.0124
		NADH dehydrogenase [ubiquinone] iron-sulfur protein 2, mitochondrial	NDUFS2	6	
60	**1656**	**2',3'-cyclic-nucleotide 3'-phosphodiesterase**	**CNP**	**9**	**0.00983**
61	**1685**	**2',3'-cyclic-nucleotide 3'-phosphodiesterase**	**CNP**	**6**	**0.00993**
62	**1765**	**Actin, cytoplasmic**	**ACTB**	**7**	**0.006**
63	**1781**	**Actin, cytoplasmic**	**ACTB**	**7**	**0.000386**
64	**1782**	**Actin, cytoplasmic**	**ACTB**	**13**	**0.000614**
65	**1783**	**Actin, cytoplasmic**	**ACTB**	**5**	**0.00258**
66	**1789**	**Actin, cytoplasmic**	**ACTB**	**6**	**0.0000701**

gel ID figure 3.2	master number	Protein name	IPA symbol	# peptides identified	1-ANOVA
67	**1790**	**Actin, cytoplasmic**	**ACTB**	**7**	**0.00542**
68	**1862**	**Septin-2**	**SEPT2**	**3**	**0.00136**
69	**1888**	**Leukocyte elastase inhibitor A**	**SERPINB1**	**3**	**0.00348**
70	**1906**	**Macrophage-capping protein**	**CAPG**	**4**	**0.0000308**
		Septin-2	**SEPT2**	**3**	
		Septin-5	**SEPT5**	**2**	
71	**1944**	**Aspartate aminotransferase, cytoplasmic**	**GOT1**	**8**	**0.00122**
72	2113	Guanine nucleotide-binding protein G(o) subunit alpha	GNAO1	7	0.0151
73	**2139**	**Isocitrate dehydrogenase [NAD] subunit alpha, mitochondrial**	**IDH3A**	**7**	**0.00537**
74	**2314**	**L-lactate dehydrogenase B chain**	**LDHB**	**4**	**0.000488**
75	2321	L-lactate dehydrogenase B chain	LDHB	10	0.0314
76	2334	L-lactate dehydrogenase B chain	LDHB	2	0.0367
77	**2373**	**L-lactate dehydrogenase B chain**	**LDHB**	**8**	**0.00312**
		Malate dehydrogenase, cytoplasmic	**MDH1**	**3**	
78	**2380**	**Isocitrate dehydrogenase [NAD] subunit alpha, mitochondrial**	**IDH3A**	**4**	**0.00393**
79	2412	Guanine nucleotide-binding protein G(I)/G(S)/G(T) subunit beta-1	GNB1	5	0.0237
80	**2543**	**Malate dehydrogenase, cytoplasmic**	**MDH1**	**2**	**0.00724**
81	**2545**	**Annexin A3**	**ANXA3**	**2**	**0.0000476**
		Malate dehydrogenase, cytoplasmic	**MDH1**	**7**	

gel ID figure 3.2	master number	Protein name	IPA symbol	# peptides identified	1-ANOVA
82	**2557**	**Beta-soluble NSF attachment protein**	**NAPB**	**8**	**0.00386**
83	**2564**	**Beta-soluble NSF attachment protein**	**NAPB**	**10**	**0.00966**
84	2629	Alpha-soluble NSF attachment protein	NAPA	10	0.0257
85	**2692**	**Annexin A4**	**ANXA4**	**4**	**0.00731**
86	2738	alpha-enolase	ENO1	2	0.0231
87	**2899**	**Chloride intracellular channel protein 1**	**CLIC1**	**4**	**0.00246**
		Phospholysine phosphohistidine inorganic pyrophosphate phosphatase	**LHPP**	**4**	
88	**2903**	**Serum albumin**	**ALB**	**2**	**0.00234**
		Neurofilament light polypeptide	**NEFL**	**5**	
		Prohibitin	**PHB**	**4**	
		Proteasome activator complex subunit 2	**PSME2**	**2**	
89	**2979**	**Dihydropyrimidinase-related protein 2**	**DPYSL2**	**2**	**0.005**
		Proteasome activator complex subunit 1	**PSME1**	**2**	
90	**3103**	**Phosphoglycerate mutase 1**	**PGAM1**	**8**	**0.000863**
91	3234	similar to desmoplakin	DSP	9	0.0441
		Junction plakoglobin	JUP	2	
92	**3319**	**Peroxiredoxin-6**	**PRDX6**	**7**	**0.00455**

Table S3.2. Cluster analysis

gel ID figure 3.2	Spot master number	IPA symbol	1-ANOVA	Av. Ratio C vs O	T-test C vs O	Av. Ratio C vs T	T-test C vs T	Av. Ratio C vs R	T-test C vs R	Av. Ratio O vs T	T-test O vs T	Av. Ratio O vs R	T-test O vs R	Av. Ratio T vs R	T-test T vs R
Cluster 1, q:87.1															
23	871	ALB	0.00162	1.21	0.436	13.62	0.000381	9.55	0.0359	11.23	0.00117	7.87	0.0514	-1.43	0.419
24	0874	ALB	0.0000141	1.2	0.462	41.55	0.000356	28.08	0.00236	34.67	0.000214	23.43	0.00223	-1.48	0.371
25	0876	ALB	0.0000289	-1.14	0.487	16.9	0.000389	11.74	0.00437	19.35	0.000256	13.44	0.00329	-1.44	0.37
26	0877	ALB	0.00613	-1.25	0.775	6.31	0.0127	4.67	0.0703	7.89	0.00366	5.85	0.0376	-1.35	0.454
86	2738	ENO1	0.0231	1.12	0.95	5.55	1.67E-03	3.36	0.0653	4.95	0.0426	3	0.0816	-1.65	0.237
Cluster 2, q:92.4															
10	0581	ACO2 TF	0.000884	1.13	0.185	3.97	0.000746	2.95	0.0259	3.5	0.00124	2.6	0.0398	-1.35	0.331
81	2545	ANXA3 MDH1	0.0000476	1.22	0.496	2.77	0.000517	5.5	0.000425	2.28	0.0137	4.53	0.00302	1.99	0.00935
Cluster 3, q:96.9															
78	2380	IDH3A	0.00393	1.12	0.461	1.78	0.0383	2.12	0.0215	1.58	0.00578	1.89	0.00508	1.19	0.278
88	2903	ALB NEFL PHB PSME2	0.00234	-1.05	0.776	1.84	0.0137	2.29	0.0175	1.93	0.00789	2.4	0.0127	1.25	0.382
89	2979	DPYSL2 PSME1	0.005	-1.04	0.954	1.75	0.061	2.15	0.0211	1.83	0.018	2.24	0.00428	1.23	0.18

gel ID figure 3.2	Spot master number	IPA symbol	1-ANOVA	Av. Ratio C vs O	T-test C vs O	Av. Ratio C vs T	T-test C vs T	Av. Ratio C vs R	T-test C vs R	Av. Ratio O vs T	T-test O vs T	Av. Ratio O vs R	T-test O vs R	Av. Ratio T vs R	T-test T vs R
Cluster 4, q:93															
51	1397	GFAP	0.00025	1.09	0.408	1.39	0.00365	1.76	0.000977	1.27	0.0397	1.61	0.00588	1.27	0.0142
52	1407	GFAP	0.00125	1.06	0.547	1.27	0.018	1.54	0.00276	1.2	0.0754	1.46	0.00949	1.21	0.0397
		NEFL													
53	1408	GFAP	0.0191	1.09	0.148	1.34	9.89E-03	1.53	0.0427	1.23	0.0304	1.41	0.0793	1.14	0.46
80	2543	MDH1	0.00724	-1.02	0.848	1.26	0.0416	1.87	0.0189	1.28	0.103	1.91	0.0268	1.49	0.0623
Cluster 5, q:96.7															
8	0562	ACO2	0.000557	1.06	0.426	2.56	0.000911	2.02	0.0207	2.43	0.00135	1.91	0.0283	-1.27	0.274
		TF													
12	0599	ACO2	0.00226	1.02	0.688	2.5	0.00274	1.95	0.0447	2.46	0.00287	1.92	0.0481	-1.28	0.34
		PFKP													
		TF													
22	0855	ALB	0.0128	-1.29	0.529	2.43	0.0364	1.48	0.291	3.14	2.24E-03	1.91	0.0564	-1.65	0.117
36	1090	ALB	0.000137	-1.14	0.582	3.22	0.0033	2.12	0.0241	3.67	0.000163	2.41	0.00331	-1.52	0.0505
		DPYSL2													
Cluster 6, q:91.2															
19	0742	IMMT	0.00425	-1.04	0.691	1.8	0.011	1.64	0.0496	1.87	0.00625	1.71	0.0162	-1.1	0.527
30	0951	ALB	0.0174	1.05	0.672	2.3	0.0269	1.91	0.0662	2.19	0.0287	1.82	0.0751	-1.2	0.625
		DPYSL2													
		SELENBP1													

gel ID figure 3.2	Spot master number	IPA symbol	1-ANOVA	Av. Ratio C vs O	T-test C vs O	Av. Ratio C vs T	T-test C vs T	Av. Ratio C vs R	T-test C vs R	Av. Ratio O vs T	T-test O vs T	Av. Ratio O vs R	T-test O vs R	Av. Ratio T vs R	T-test T vs R
Cluster 6, q:91.2 (continued)															
35	1089	DPYSL2	0.000767	1.02	0.901	2.03	0.00313	1.5	0.0215	1.99	0.0047	1.46	0.0327	-1.36	0.0163
87	2899	CLIC1 LHPP	0.00246	-1.58	0.119	1.84	0.0314	1.37	0.255	2.92	0.00037	2.16	0.0124	-1.35	0.106
Cluster 7, q:97.8															
27	0882	ALB SDHA	0.024	-1.01	0.984	1.58	0.0695	1.51	0.0423	1.59	0.0482	1.52	0.0195	-1.04	0.87
39	1149	PDIA3 TUBB1	0.00597	1.03	0.808	1.41	0.023	1.56	0.0281	1.37	0.01	1.52	0.0213	1.11	0.383
63	1781	ACTB	0.000386	-1.07	0.473	1.44	0.0135	1.47	0.0132	1.54	0.000944	1.57	0.00128	1.02	0.811
66	1789	ACTB	0.0000701	1.02	0.753	1.45	0.00219	1.61	0.00014	1.42	0.0101	1.57	0.00216	1.11	0.161
69	1888	SERPINB1	0.00348	-1.08	0.45	1.43	0.0294	1.5	0.0111	1.55	0.0214	1.62	0.00966	1.05	0.698
Cluster 8, q:91.4															
17	0683	THOP1	0.00929	1.01	0.881	1.29	0.0229	1.33	0.0444	1.28	0.00743	1.32	0.0309	1.03	0.721
20	0761	EEF1A1 GARS LOC674678	0.00283	1.09	0.33	1.29	0.0233	1.41	0.00651	1.18	0.0609	1.29	0.0118	1.09	0.104
57	1464	ACTR3 NEFH	0.00171	1.02	0.727	1.22	0.0278	1.26	0.013	1.2	0.0078	1.23	0.00119	1.03	0.526
85	2692	ANXA4	0.00731	1.02	0.711	1.2	0.0164	1.22	0.0239	1.18	0.0231	1.19	0.0331	1.01	0.768

gel ID figure 3.2	Spot master number	IPA symbol	1-ANOVA	Av. Ratio C vs O	T-test C vs O	Av. Ratio C vs T	T-test C vs T	Av. Ratio C vs R	T-test C vs R	Av. Ratio O vs T	T-test O vs T	Av. Ratio O vs R	T-test O vs R	Av. Ratio T vs R	T-test T vs R
Cluster 9, q:86.1															
6	0558	DNM1	0.00106	1.03	0.847	-1.65	0.000934	-1.32	0.0179	-1.69	0.00712	-1.36	0.0539	1.24	0.0579
16	0676	DSP	0.00059	1.09	0.0123	1.93	0.000987	1.48	0.031	1.77	0.00154	1.36	0.0641	-1.3	0.118
58	1556	IFI47	0.018	1.03	0.84	1.91	0.065	1.84	0.0104	1.85	0.0754	1.79	0.013	-1.04	0.999
74	2314	LDHB	0.000488	1.15	0.298	2.56	0.000313	1.61	0.0391	2.23	0.00203	1.4	0.131	-1.59	0.0339
Cluster 10, q:94.2															
2	0499	ATP5B	0.00313	1.02	0.704	1.47	0.0133	1.32	0.0245	1.45	0.0115	1.3	0.0206	-1.11	0.373
13	0606	PFKP	0.00887	1.01	0.877	1.33	0.0283	1.22	0.0179	1.31	0.0334	1.21	0.0243	-1.09	0.379
14	0619	ACO2 PFKP	0.00453	-1.06	0.424	1.44	0.0226	1.3	0.0291	1.52	0.0147	1.37	0.0165	-1.11	0.403
18	0700	HSPA12A	0.00811	-1.05	0.52	1.25	0.0322	1.29	0.0418	1.32	0.0139	1.36	0.0212	1.03	0.754
Cluster 11, q:95.6															
29	0912	WDR1	0.0104	-1.12	0.0774	1	0.999	1.13	0.0451	1.13	0.111	1.28	0.0169	1.13	0.0765
43	1242	LAP3	0.00527	-1.11	0.15	1.07	0.213	1.11	0.0975	1.19	0.00636	1.23	0.00416	1.04	0.127
Cluster 13, q:78.1															
1	0377	EEF2	0.00494	-1	0.984	1.55	0.0675	1.29	0.0689	1.56	0.00809	1.3	0.0104	-1.2	0.158
4	0521	DDX1	0.00636	-1.04	0.225	1.37	0.046	1.23	0.0000662	1.43	0.0347	1.27	0.00105	-1.12	0.391
15	0674	HSP4A	0.00286	1.16	0.243	1.66	0.00742	1.5	0.00775	1.43	0.0305	1.3	0.0472	-1.1	0.35
33	1063	AARS DPYSL2	0.00776	-1.03	0.723	1.84	0.0399	-1.07	0.483	1.89	0.0347	-1.04	0.677	-1.97	0.0313

gel ID figure 3.2	Spot master number	IPA symbol	1-ANOVA	Av. Ratio C vs O	T-test C vs O	Av. Ratio C vs T	T-test C vs T	Av. Ratio C vs R	T-test C vs R	Av. Ratio O vs T	T-test O vs T	Av. Ratio O vs R	T-test O vs R	Av. Ratio T vs R	T-test T vs R
Cluster 13, q:78.1 (continued)															
33	1063	DPYSL3	0.00776	-1.03	0.723	1.84	0.0399	-1.07	0.483	1.89	0.0347	-1.04	0.677	-1.97	0.0313
34	1088	DPYSL2 DPYSL3	0.00951	-1.04	0.678	1.56	0.0148	1.34	0.0648	1.62	0.017	1.39	0.0627	-1.17	0.321
37	1092	DPYSL3	0.00814	-1.02	0.685	1.37	0.0242	1.25	0.0322	1.41	0.0227	1.28	0.0307	-1.1	0.424
62	1765	ACTB	0.006	-1.19	0.11	1.48	0.0531	1.32	0.0766	1.75	0.0105	1.56	0.00813	-1.12	0.498
65	1783	ACTB	0.00258	1.05	0.287	1.4	0.00457	1.3	0.0368	1.33	0.00285	1.23	0.0495	-1.08	0.374
67	1790	ACTB	0.00542	-1.07	0.287	1.3	0.0164	1.2	0.098	1.39	0.00338	1.28	0.0306	-1.08	0.4
70	1906	CAPG SEPT2 SEPT5	0.0000308	-1.06	0.0388	1.37	0.00283	1.43	0.00163	1.45	0.00123	1.51	0.000731	1.04	0.562
Cluster 14, q:79.3															
3	0516	PTPN1	0.0277	1.01	0.892	1.26	0.0312	1.15	7.31E-04	1.24	0.0823	1.13	0.122	-1.1	0.259
28	0902	STXBP1 WDR1	0.0192	-1.11	0.0688	1.04	0.345	1.06	0.26	1.15	0.0191	1.17	0.0243	1.02	0.651
38	1135	PKM2	0.000318	1.04	0.35	1.27	0.00176	1.14	0.0192	1.23	0.0025	1.1	0.0431	-1.12	0.0236
64	1782	ACTB	0.000614	1.01	0.812	1.2	0.0123	1.32	0.000756	1.18	0.04	1.31	0.00511	1.11	0.0764
68	1862	SEPT2	0.00136	-1.07	0.0193	1.13	0.0266	1.1	0.0501	1.21	0.00358	1.18	0.00563	-1.02	0.619
Cluster 15, q:20.7															
50	1358	DLST	0.0471	-1.05	0.096	-1.12	0.0625	-1.14	0.0162	-1.06	0.27	-1.08	0.108	-1.02	0.767

gel ID figure 3.2	Spot master number	IPA symbol	1-ANOVA	Av. Ratio C vs O	T-test C vs O	Av. Ratio C vs T	T-test C vs T	Av. Ratio C vs R	T-test C vs R	Av. Ratio O vs T	T-test O vs T	Av. Ratio O vs R	T-test O vs R	Av. Ratio T vs R	T-test T vs R
Cluster 15, q:20.7 (continued)															
60	1656	CNP	0.00983	1.04	0.608	-1.28	0.00766	-1.09	0.235	-1.33	0.0118	-1.13	0.177	1.17	0.0767
76	2334	LDHB	0.0367	-1.16	0.162	-1.08	0.48	-1.29	0.0548	1.08	0.0984	-1.11	0.101	-1.2	0.026
79	2412	GNB1	0.0237	-1.01	0.807	-1.14	0.0145	-1.02	0.697	-1.13	4.10E-03	-1.01	0.758	1.12	0.0759
90	3103	PGAM1	0.000863	-1.08	0.0561	-1.18	0.00546	-1.19	0.00941	-1.09	0.00371	-1.11	0.0203	-1.02	0.598
91	3234	DSP	0.0441	1.63	0.0348	1.09	0.464	1.44	0.0507	-1.5	0.0852	-1.13	0.578	1.33	0.148
		JUP													
92	3319	PRDX6	0.00455	-1.04	0.32	-1.05	0.228	-1.22	0.0131	-1.01	0.761	-1.16	0.0186	-1.15	0.0208
Cluster 16, q:70.4															
5	0545	HSP90AA1	0.044	1.33	0.295	-1.81	0.103	-1.33	0.0738	-2.42	0.0642	-1.78	0.0651	1.36	0.287
11	0588	ACO2	0.0019	1.02	0.841	1.78	0.0104	1.45	0.0396	1.75	0.00397	1.43	0.0175	-1.23	0.125
		HSPD1													
		PKM2													
		TUBB													
7	0560	DNM1	0.000783	1.09	0.401	-1.37	0.0000314	-1.23	0.00143	-1.49	0.00936	-1.33	0.0312	1.12	0.0142
9	0566	TF	0.00954	1.07	0.623	-1.28	0.00298	-1.27	0.000729	-1.37	0.0522	-1.36	0.0515	1.01	0.843
21	0814	TRAP1	0.00243	-1.06	0.595	-1.41	0.0148	-1.56	0.00244	-1.33	0.0541	-1.48	0.0136	-1.11	0.221
31	0972	DPYSL2	0.00351	-1.14	0.117	-1.51	0.00422	-1.39	0.0309	-1.33	0.00608	-1.22	0.0892	1.09	0.44
		LTA4H													
32	0990	DPYSL2	0.0476	-1.08	0.542	-1.44	3.83E-03	-1.19	0.073	-1.33	0.113	-1.1	0.598	1.21	0.0426

gel ID figure 3.2	Spot master number	IPA symbol	1-ANOVA	Av. Ratio C vs O	T-test C vs O	Av. Ratio C vs T	T-test C vs T	Av. Ratio C vs R	T-test C vs R	Av. Ratio O vs T	T-test O vs T	Av. Ratio O vs R	T-test O vs R	Av. Ratio T vs R	T-test T vs R
Cluster 16, q:70.4 (continued)															
40	1188	DPYSL2 TUBB1	0.00788	1.03	0.832	-1.43	0.0223	-1.36	0.0385	-1.46	0.0162	-1.4	0.0279	1.05	0.622
41	1190	DPYSL2	0.012	-1.03	0.747	-1.47	0.013	-1.36	0.033	-1.43	0.0316	-1.32	0.0726	1.08	0.536
42	1198	TUBB3	0.0201	-1.04	0.545	-1.35	0.0166	-1.15	0.113	-1.3	0.0601	-1.11	0.253	1.17	0.178
44	1276	TUBA1A TUBB2A	0.0209	-1.12	0.149	-1.28	0.0453	-1.23	0.0222	-1.14	0.128	-1.1	0.0372	1.03	0.601
45	1297	SEPT8 TUBB2A	0.00818	-1.1	0.0375	-1.3	0.00558	-1.21	0.0467	-1.18	0.0183	-1.1	0.202	1.08	0.392
46	1316	DLD GLUD1	0.00642	-1.06	0.276	-1.28	0.082	-1.28	0.000172	-1.2	0.0866	-1.21	0.00756	-1	0.98
47	1331	GLUD1	0.00261	-1.04	0.572	-1.28	0.0221	-1.39	0.016	-1.23	0.00854	-1.33	0.0101	-1.09	0.276
48	1338	ATP6V1B2	0.00184	1.01	0.883	-1.27	0.033	-1.31	0.0125	-1.28	0.0102	-1.32	0.00112	-1.03	0.663
49	1357	TUBA1A	0.00451	-1.05	0.444	-1.28	0.0605	-1.42	0.00736	-1.21	0.0626	-1.34	0.00178	-1.11	0.32
54	1428	ALDH5A1 SEPT11	0.00761	-1.05	0.371	-1.27	0.0259	-1.24	0.00403	-1.21	0.0631	-1.18	0.0205	1.02	0.69
55	1437	ABAT	0.0142	1.01	0.945	-1.42	0.0254	-1.26	0.0936	-1.43	0.0153	-1.26	0.0621	1.13	0.196
56	1439	ABAT	0.000524	-1.11	0.155	-1.44	0.00117	-1.26	0.0165	-1.3	0.00354	-1.14	0.0856	1.14	0.0372
59	1638	GFAP NDUFS2	0.0124	-1.06	0.577	-1.67	0.0175	-1.26	0.11	-1.58	0.0206	-1.19	0.174	1.33	0.0796

gel ID figure 3.2	Spot master number	IPA symbol	1-ANOVA	Av. Ratio C vs O	T-test C vs O	Av. Ratio C vs T	T-test C vs T	Av. Ratio C vs R	T-test C vs R	Av. Ratio O vs T	T-test O vs T	Av. Ratio O vs R	T-test O vs R	Av. Ratio T vs R	T-test T vs R
Cluster 16, q:70.4 (continued)															
61	1685	CNP	0.00993	-1.02	0.722	-1.36	0.0227	-1.16	0.0121	-1.33	0.0424	-1.13	0.1	1.18	0.11
71	1944	GOT1	0.00122	-1.07	0.132	-1.28	0.00251	-1.18	0.0101	-1.2	0.0138	-1.11	0.0781	1.08	0.147
72	2113	GNAO1	0.0151	-1.03	0.761	-1.36	0.0443	-1	0.986	-1.33	0.0315	1.02	0.699	1.36	0.0327
73	2139	IDH3A	0.00537	-1.05	0.327	-1.27	0.000484	-1.16	0.0234	-1.2	0.0286	-1.1	0.226	1.09	0.123
75	2321	LDHB	0.0314	1.05	0.445	-1.2	0.0424	-1.14	0.195	-1.26	8.75E-03	-1.19	0.0756	1.06	0.552
77	2373	LDHB	0.00312	1.03	0.564	-1.21	0.0021	-1.09	0.123	-1.24	0.00422	-1.12	0.0928	1.11	0.0733
		MDH1													
82	2557	NAPB	0.00386	-1.12	0.142	-1.38	0.00496	-1.26	0.0437	-1.24	0.0029	-1.13	0.126	1.09	0.254
83	2564	NAPB	0.00966	-1.03	0.599	-1.19	0.0154	-1.17	0.0186	-1.16	0.0407	-1.13	0.0549	1.02	0.587
84	2629	NAPA	0.0257	-1.04	0.521	-1.16	0.151	-1.26	9.41E-03	-1.12	0.198	-1.21	1.89E-03	-1.08	0.387

Table S3.3. IPA networks

75 unique proteins	networks		
	DLG4/KCNMA1	APP/ACTB	AGT
AARS			
ABAT			
ACO2	x		
ACTB	x	x	x
ACTR3	x		
ALB	x	x	x
ALDH5A1	x		
ANXA3	x		x
ANXA4		x	x
ATP5B	x	x	x
ATP6V1B2	x		
CAPG	x		
CLIC1		x	x
CNP	x		
DDX1	x		x
DLD	x	x	x
DLST		x	x
DNM1	x	x	x
DPYSL2	x	x	x
DPYSL3			
DSP		x	x
EEF1A1	x	x	x
EEF2			x
ENO1	x	x	x
GARS			
GFAP	x	x	x
GLUD1	x		
GNAO1	x	x	x
GNB1	x	x	x
GOT1	x		
HSP4A		x	x
HSP90AA1	x	x	x
HSPA12A	x		
HSPD1	x	x	x
IDH3A	x		
IFI47			
IMMT	x		
JUP		x	x
LAP3	x		
LDHB	x		
LHPP			
LOC674678			
LTA4H			
MDH1			
NAPA	x		
NAPB	x		

75 unique proteins	networks		
	DLG4/KCNMA1	APP/ACTB	AGT
NDUFS2	x	x	x
NEFH	x	x	x
NEFL	x	x	x
PDIA3	x	x	x
PFKP	x	x	
PGAM1	x	x	
PHB	x	x	x
PKM2	x		
PRDX6			
PSME1		x	x
PSME2		x	x
PTPN1	x	x	x
SDHA	x		x
SELENBP1			
SEPT11	x	x	x
SEPT2	x	x	x
SEPT5	x	x	x
SEPT8		x	x
SERPINB1			
STXBP1	x	x	
TF	x	x	x
THOP1		x	x
TRAP1			
TUBA1A	x	x	x
TUBB	x	x	x
TUBB1			
TUBB2A	x	x	x
TUBB3		x	x
WDR1			x

4

CRMP2 EXPRESSION IN MS RELATED IMMUNE CELL SUBSETS

ABSTRACT

Collapsin-response mediator protein 2 (CRMP2) is a member of the collapsin-response mediator protein family. This family of proteins is involved in brain development, neuronal guidance, neurite-axon differentiation and growth-cone collapse. CRMP2 was identified in 10 differential protein spots in the 2D-DIGE study of EAE brainstem (chapter 3). These spots represent different isoforms, post-translational modifications and/or breakdown products of the protein. Some of these spots were upregulated during EAE, while others were down regulated. CRMP2 was previously identified as a downstream molecule of the Nogo-A pathway and suggested to be involved in the axonopathy of EAE. Here, we propose that CRMP2 is also involved in the MS pathogenesis by affecting the immunological aspect of the disease. Indeed, CRMP2 was shown to be involved in T cell migration during viral infections. In this study, we show that CRMP2 expression levels are higher in $CD4^+$ T cells compared to $CD8^+$ T cells. Within the $CD4^+$ T cell subtypes, CRMP2 expression was higher in regulatory subtypes compared to conventional subtypes related to an elevation in the memory T cell compartment. The percentage of CRMP2 positive cells is even higher in monocytes compared to T cells. Monocyte subsets also show differences in CRMP2 expression, with the highest expression levels in the intermediate monocytes, the lowest expression in non-classical monocytes. A decrease in CRMP2 expression was seen in immune-cell subsets of MS patients when compared to controls. These findings suggest that CRMP2 is also involved in the immune-cell infiltration process into the CNS, and not only in the neuronal part of the pathogenesis.

4.1 Introduction

One of the identified proteins in the EAE 2D-DIGE study (Chapter 3) is dihydropyrimidinase-related protein 2 (DPYSL2) or collapsin-response mediator protein 2 (CRMP2). CRMP2 is a member of the collapsin-response mediator protein family, which consists of phosphoproteins CRMP1-5 (171). These proteins are involved in the development of the brain, mainly in neurite-axon differentiation. They are also involved in facilitation of neuronal guidance, growth and polarity, and growth cone collapse (172). CRMP2 binds and stabilizes tubulin at the positive end of the microtubules (173). Expression of CRMP2 is mostly found in the plastic areas of the brain, such as the hippocampus (174).

CRMP2 phosphorylation is known to cause a decrease in tubulin and actin stability, leading to growth cone collapse and axonal retraction (175-180). Semaphorin 3A mediated growth cone collapse for example (171, 181), semaphorin 3A (sema3A) is an acknowledged inhibitory signaling molecule for axonal outgrowth and promotes growth of apical dendrites. It activates GSK3β, a kinase that phosphorylates CRMP2 at Thr509 and Thr514. This double phosphorylation inhibits the binding of CRMP2 to kinesin 1, a microtubule motor protein, thereby limiting microtubule growth and thus resulting in axonal retraction (179, 180, 182-184).

In MS, CRMP2 is speculated to be involved as a downstream molecule in the Nogo-A-pathway. Nogo-A is an axonal growth inhibitor possibly involved in neurodegeneration during MS. When Nogo-A is inhibited or its receptor, Nogo-66 receptor 1 (NgR1), is blocked, a reduced EAE progression was observed (112). Binding of Nogo-A to NgR1 results in the phosphorylation of CRMP2 at Thr555. This phosphorylation inhibits axonal growth and thereby hampers neuroregeneration. It has been shown that NgR1 deletion results in a reduced amount of PThr555-CRMP2, reduced EAE symptoms and a delayed EAE onset (112).

In addition, CRMP2 was reported to be involved in T cell proliferation and migration in the context of viral infections (185). CXCL12, a chemokine associated with certain viral infections, is responsible for modifications in CRMP2 expressed by T cells. Binding of CXCL12 to the CXCR4 receptor on T cells activates Yes-kinase (phosphorylating CRMP2 at Tyr479) and inhibits GSK3β (inhibition of

PThr509/514 modification of CRMP2). These phosphorylation conditions lead to a more active form of CRMP2 that localizes to the uropod of the migrating T cell and assists in their proliferation and migration (113, 181, 185-187).

Based on the importance of CRMP2 in T cell migration during viral infections and the fact that CXCL12 is upregulated on the luminal side of de blood-brain barrier during MS (188-190), the role of CRMP2 in T cell migration during the MS disease course could be crucial. Therefore, we first investigated the expression of CRMP2 among different T cell subtypes in HC, followed by an exploration of its expression in healthy controls compared to MS-patients.

4.2 Materials and Methods

4.2.1 Study subjects

Peripheral blood samples were collected from 10 healthy controls (HC) and 10 patients with clinically definite RRMS by the University Biobank Limburg (UBiLim). Clinical data of MS patients and HC are summarised in Table 4.1. MS patients were untreated for at least three months at the time of sample collection and had a mean age of 47.8 years (range 24-69) and a mean EDSS disease score of 3.35 (range 1.5-6.5). This study was approved by the local Medical Ethical committee of Hasselt University and the Medical Ethical Committee of the University Hospital K.U.Leuven, an informed consent was obtained from all study subjects.

Table 4.1. Study subjects

	RRMS	HC
Mean age (range)[a]	47.8 (24-69)	29.8 (22-43)
Female/Male	10/0	10/0
Mean disease duration (range)[a]	7.37 (0.25-23.58)	-
Mean EDSS score (range)	3.35 (1.5-6.5)	-

[a] in years

4.2.2 Sample collection and preparation

For all donors included in this study, peripheral blood mononuclear cells (PBMC) were isolated from whole blood by density gradient centrifugation (Histopaque; Sigma-Aldrich, St. Louis, MO, USA). Cells were suspended in 10% DMSO in fetal bovine serum (FBS) at a concentration of 10 million cells/ml. Fractions of 2 ml were frozen at a cooling rate of approximately -1°C/minute (Mr. Frosty) for at least 24 hours at -80°C. Next, samples were transferred to liquid nitrogen. For this study, cells were thawed using 20% FBS in RPMI medium. Cells were rinsed, diluted in culture medium (RPMI, 10% FBS, 0.2% NaPyr, 0.2% NEAA) and kept on ice until used for flow cytometry staining.

4.2.3 Flow cytometry

To phenotype immune subsets, three flow cytometric staining panels were used. An overview of the panels is presented in table 4.2.

Table 4.2. Antibody panels flow cytometry

T cells	Th subsets	Monocyte subsets
CRMP2[a]	CRMP2[a]	CD16 FITC
CD127 PE	CD3 PE	HLA-DR PE
CD45RO PE-CF594	CXCR3 PE-CF594	
CD25 PERCP-Cy5.5	CCR6 PERCP-Cy5.5	CD14 PERCP
CD8 PE-Cy7	CD4 PE-Cy7	
CD4 APC	CCR4 Alexa 647	CRMP2[b]
CD45RA APC-H7	CD45RA APC-H7	

[a] an Alexa 488 or [b] an Alexa 647 secondary goat anti-rabbit antibody was used for staining.

A multi-step staining protocol was performed since CRMP2 is an intracellular protein, and the antibody to CRMP2 is not directly labeled. First, a surface stain was performed using antibodies to the extracellular molecules. Cells were then permeabilised using the Cytofix/Cytoperm kit (BD Biosciences). CRMP2 primary antibody (LSBio, LS-C154410) was added, followed by the matched secondary antibody, depending on the staining panel (see Table 4.2). This CRMP2 antibody binds to the C-terminus of the protein, staining all CRMP2 positive cells independent of PTMs. Stained samples were analysed by flow cytometry using a FACSAria II (BD Biosciences). Data processing was performed using the FACS Diva software (BD Biosciences).

4.2.4 Statistical analysis

Statistical analyses were performed using SAS JMP Pro 11. If distribution was normal, matched pairs comparison was performed to compare different cell types of the same sample group. A Bonferroni correction was performed if more than 2 cell types were compared. In case of a non-normal distribution, a Wilcoxon rank test was performed. To compare HC and RRMS for a given cell type, a 1way-ANOVA was performed for normal distribution or a Kruskal Wallis test for non-normal distribution. A p-value of less than 0.05 was considered significant. Results are expressed as mean values ± standard error of the mean (SEM).

4.3 Results

4.3.1 CRMP2 expression in EAE brainstem

CRMP2 was identified in 10 differential protein spots in our EAE 2D-DIGE study (spot 30-36, 40, 41 and 89, see figure 4.1, chapter 3 and supplemental table 1). Six spots were more intense during EAE while 4 spots were less intense during EAE. These protein spots are present on the 2D gel at different molecular weights, indicating different isoforms, but also a breakdown product (spot 89).

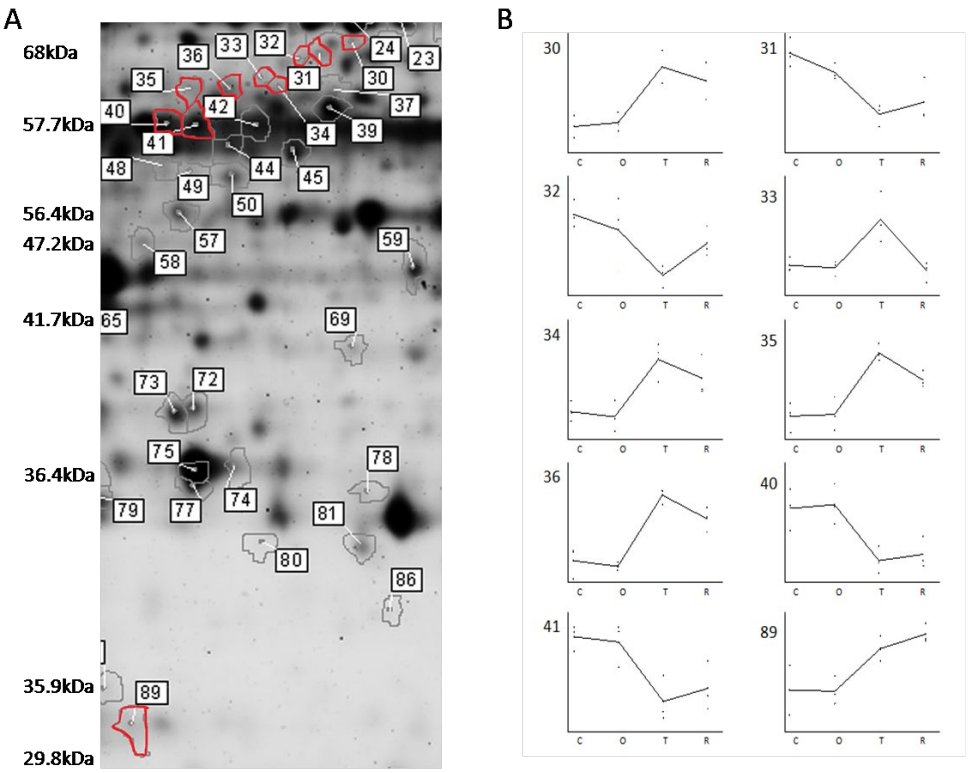

Figure 4.1. CRMP2 expression patterns. Gel overview (A) and expression pattern over time (B) of the spots containing CRMP2. (A) MW is indicated in the gel based on known identifications in the area. (B) Vertical axis distribution varies between the graphs. C: control, O: onset, T: top, R: recovery.

Different CRMP2 isoforms have been described, ranging from 58 to 66 kDa (113). In T cells, major attention has been given to the 58kDa and 62kDa isoforms (187). These could potentially be represented here by spots 40,41 and 33-36 respectively. These protein spots are at the same molecular weight (MW), but with a difference in pI. This could indicate post-translational modifications such as phosphorylation (171, 173). Phosphorylation causes a shift towards the acidic side (left), indicating that spot 40, 34-36 could be phosphorylated.

4.3.2 CRMP2 expression in immune-cell subsets

CRMP2 is involved in T cell migration during viral infections, and in the migration towards CXCL12, a chemokine that is upregulated on the luminal side of the BBB during MS (113, 185). Here we study the distribution of CRMP2 in different T cell and monocyte subsets in healthy controls and MS patients.

We first defined which immune-cell subsets express CRMP2. T cells are subdivided into $CD4^+$ T helper cells (Th) and $CD8^+$ cytotoxic T cells (Tcyt). Th cells are further subcategorised in two populations, conventional T cells (Tconv, $CD4^+CD25^{low}CD127^+$) and regulatory T cells (Treg, $CD4^+CD25^{hi}CD127^{low}$). These two populations are each subdivided in two additional categories, namely naïve and memory T cells ($CD4^+CD45RA^+$ and $CD4^+CD45RO^+$ respectively) (191-193). When naïve $CD4^+$ T cells encounter an antigen, they are activated and migrate towards the site of inflammation. Activation triggers these Th cells to differentiate into different Th subsets, namely Th1 ($CD3^+CD4^+CD45RA^-CXCR3^+$), Th2 ($CD3^+CD4^+CD45RA^-CXCR3^-CCR4^+CCR6^-$) and Th17 ($CD3^+CD4^+CD45RA^-CXCR3^-CCR6^+$) (193-198). Th1 and Th17 have been associated with autoimmune diseases, while Th2 is associated with allergies (199, 200).

Whenever necessary, circulating monocytes migrate into tissues to differentiate into macrophages based on the cytokines and growth factors at hand (201-203). There are 3 main groups of circulating monocytes. Classical monocytes ($CD14^+$HLA-DR^+CD16^-), intermediate ($CD14^+$HLA-DR^+CD16^+) and non-classical monocytes ($CD14^{low}$HLA-DR^+CD16^+) (201, 204-206). The classical monocytes are easily attracted to sites of inflammation and display a high potential for phagocytosis (203, 207). This population accounts for 80-90% of circulating monocytes. Intermediate monocytes express an array of pro-inflammatory

cytokines, while the non-classical monocytes are more anti-inflammatory and display a patrolling function (201).

Flow cytometric stainings were performed on PBMC of 10 healthy donors to investigate CRMP2 expression in the above mentioned immune cell subsets. Of $CD4^+$ T cells, 73.13±3.84% express CRMP2 while 56.30±3.93% of $CD8^+$ T cells and 95.92±0.67% of monocytes express it (Fig. 4.2A).

$CD4^+$ T cells express significantly higher levels of CRMP2 compared to cytotoxic $CD8^+$ T cells (Fig. 4.2B). Furthermore, Tregs express higher CRMP2 levels compared to Tconv. Memory T cells have a higher CRMP2 expression compared to their naïve counterparts, both in the conventional as well as in the regulatory population (Fig. 4.2D). Th subsets associated with pro-inflammatory functions, Th1 and Th17, show a lower expression of CRMP2 compared to their anti-inflammatory counterpart, the Th2 cells (Fig. 4.2F). For monocytes (Fig. 4.2H), the intermediate monocytes display the highest CRMP2 expression levels. The non-classical monocytes have the lowest CRMP2 expression and the lowest percentage of CRMP2 positive cells of all three monocyte subtypes.

Figure 4.2. CRMP2 expression in different immune cell subsets. The expression of CRMP2 in different immune cell subsets was measured by flow cytometry. Three staining panels enabled staining of different cell types in PBMC of 10 healthy controls. The percentage of CRMP2 positive cells (A/C/E/G) was plotted as well as the median fluorescence intensity (MFI), indicating the expression level of CRMP2 within the different populations (B/D/F/H) ±SEM. **: $p \leq 0.01$. Th: Thelper cells, Tconv: conventional T cells, Treg: regulatory T cells, nT cells: naïve T cells and mT cells: memory T cells.

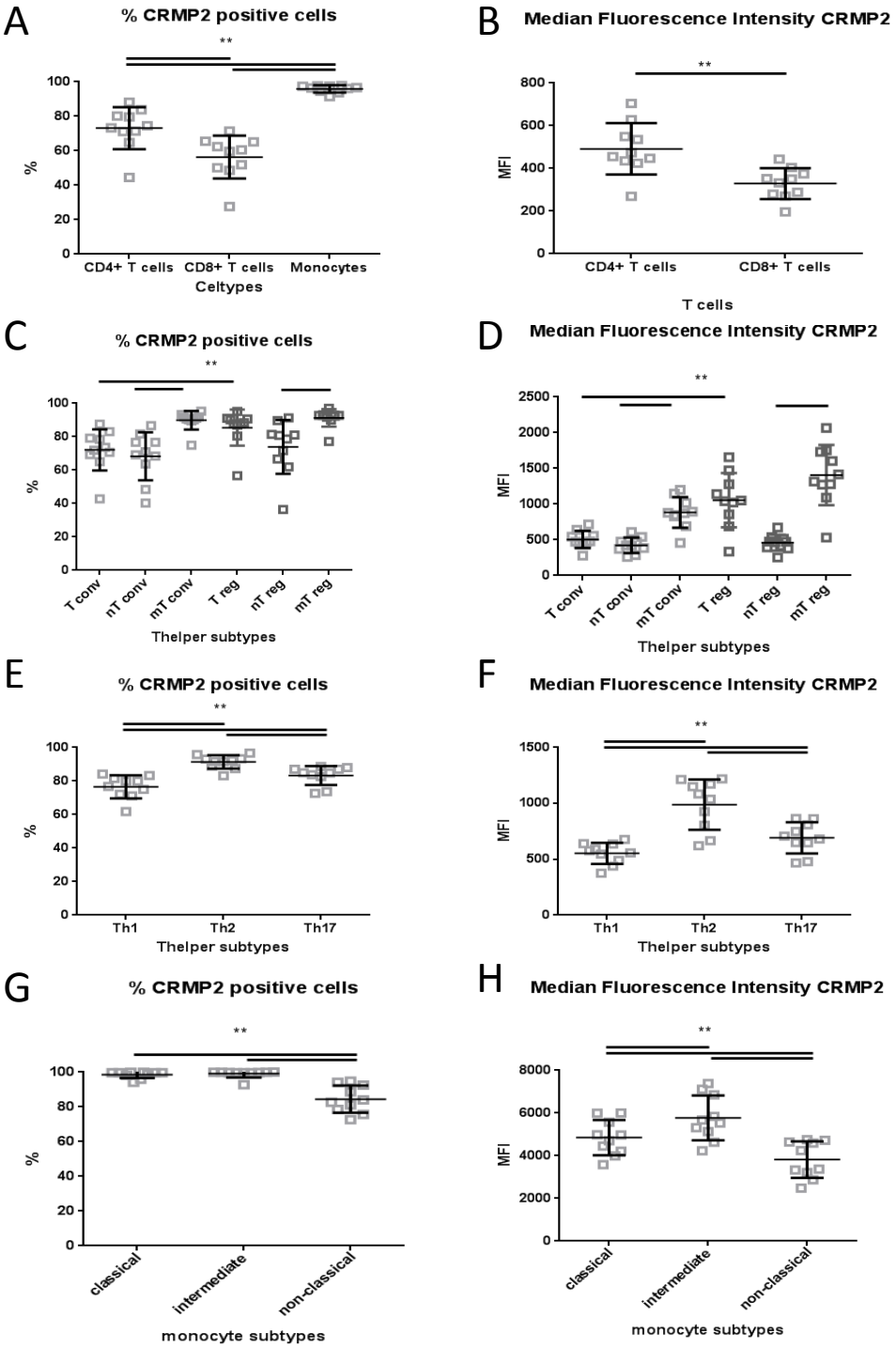
A
% CRMP2 positive cells
**
%
CD4+ T cells
CD8+ T cells
Monocytes
Celtypes
B
Median Fluorescence Intensity CRMP2
**
MFI
CD4+ T cells
CD8+ T cells
T cells
C
% CRMP2 positive cells
**
%
T conv
nT conv
mT conv
T reg
nT reg
mT reg
Thelper subtypes
D
Median Fluorescence Intensity CRMP2
**
MFI
T conv
nT conv
mT conv
T reg
nT reg
mT reg
Thelper subtypes
E
% CRMP2 positive cells
**
%
Th1
Th2
Th17
Thelper subtypes
F
Median Fluorescence Intensity CRMP2
**
MFI
Th1
Th2
Th17
Thelper subtypes
G
% CRMP2 positive cells
**
%
classical
intermediate
non-classical
monocyte subtypes
H
Median Fluorescence Intensity CRMP2
**
MFI
classical
intermediate
non-classical
monocyte subtypes

4.3.3 CRMP2 expression in immune cells of MS patients

T cell migration to the CNS is an important process associated with MS pathogenesis (10, 38). $CD8^+$ cytotoxic T cells are the most prominent T cells present in MS lesions (208-211). Moreover, a great pathogenic role is acknowledged for Th1 and Th17 cells in the pathogenesis of MS, and a reduced function of regulatory T cells has been described (212-214). The role of monocytes in MS pathogenesis is part of an ongoing debate, as the functions of these cells can be pro-inflammatory as well as neuroprotective, based on the activation cues present in the lesion environment (46, 203, 215). The relative distribution of different immune cell subsets in PBMC samples of HC was compared to RRMS. No difference in the percentage of circulating total $CD4^+$/$CD8^+$ T cells and different T cell subtypes was found (Figure 4.3A and data not shown). A minimal decrease in the overall percentage of CD14+ monocytes was seen, which related to the decrease in circulating classical monocytes in RRMS patients compared to HCs (Fig. 4.3).

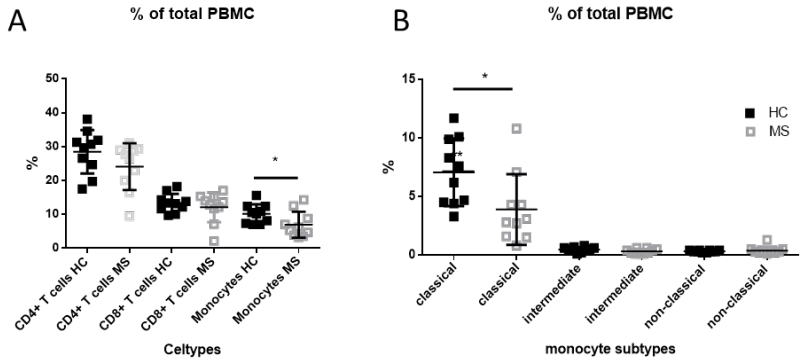

Figure 4.3. Immune cell population size in HC versus RRMS. The percentage of PBMCs that was occupied by a certain immune-cell subpopulation was plotted for HCs and RRMS patients. A: T cells and monocytes, B: Different monocyte populations. *: $p \leq 0.05$

As reported above (fig 4.2) there is a clear difference in CRMP2 expression between different T cell and monocyte subsets. Since altered immune-functions are part of the MS pathogenesis (39, 192) and CRMP2 is important for the migratory behavior of immune cells, we determined expression levels of CRMP2 on different immune cell subsets of HCs and RRMS patients. While no difference

in mean CRMP2 expression levels or percentage of CRMP2 positive cells was found for $CD4^+$ and $CD8^+$ T cells, we did find a decrease in the percentage of CRMP2 positive monocytes in RRMS patients (Fig 4.4).

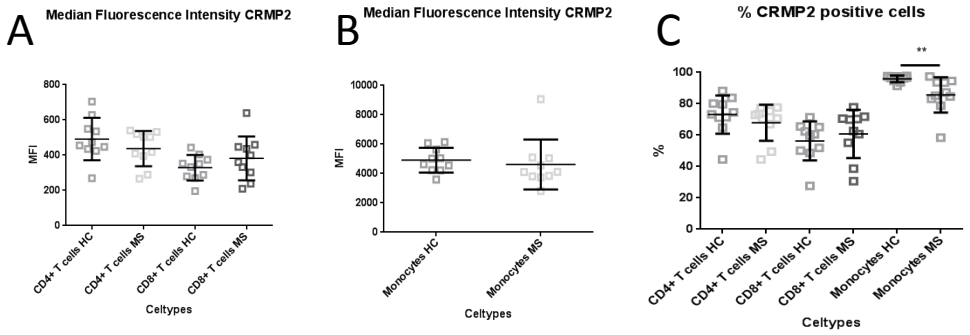

Figure 4.4. CRMP2 expression in immune-cells in RRMS . The mean CRMP2 expression in $CD4^+$ and $CD8^+$ T cells (A) and monocytes (B) was plotted for HCs and RRMS patients. The percentage of CRMP2 positive cells was compared for different immune-cells (C). **: $p \leq 0.01$

A significant decrease in CRMP2 expression was seen in certain $CD4^+$ T cell subsets (Fig. 4.5), while no overall reduction of CRMP2 expression was found on total $CD4^+$ T cells. Naive $CD4^+$ T cells, both conventional as well as regulatory, show a decrease in CRMP2 expression in the RRMS samples compared to controls. This is accompanied by a reduction in the percentage of CRMP2 positive cells in these subtypes. No difference in CRMP2 expression was seen for the memory T cells, apart from a decrease in the percentage of CRMP2 positive memory Treg cells in MS patients. Moreover, Th1 and Th17 cells of RRMS patients show a reduced mean CRMP2 expression paralleled by a decreased percentage of CRMP2 positive cells for MS patients compared to controls (Fig. 4.6).

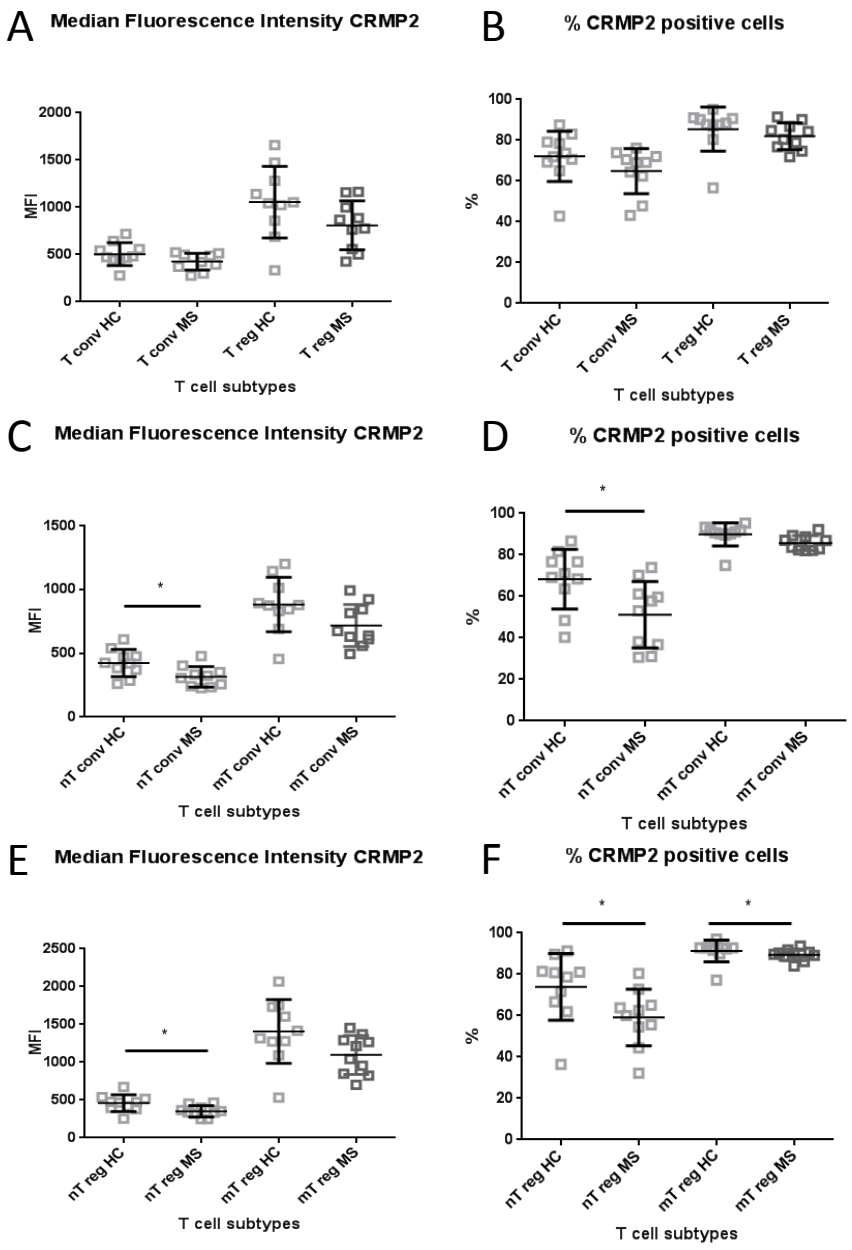

Figure 4.5. CRMP2 expression in HC and RRMS derived T cell subsets. The expression of CRMP2 in different T cell subsets was measured by flow cytometry for 10 HC and 10 RRMS samples. The expression level of CRMP2 (MFI) within the populations was plotted (A/C/E) as well as the percentage of CRMP2 positive cells (B/D/F). *: $p \leq 0.05$

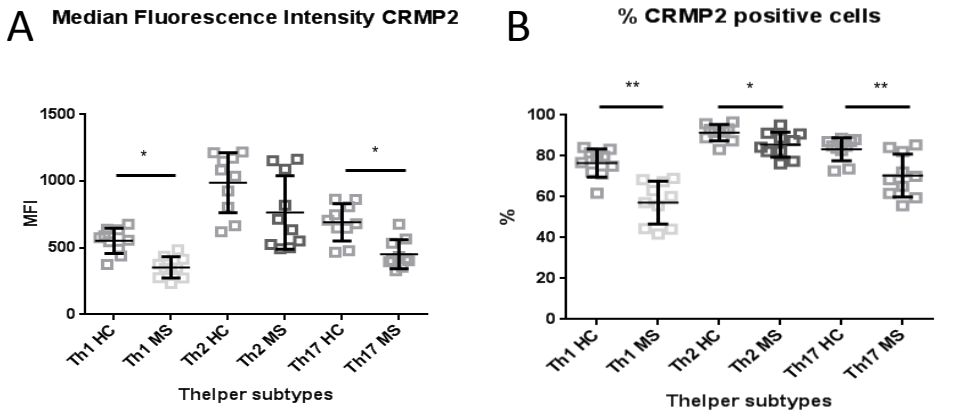

Figure 4.6. CRMP2 expression in T helper subsets. The expression of CRMP2 in different Th subsets was measured. The expression level of CRMP2 (MFI) within the populations was plotted (A) as well as the percentage of CRMP2 positive cells (B). *: p≤0.05, **: p≤0.01

The decrease in percentage of CRMP2 positive monocytes in RRMS (Fig. 4.4) is explained by a decrease in CRMP2 positive intermediate and non-classical monocytes (Fig 4.7). This decrease is most prominent in the non-classical monocyte population, with a decrease of about 35%. A slight decrease of the CRMP2 expression levels in this population was also seen. Overall, a significant decrease in CRMP2 expression is apparent in several immune-cell subsets in RRMS compared to HC.

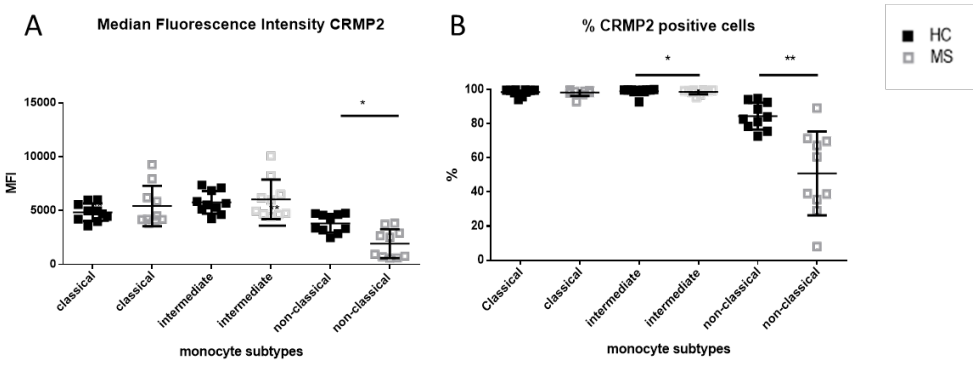

Figure 4.7. CRMP2 expression in HC and RRMS monocyte subsets. The expression of CRMP2 in different monocyte subsets. The expression level of CRMP2 (MFI) within the populations was plotted (A) as well as the percentage of CRMP2 positive cells (B). *: p≤0.05, **: p≤0.01

4.3.4 CRMP2 expression in activated lymphocytes

We further checked CRMP2 expression in non-activated versus activated lymphocytes. An increased CRMP2 expression (MFI) was found in activated (CD25+) lymphocytes, as well as an increase in the percentage of CRMP2 positive cells (Fig. 4.8, A and B respectively). When comparing the CRMP2 expression between HC and RRMS, a decrease of CRMP2 expression levels and the % of CRMP2 positive cells was observed in the activated lymphocytes of RRMS patients (Fig. 4.8, C and D respectively). The increase in CRMP2 in activated versus non-activated lymphocytes remained significant for RRMS samples (data not shown).

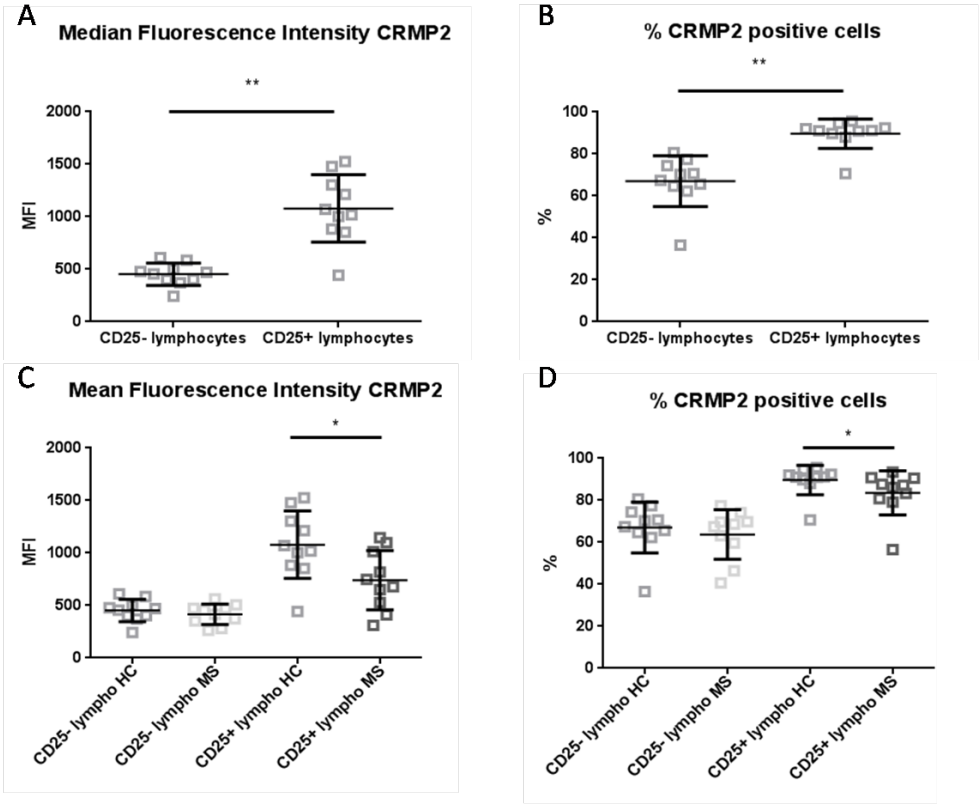

Figure 4.8. CRMP2 expression in activated versus non-activated lymphocytes. The expression level of CRMP2 (MFI) within the activated (CD25+) and non-activated (CD25-) lymphocytes was plotted (A/C) as well as the percentage of CRMP2 positive cells (B/D). CRMP2 expression was also compared between HC and RRMS samples. *: $p \leq 0.05$, **: $p \leq 0.01$

4.4 Discussion

The expression of CRMP2 in EAE brainstem changes during the disease course of EAE. A neuronal role for CRMP2 in MS has already been proposed (112, 216), but the role of this protein in immune-cell function during MS is unknown. We show that CRMP2 expression is different for the diverse T cell and monocyte populations, and that this expression is reduced in RRMS patients.

CRMP2 expression was higher in regulatory T cells compared to the conventional $CD4^+$ T cell population. An increased CRMP2 expression in activated T cells (CD69+ or HLA-DR+) has been described and linked to increased migration capacity (181, 185). It should however be mentioned that 30 percent of HLA-DR positive T cells are regulatory T cells, and not activated effector T cells (217). The elevation of CRMP2 expression in a population that is partly regulatory fits with our results. CRMP2 expression in regulatory T cell populations decreased in RRMS patients, which could indicate a reduced migration capacity of Treg to the CNS during MS. This could lead to an ongoing inflammatory cascade in the brain.

A high percentage of effector T cells (Th1,2,17 and memory T cells) is CRMP2 positive and show high levels of CRMP2 expression. An enhanced expression of CRMP2 in $CD45RO^+$ memory T cells has been reported by P. Giraudon et al. in the context of viral infections (181, 185). They linked the higher expression of CRMP2 in T cells to an increased migratory capacity towards the infected region. There are strong indications that the association of CRMP2 with vimentin and their co-localisation at the uropod during T cell polarization are involved in this mechanism. Furthermore, they show an increased CRMP2 expression in activated T cells (CD69+ or HLA-DR+), leading to a better migration capacity of the activated effector T cells (181). In these experiments, migration was tested towards CXCL12, a cytokine that is also expressed at the BBB during MS (188-190, 218). We included CD25 as an activation marker for lymphocytes in our panel and confirmed the elevation of CRMP2 expression in activated lymphocytes. In the case of MS pathology, this could indicate that activated effector T cells migrate easily to the CNS because of the elevated CRMP2 expression.

In HC, CRMP2 expression is higher in Th2 cells (anti-inflammatory) compared to Th1 and Th17 (pro-inflammatory). A decrease in the percentage of CRMP2 positive cells and mean CRMP2 expression is observed for Th1 and Th17 cells during MS.

These Th1 and Th17 cells are highly associated with MS, and a decrease in CRMP2 expression during RRMS, linked to a decreased migratory capacity is not what we expected. This is also in contrast with the findings of the group of P. Giraudon, where an increase of CRMP2 expression was seen during viral CNS inflammation (185). A possible explanation for the decreased CRMP2 expression in Th1 and Th17 cells could be that cells with high levels of CRMP2 already migrated into the CNS, leaving the low CRMP2 expressors in circulation. This could also explain the reduced CRMP2 expression in activated lymphocytes during MS.

The percentage of CRMP2 positive cells is higher in monocytes compared to T cells. Both classical and intermediate monocytes show a high percentage of CRMP2 positive cells. The non-classical monocytes show less CRMP2 positive cells and also the lowest mean CRMP2 expression among the monocyte subsets. Highest CRMP2 expression was seen in the intermediate monocytes. These intermediate monocytes are seen as the pro-inflammatory subtype compared to the non-classical anti-inflammatory monocytes and the phagocytosing, patrolling classical monocytes (201). Migration efficiency is crucial for the function of classical and intermediate monocytes as they are the patrolling and pro-inflammatory monocytes in charge for a quick response to inflammatory signals. The fact that these two monocyte subtypes show the highest CRMP2 expression here indicates a possible role for CRMP2 in migration of monocytes similar to its role in T cells. This, however, has not been studied so far.

The decrease in population size of the classical monocytes during MS that was seen, has already been reported (219). This decrease could be a result of the differentiation of these classical monocytes to $CD16^+$ intermediate or non-classical monocytes as they are their precursors (220). Another possible explanation for the decrease in population size is the increased migration of these phagocytic, patrolling monocytes out of circulation and into the site of inflammation, the CNS. Increased migration of these monocytes, and their subsequent differentiation to macrophages and dendritic cells could add to the ongoing inflammation. The imbalance caused by the decrease in classical monocytes could thus be involved in MS pathogenesis.

When CRMP2 levels of these monocyte subtypes are compared between HC and RRMS samples, a decrease in CRMP2 expression and percentage of CRMP2 positive cells is observed in the non-classical monocytes. This would mean that the anti-

inflammatory compartment of monocytes is impaired during MS. Changes in monocyte subsets during MS have been reported but CRMP2 levels have not been checked previously.

This preliminary study shows that there are differences in CRMP2 expression between different immune-cell populations as well as in RRMS compared to HC. An in depth study is needed to further unravel the role of CRMP2 in these immune-cells using for instance CRMP2 KD models. The role of CRMP2 in MS pathogenesis was previously always linked to its potential roles in axonal regeneration and neuronal development. This study indicates that CRMP2 can also be involved in immune-mediated disease mechanisms.

5

MYELIN UPTAKE: A ROLE FOR KCNMA1?

ABSTRACT

KCNMA1, a widely expressed calcium-activated potassium channel is an important network node connecting 64% of the differential proteins found in our EAE brain 2D-DIGE study. In the immune system, KCNMA1 is primarily expressed in macrophages and microglia. Both cell types play a crucial role in myelin uptake during MS pathogenesis. In this chapter, the role of this ion channel in the innate immune system was further explored.

Paxilline treatment to block KCNMA1 decreased myelin uptake in primary peritoneal macrophages, in line with what was reported for the macrophage cell line NR8383 in chapter 3. While microglia play a crucial role in the cuprizone induced demyelination model, no prominent effect on demyelination was found in KCNMA1 KO mice. Further investigation revealed that peritoneal macrophages of KCNMA1 KO mice showed no difference in myelin uptake compared to WT controls, indicating that compensatory mechanisms could be involved. Control experiments however show that paxilline affected myelin uptake in KCNMA1 KO macrophages, demonstrating cellular changes that are independent of KCNMA1.

5.1 Introduction

After network analysis of all identified proteins from our EAE 2D-DIGE study, the large conductance calcium-activated potassium channel, KCNMA1, was identified as a central protein node in one of the networks. This network connects 64% of the differential proteins. KCNMA1 is a calcium-activated potassium channel that is widely expressed, for example in smooth muscle, endothelium, neuronal tissue, microglia and macrophages (159, 221-224). It forms a tetramer which is completed by addition of a β-subunit; KCNMB (159, 225). Activation of this channel opens the potassium pore and leads to the efflux of potassium from the cell. This results in membrane hyperpolarisation, and thus decreased cell excitability (226). Functionally, this mechanism is involved in the regulation of smooth muscle tone and neuronal excitability (227).

Given the fact that a lot of differentially expressed proteins in EAE brain connected to KCNMA1, this could indicate that this channel plays a role during EAE/MS. Besides its obvious task in the control of neuronal excitability, KCNMA1 might modulate the microglial phagocytosis as a connection between KCNMA1 and macrophage-capping protein (CAPG) was evident in the protein network. CAPG is a calcium sensitive protein involved in actin-based cell motility, important for macrophage migration and myelin phagocytosis, processes involved in EAE/MS (17). The possible functional connection between KCNMA1 and CAPG was shown by the fact that blocking of KCNMA1 in macrophages lead to a decreased ability to phagocytose myelin (chapter 3).

Blocking of potassium channels has been described to be beneficial in EAE, with an effect on disease score and delay of disease onset (115, 228, 229). 4-aminopyridine (4-AP) is a general blocker for a variety of voltage-gated potassium channels that improves neuronal conduction in MS patients (230). It does not block KCNMA1 at clinical concentrations (230). Due to epileptogenic side effects, this drug is not used as a first-line treatment (115, 230). Although the effect of KCNMA1 blockage on EAE has not been described yet, the fact that other potassium channels are important indicates that research focussed on evaluating the role of KCNMA1 in the disease processes of EAE/MS is certainly relevant.

Blocking KCNMA1 might improve neuronal excitability like 4-AP, however side effects might be less pronounced as only one potassium channel is blocked.
As blockage of KCNMA1 in macrophages results in a decreased uptake of myelin (see chapter 3), we further explored the role of this channel in the immune system. Expression of KCNMA1 in the immune system is primarily found on macrophages and microglia (115). In light of MS pathogenesis, these cells are important in perivascular reactivation of T cells, secretion of reactive nitrogen species and cytokines, and for the uptake of myelin debris at the lesion site (38, 41, 231). Here we further investigated the role of KCNMA1 in immune-related MS disease processes.

5.2 Materials and methods

5.2.1 Animals

KCNMA1 knock-out mice (FVB background) were kindly donated by Prof. Dr. A. L. Meredith, Stanford University and provided by the Friedrich-Schiller-University Jena. Animals were generated as previously described (223), heterozygous mice were used as breeding pairs. Animals were housed in an accredited animal facility with free access to food and water. All animal procedures were in accordance with the EU directive 2010/63/EU and were approved by the Hasselt University ethics committee for animal experiments.

5.2.2 Genotyping

Tailsnips were collected and DNA was extracted with the Extracta™ DNA prep for PCR – tissue kit (Quanta Biosciences) as indicated by the manufacturer. Genomic DNA concentrations were determined with the nanodrop spectrophotometer (Isogen Life Science) and 200-500ng of DNA was used in the PCR reaction. PCR buffer, Taq polymerase and dNTP's (NEB, SigmaAldrich) were used according to manufacturer's instruction. Primers and PCR program were as described (223), however, we did not combine both primer sets in 1 PCR reaction.

5.2.3 Isolation of peritoneal macrophages

Resident peritoneal macrophages were isolated as described (158), with the exception of the thioglycolate injection prior to isolation. In short, a peritoneal lavage with 10ml of ice cold PBS (Lonza) supplemented with 5mM ethylenediamine tetraacetic acid (EDTA, VWR) was performed. Peritoneal exudate cells (PECs) were

cultured for 2 hours in RPMI 1640 medium. Non-adherent cells were washed away after 2 hours incubation at 37°C with 5% CO_2.

5.2.4 Myelin phagocytosis assay

DiI-labeled myelin (100µg/ml), isolated and labeled as previously described (158), and paxilline (Sigma; P2928) were diluted in RPMI 1640 medium (Invitrogen) enriched with 10% fetal calf serum (Cyclone, Erenbodegem, Belgium), 50 U/ml penicillin and 50 U/ml streptomycin (Invitrogen). For paxilline treatment, different concentrations were used (3, 30 and 300nM). A concentration of 300nM leads to a total blockage of the KCNMA1 channel (159). Medium containing DiI-myelin and paxilline was added to the macrophages for 90 minutes (100 000 cells). Flow cytometry was used to assess the degree of myelin internalization by measuring cellular fluorescence intensity.

5.2.5 Cuprizone model

Eight week old mice were put on a diet containing 0.2% cuprizone (Sigma-Aldrich). Cuprizone was homogenously mixed into powdered chow and renewed three times a week. Wild type, KCNMA1 knock-out and heterozygous mice (littermates) received a cuprizone diet for 5 weeks to induce acute demyelination (53, 232).

Mice were transcardially perfused with Ringer's solution followed by 4% PFA, brains were dissected and incubated overnight in 5% sucrose/PBS. Brains were then transferred to a 15% sucrose/PBS solution until they stopped floating. This was repeated in a 30% sucrose/PBS solution. Tissues were then imbedded in Tissue-Tek and frozen by means of isopentane (-50°C) on liquid nitrogen. Samples were stored at -80°C.

5.2.6 Histochemistry

Ten micrometer cryosections were prepared using the Leica CM3050S cryostat (Leica Microsystems). A Luxol Fast Blue (LFB) staining was performed to quantify the myelinated area in the corpus callosum (4-5 sections per animal). Sections were first fixed in ice cold acetone, followed by a 16 hour incubation in LFB solution

at 56°C. Differentiation in 0.5% lithium carbonate was followed by counterstaining in cresyl violet (Sigma-Aldrich). Microscopic analysis was performed with the Eclipse 80i microscope (Nikon) and the Nis-Elements Basic Research version 2.3 microscopy software.

5.2.7 Statistical analysis

Statistical analyses were performed using SAS JMP Pro 11. For data with a normal distribution a t-test (2 groups) or 1way-ANOVA (3 or more groups) was performed. For non-parametric data the Mann-Whitney (2 groups) or Kruskal Wallis (3 or more groups) analysis was performed. A p-value of less than 0.05 was considered significant. Results are expressed as mean values ± standard error of the mean (SEM). A Bonferroni correction was performed if more than 2 analysis were compared.

5.3 Results

5.3.1 Paxilline treatment reduces myelin uptake by peritoneal macrophages

Different concentrations of paxilline were added to primary peritoneal macrophages to check for dose-dependent effects on myelin uptake. In line with Fig 3.10, blocking of KCNMA1 resulted in a reduced uptake of myelin with increasing paxilline concentration, becoming significant at the highest paxilline concentration (300nM) used in this study (Fig. 5.1). This concentration known to cause a full blockage of KCNMA1, lower paxilline concentrations only partially block KCNMA1 (159). Cell viability was not affected by paxilline treatment (data not shown).

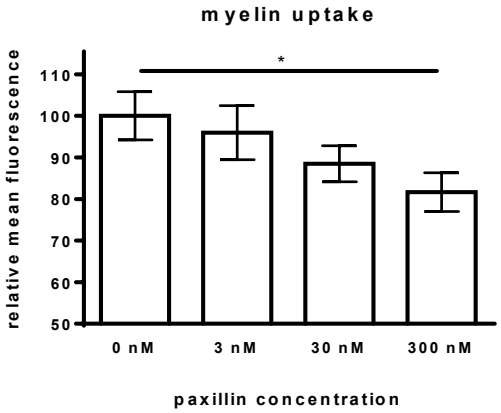

Figure 5.1. Myelin uptake by primary macrophages. The influence of KCNMA1 blockage on myelin uptake in peritoneal macrophages was assessed by means of flow cytometry. Data represent mean ± SEM of 3 independent experiments performed in triplicate. For each concentration a pool of peritoneal macrophages of 5 mice was used. *: $p \leq 0.05$

5.3.2 Cuprizone induced demyelination is not affected in KCNMA KO mice

Uptake of myelin debris by macrophages and microglia is an important mechanism that influences de- and remyelination (45, 232, 233). To analyse the involvement om KCNMA1 in this process we selected the cuprizone animal model. Traditionally

the EAE animal model is used to study the immune-mediated processes in MS (52). However, to study de- and remyelination the cuprizone induced demyelination model has gained more and more attention (53, 232). KCNMA1 WT, KO and heterozygous mice were obtained, no differences in basal myelination of the corpus callosum were observed in these mice (data not shown). Cuprizone induced demyelination in all 3 genotypes, but no differences in demyelination of the corpus callosum were seen between the different genotypes (Fig. 5.2).

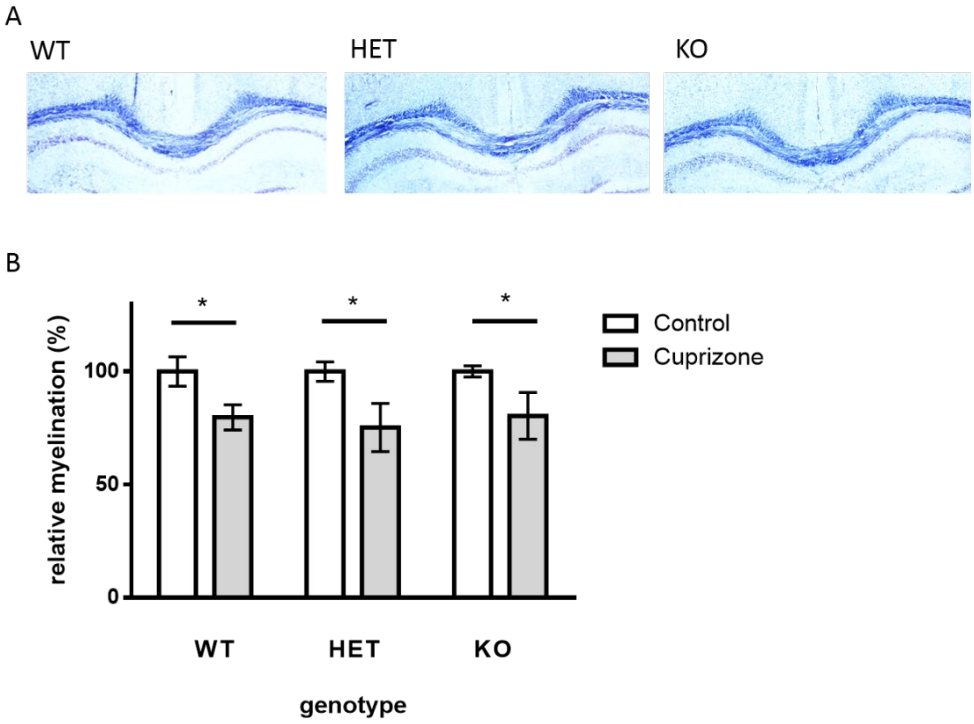

Figure 5.2. Demyelination of the corpus callosum. A: Representative LFB staining of the corpus callosum after 5 weeks of cuprizone treatment. B: Relative myelination of the corpus callosum in the different genotypes was analysed (mean ± SEM), both in the control group and in the cuprizone treated animals (n=5). *: $p \leq 0.05$, WT: wild type, HET: heterozygous, KO: knock out.

Since compensatory mechanisms may mask direct effects of KCNMA KO *in vivo*, an *in vitro* assay was set up using purified peritoneal macrophages of wild type and KCNMA1 KO mice. KCNMA1 deficiency did not affect myelin phagocytosis by peritoneal macrophages. (Fig. 5.3).

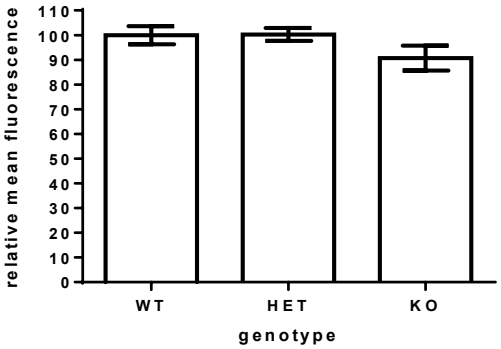

Figure 5.3. Myelin uptake by KCNMA1 KO macrophages. The influence of KCNMA1 KO on myelin uptake in peritoneal macrophages was assessed by means of flow cytometry (mean ± SEM). Each genotype was represented by a pool of peritoneal macrophages of 5 mice. All samples were measured in triplo. Data represent 3 independent experiments.

The effects of blocking KCNMA1 and gene knock out are thus different. In KCNMA1 KO macrophags no KCNMA1 channels are present, and thus no effect of paxilline should be observed. While paxilline is an acknowledged blocker for KCNMA1 (159, 225, 226, 234), unexpectedly we did see a decrease in myelin uptake in the KCNMA1 KO macrophages treated with paxilline (Fig. 5.4).

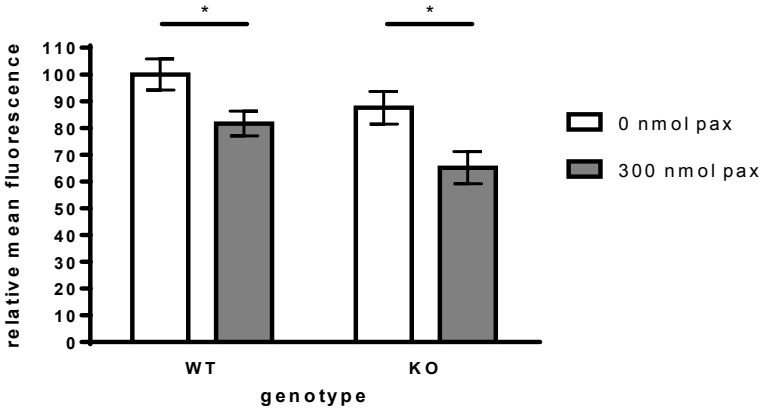

Figure 5.4. Myelin uptake by KCNMA1 KO macrophages after paxilline treatment. The influence of paxilline on myelin uptake by KCNMA1 KO peritoneal macrophages was assessed by means of flow cytometry (mean ± SEM). Each genotype was represented by a pool of peritoneal macrophages of 5 mice. All samples were measured in triplo. Data represent 3 independent experiments. *: $p \leq 0.05$

5.4 Discussion

Decrease of myelin uptake by cultured macrophages after paxilline treatment was confirmed in primary peritoneal macrophages. To evaluate the effect of impaired myelin uptake on demyelination, demyelination of the corpus callosum was assessed in WT, HET and KCNMA1 KO mice after a 5 week cuprizone diet. No differences in basal CC myelination were found, and cuprizone induced equal levels of demyelination in all three genotypes. Further investigation showed that there were no in vitro differences in myelin uptake by peritoneal macrophages of WT and KCNMA1 KO mice.

KCNMA1 KO mice have alterations in circadian rhythm, heart rate, blood pressure, urination and reproductive function (221, 223, 227, 234). Compensation for KCNMA1 loss of function has been reported for aspects of cardiac, bladder and renal function (221, 235, 236). Similarly, a compensation effect could be responsible for the lack of difference in the amount of demyelination seen in WT versus KCNMA1 KO animals. In contrast to acute blockage of KCNMA1 with paxilline, compensation mechanisms can be expected to be more pronounced in KO animals, were loss of function is long-lived and adaptive processes during development may play a role (235). KCNMA1 is a large conductance (BK) calcium-sensitive potassium channel. Compensation for its calcium-induced activation could be the result of overexpression or overactive intermediate (IK) or small (SK) conductance potassium channels (222, 226). KCNMA1 is also voltage-sensitive, while IK and SK are only calcium-sensitive. In macrophages and microglia, however, voltage activated potassium channels are upregulated during strong activation and these channels might compensate for the loss of the BK channels during changes of the membrane potential (237, 238). Compensation is thus a plausible explanation for the differences between the effect of paxilline and that of KCNMA1 KO.

To make sure that the results we see with paxilline are a result of KCNMA1 blockage, KCNMA1 KO macrophages were also treated with paxilline. While no effect was expected as KO cells do not express KCNMA1, myelin uptake was significantly impaired by paxilline in these KO macrophages as was seen in WT cells. This indicates that even low concentrations of paxilline are responsible for cellular changes that are not KCNMA1 linked and the reduction in myelin uptake

seen after paxilline treatment cannot be solely linked to KCNMA1 modulation. Although paxilline is known to be a specific blocker, it does block SERCA channels in the µM range (239). SERCA channels are sarco/endoplasmatic reticulum Ca^{2+} ATPases that keep the calcium levels in the cell low, and are important in myelin uptake because small changes in calcium levels can influence cytoskeletal reorganization and thus process motility (168). In our experiments blockage of SERCA by paxiline should not occur as we are working in the pM range. However, this should be considered as a possible explanation for the effects of paxilline on KCNMA1 KO cells. Furthermore, we should also consider the possibility that our KO animals still express KCNMA1. KO animals were genotyped, checking the presence of KCNMA1 exon 1 which encodes the translation start and first transmembrane region S0, confirming the absence of KCNMA1. However, a KCNMA1 staining of KO tissue was not performed.

Both blockage of KCNMA1 by paxilline and gene KO are approaches that have limitations for further research. Furthermore, cellular functions other than myelin uptake can contribute to the involvement of KCNMA1 in MS disease mechanisms. Macrophage activation for example by lipopolysaccharide (LPS) occurs via Toll-like receptor 4 (TLR4) (224). This activation results in the expression and release of proinflammatory cytokines. This effect is a result of NF-κB relocalisation to the nucleus. It has been shown that KCNMA1 blockers inhibit this process which provides evidence that KCNMA1 could also be involved in cytokine production in EAE and MS (224, 240, 241). As KCNMA1 is a widely expressed potassium channel, other cell types should not be forgotten. Unravelling the role of KCNMA1 in EAE and MS disease pathways will thus be a challenge for further research.

6

SUMMARY, GENERAL DISCUSSION & FUTURE PERSPECTIVES

6.1 Summary and general discussion

The open approach of proteomic studies allows for the identification of dysregulated proteins involved in disease mechanisms without prior knowledge of the involvement of these proteins/mechanisms. This, in contrast to a candidate approach, can give new insights and provide more detailed knowledge about unknown disease mechanisms. The proteomic identification of dysregulated proteins in autoimmune disease could be the starting point for better diagnosis and prognosis and the development of novel. Here we studied changes in the proteomic profile of tissues representative for two autoimmune diseases in a time-dependent manner. In this chapter, obtained results are summarised and discussed.

PART 1: PROTEOMICS

In myasthenia gravis autoantibodies react to proteins of the neuromuscular junction. In 85% of patients, autoantibodies against the AChR are found (59). The presence of these autoantibodies impairs neuromuscular signal transduction, leading to severe muscle weakness (60, 62). How these autoantibodies cause a loss in signal transmission and thus mediate muscle weakness is relatively well known (60). But how this neuromuscular transmission failure is reflected at the protein level remains largely uncharacterised. In **chapter 2** we determined the proteomic profile of the tibialis anterior muscle at different stages of EAMG, the animal model of MG. Protein abundance changes between the experimental groups (different disease scores) were observed for twenty-six protein spots in the 2D-DIGE study. In these spots a total of twenty-two unique proteins were identified, pointing among others to a reduction in glycolytic capacity of the muscle and the loss of fast twitch muscle fibres as EAMG disease symptoms aggravated. Similar changes were previously reported in other conditions that impair muscle contraction such as denervation (121, 122) and are probably a consequence of impaired nerve-muscle signalling. Furthermore, additional protein abundance changes found in this study are of interest as well and could drive further research.

In contrast to MG, the antigenic targets and underlying molecular mechanisms of MS are largely unknown. In **chapter 3** we performed a proteomics study to

identify proteins and pathways involved in inflammatory brain lesion development during acute EAE, an animal model of MS. Protein abundances in brainstem were compared at three different time points: before onset of the disease, at the top of clinical symptoms and after recovery. Proteins present in the ninety-two protein spots that showed a significant change in abundance at different stages of the disease were identified. This yielded a list of seventy-five unique proteins. Identification of changes in protein abundance representative of processes actively involved in MS pathogenesis confirmed the experimental design and the ability to pick up disease-related differences.

Multivariate principal component analysis indicated that the brainstem proteome could differentiate early from late EAE. Network analysis was performed to disclose disease-related pathways and interactions between the identified proteins. Four focus networks were built using our dataset. These suggest an integrated regulation of the identified proteins together with four putative key proteins. Presence of two of these key proteins in our samples was confirmed, and blockage of one of these, KCNMA1, in macrophages resulted in a decreased myelin phagocytosis. Therefore, this study of the EAE brainstem proteome has provided information on biological events involved in neuro-inflammation, whereas network analysis revealed the connections within our data. This study is a first step in finding disease-related cellular changes and further research is needed to explore the possible implications of these findings as to what the functional role of these proteins is in the disease pathogenesis.

What is the added value of network analyses for proteomic research?

The data generated in proteomics are often long lists of identified proteins present in a sample, possibly supplemented with information about differences in abundance between different samples or about PTM's. These lists often fail to offer insights in underlying biological mechanisms. Reducing the complexity of these data by classification, clustering and identification of active pathways helps to extract biological meaning and functional insights. This not only helps to organize the data but also enables the interpretation of the molecular mechanisms behind the altered protein levels and thus increases the explanatory power (242, 243).

The assignment of functional and biological information to proteins and the exploration of different relationships between proteins in a dataset can be

accomplished by a still growing array of available tools (242, 243). In chapter 3 Ingenuity Pathway Analysis (IPA)(244) revealed the cellular compartments the identified proteins belong to. The list of identified proteins was mapped onto biological pathways, disease networks and focus networks were built that represent the integrated regulation of the identified proteins. These focus networks do not take into account whether a protein is up or down regulated, but show real interactions between the identified proteins based on the IPA Knowledge Base. Furthermore, these proteins were compared to a list of MS-related proteins present in the IPA knowledge base, which is based on primary literature and public databases (244). The results reveal some of the great advantages of network analysis. Gel-based proteomic approaches such as 2D-DIGE have technical limitations such as the reduced separation potential of both high and low molecular weight proteins as well as proteins with an extreme pI and hydrophobic proteins such as membrane proteins (245). As expected due to the limitations mentioned above, 76% of the identified proteins in our study were cytoplasmic. By means of IPA, our data were compared to a list of known MS-related proteins that are largely membrane bound. The overlap was thus limited, but a clear connection between the two datasets was seen, as our proteins mostly operated in the downstream biochemical pathways of the membrane-bound MS-related proteins. Furthermore, proteins that were not identified in the EAE proteomics study were found to be highly connected to our dataset. One such example is KCNMA1, a membrane protein that plays a central role in one of the focus networks. This shows that apart from the reduction in complexity and identification of active biological pathways, network analysis can also help overcome the technical limitations that may be associated with the proteomic techniques at hand.

2D-DIGE or gel-free quantitative proteomics?

Network analysis helps to overcome technical limitations in proteomics studies, but the techniques at hand for proteomic research also advance to overcome these limitations. Gel-free quantitative proteomic methods have improved drastically in recent years. For protein separation better nano-flow LC and column resins are now available, for protein identification higher sensitivity and better resolution are achieved as a result of technical advances in instrumentation. Furthermore, mass

spectrometric data analysis software has been improved and automated (246). For gel-free quantification several strategies have been developed, with and without labels, but also for absolute quantitation (247). Due to the advances made, gel-free methods are currently more sensitive and reproducible than 2D-DIGE. While 2D-DIGE allows great protein separation, the limitations discussed above, and the complex procedures make this gel-based technique less attractive nowadays.

PART 2: UNRAVELING THE ROLE OF PROTEINS IN HEALTH AND DISEASE

With information about differences in protein profile at different stages of EAE, identification of the proteins and an analysis of their biological roles and the connections between them, functional analysis of the involvement of these proteins in health and disease awaits. In the context of MS, two proteins were selected for further research, namely CRMP2 and KCNMA1. The role of both proteins in normal CNS function has been studied (172, 227), and the downstream function of CRMP2 in the Nogo-A pathway has previously been linked to MS (112). Their function in the immune-system however, and its relation to MS pathogenesis has received little or no attention. In **chapters 4 and 5** the possible roles of CRMP2 and KCNMA1 in the immune-system were characterised.

What is the role of CRMP2 in immune cells during MS?

In our 2D-DIGE study, the CRMP2 protein was present in ten protein spots with an altered protein abundance during EAE, indicating changes in protein isoform expression, post-translational modifications and protein breakdown. Different phosphorylation forms of CRMP2 have altered functional properties such as induction of growth cone collapse (Thr555) and T cell polarisation (Tyr479) (176, 186), which could be involved in EAE progression. The recurring appearance of CRMP2 in the list of differential proteins was a first hint towards selection of this protein for further research. Furthermore, CRMP2 is known to function as a downstream molecule in the Nogo-A pathway (112). Nogo-A induces the phosphorylation (pThr555) of CRMP2, inhibiting the normal role of CRMP2 in axonal growth and thus inducing axonal growth inhibition. It was shown that blocking the Nogo-A pathway resulted in reduced CRMP2 phosphorylation, limited axonal degeneration and reduced EAE progression (112). This association of CRMP2 with neurodegeneration in MS but also the involvement of CRMP2 in T cell

migration during viral induced neuroinflammation (185) added to the curiosity and led to the selection of this protein for further analysis.

In **chapter 4** the expression of CRMP2 in different monocyte and T cell subsets was assessed and a comparison of these expression levels between healthy controls and RRMS patients was completed. In T cells, the expression of CRMP2 was higher in regulatory T cells compared to conventional T cells, memory T cells had a higher expression than naïve T cells and expression of CRMP2 was higher in Th2 cells compared to Th1 and Th17 cells. Furthermore, activated lymphocytes showed increased CRMP2 expression levels. An overall decrease of CRMP2 expression in peripheral T cells of RRMS patients was observed. CRMP2 expression in monocytes was even higher than in T cells, with the highest expression for the intermediate pro-inflammatory monocytes. These expression levels were higher in HC compared to RRMS patients. CRMP2 levels are thus variable over different T cell and monocyte subsets and significantly decreased in RRMS patients. Although there is a difference in age between our MS patients and HC, we do not believe this affects our results as no age dependent changes in CRMP2 expression in T cells has been published. Furthermore, also in our data no age dependent effect on CRMP2 expression was seen.

In T cells, CRMP2 is an important activator of cell migration, as explained below (181). A decrease of CRMP2 expression could thus indicate a reduced migratory capacity of these cells. In case of regulatory T cells, a decreased migration towards the CNS can lead to the decreased control of the ongoing brain inflammation. Thelper cells however, also show a decreased expression level of CRMP2 in RRMS samples. This decrease of CRMP2 expression was most prominent in Th1 and Th17 cells, which are highly associated with MS. A decrease in CRMP2 expression, and thus a diminished migratory capacity for these Thelper cells is not in line with the observation that effector T cells are present in MS lesions. A possible explanation for this could be an increased migration of CRMP2 high T cells to the CNS and thus an apparent parallel decrease in CRMP2 levels in T cells remaining in the circulation.

The increased migratory capacity associated with increased CRMP2 expression in T cells has been studied in more detail (181, 185-187). The different phosphorylation forms of CRMP2 play an important role in T cell migration, especially in relation to CXCL12 (186, 187), a cytokine that is also expressed in

MS. The molecular pathway that is activated once CXCL12 binds its receptor CXCR4 on T cells includes the polarization of T cells, relocalization of CRMP2 to the uropod and a higher association of CRMP2 with the cytoskeleton, processes required for cellular migration. Phosphorylation of CRMP2 at Thr509 and Thr514 decreases while Tyr479 gets phosphorylated (186). CRMP2 was detected to be differentially abundant in 10 different protein spots in our EAE 2D-DIGE study, indicating different isoforms, but also different PTM. The antibody we used for our study of CRMP2 expression in immune cells cannot differentiate between different CRMP2 phosphorylation forms and an in depth study of different CRMP2 isoforms and phosphorylation is needed to further elucidate the role of CRMP2 in T cell migration during MS pathogenesis.

The functional role of CRMP2 in monocytes remains to be uncovered. The differential expression of this protein in different monocyte populations and the decrease of this expression during RRMS could indicate a role for CRMP2 in migration of these monocytes similar as was shown for T cells. This is however speculation, and further research is warranted to test this hypothesis.

What is the role of KCNMA1 in macrophages/microglia during MS

KCNMA1 was identified as a central node in one of the differentially regulated protein networks in the EAE 2D-DIGE study (**chapter 3)**. While the protein itself was present in our samples, it was not differentially expressed at the different time points during EAE. Still, the central location of this protein in our network analysis could indicate that changes in the activation pathway occur. This potassium channel is important for membrane hyperpolarisation and thus cell excitability (226, 227). This hyperpolarisation can drive extra calcium into the cell, enhancing cell motility and thus fagocytosis. The possible functional role of this protein in EAE was proven by the reduced myelin uptake by macrophages as a result of paxilline treatment (chapter 3). Blockage of potassium channels, other than KCNMA1, is effective in reducing EAE score and improving neurological conduction in MS (228, 230). The role of KCNMA1 in macrophage myelin uptake and possible consequences for disease where therefore selected for further research.

Activated macrophages/microglia, present in MS lesions, can exert different functions, both beneficial and detrimental (231). They are involved in clearance

of myelin debris, release of neurotropic factors, boosting of remyelination and axonal regeneration, all processes that promote recovery. However, macrophages and microglia also participate in detrimental processes such as demyelination, the release of inflammatory cytokines and free radicals and the recruitment and activation of T cells. KCNMA1 expression in the immune system is primarily located on macrophages and microglia, with 76-78% of microglia expressing KCNMA1. The expression on microglia is age-independent, unlike that of voltage-activated potassium channels (168). We investigated the role of KCNMA1 in myelin uptake by macrophages and microglia.

In **chapter 5** the role of KCNMA1 in macrophages was explored. Paxilline treatment decreased myelin uptake, however the effect on myelin phagocytosis was only achieved after total blockage, no dose-dependent effects were observed. Moreover, cuprizone induced demyelination was comparable for WT and KCNMA1 KO mice. This demyelination model mostly depends on microglia (53), while in MS both microglia and macrophages are responsible for the uptake of myelin debris. The mechanisms of myelin uptake however, are comparable. The lack of an effect in KO cells/animals could relate to compensatory mechanisms, that are more pronounced in a KO model compared to a short term blockage using a chemical blocker. In a control experiment however, an effect of the KCNMA1 blocker paxilline on myelin uptake was also observed in KCNMA1 KO macrophages, indicating that the observed effects of paxilline could relate to other mechanisms than KCNMA1 blockage. One possibility is the aspecific blockage of SERCA channels, which normally only occurs in the µM range. These channels are important for the intracellular calcium homeostasis and involved in cytoskeletal reorganization necessary for myelin uptake. Furthermore, these channels can be linked to MS pathology, as they are important in peroxisome proliferator-activated receptor (PPAR) related calcium homeostasis (248). PPAR plays an important role in the inate and adaptive immune system and PPAR agonists are protective in EAE. In macrophages, PPAR agonists can decrease the production of inflammatory and neurotoxic mediators (249).

The exact functional role of KCNMA1 in macrophages and microglial cells remains to be elucidated, although some functional roles have been described. The activation of proinflammatory microglia induces an upregulation of KCNMA1 (168), suggesting that KCNMA1 is an activation marker for M1 microglia and has

functional relevance in this subset. Activation of macrophages through TLR4 leads to the induction of M1 macrophages, and also induces elevated KCNMA1 expression and the release of inflammatory cytokines (TNF-α, IL6) (224). The release of these cytokines is inhibited by blocking KCNMA1. TLR4 can be activated by LPS, but also by heparan sulphate, a proteoglycan of the extracellular matrix that is released after tissue damage or during inflammation (241), processes that are important in MS pathogenesis. Furthermore, also IL-1 dependent macrophage activation and associated inflammatory cytokine release is dependent on KCNMA1 (240). Changes in cytoskeletal reorganisation, needed for shape changes and migration have been linked to ion channels. KCNMA1 could enhance process motility, as increased potassium efflux decreases the osmolarity and increases water efflux which induces process retraction (168). Other cellular functions linked to ion channels are proliferation, ROS production and the release of neurotropic factors, all involved in the pathogenesis of MS.

Is there a link between CRMP2 and KCNMA1?

Both CRMP2 and KCNMA1 are widely expressed and have previously been linked to cell motility (168, 172, 173, 185, 250-252). CRMP2 is known to stabilize tubulin (173), and phosphorylation is responsible for a decreased tubulin and actin stability (175). This function of CRMP2 has been linked to axonal growth cone collapse (173) and T cell migration (187). Furthermore, CRMP2 has been linked to MS as a down-stream molecule of the Nogo-A pathway, which is responsible for axonal growth inhibition and could thus be related to neurodegeneration (112). In chapter 4, focus was on CRMP2 expression in T cells, as a role for CRMP2 in T cell migration towards CXCL12 was previously described (186). This mechanism could also be important in MS pathogenesis.

Increased expression of KCNMA1 has been linked to augmented invasiveness of cancer cells, increasing cell migration. Blockage of KCNMA1 blocked cell migration (250, 251). By means of pathway analysis KCNMA1 was also linked with axon guidance (250). Focus of potassium channel research in MS however is on membrane hyperpolarisation and cell excitability, as blockage of potassium channels can improve neurological conduction (230). To my knowledge, no direct link between CRMP2 and KCNMA1 has been established. They are however both

linked to cell motility, and could both be responsible for immune cell migration and axonal growth, processes that are linked to MS.

6.2 Concluding remarks & future perspectives

The results presented in this thesis are an effort to identify proteins involved in autoimmune diseases to further unravel disease mechanisms. Knowledge of precise disease mechanisms is indispensable for (pre-symptomatic) diagnosis, clear prognosis and the development of effective therapies. Identification is thus not enough, functional exploration and in depth analysis are required as well. Proteins involved in the disease mechanisms of MS and MG were identified, and two proteins involved in EAE pathogenesis, CRMP2 and KCNMA1, were selected for functional exploration. In depth analysis of their functional roles in the disease mechanisms and further exploration of the other identified proteins is however still needed.

CRMP2 as a target in MS therapy?

CRMP2 has previously been linked to MS as a downstream molecule of Nogo-A, an axonal growth inhibitor. Blocking this pathway delays EAE onset and reduces clinical signs (112). In this manuscript, this effect was stated to be attributed to the neurological role of this pathway. Still, an effect on the immune system cannot be excluded as Nogo-A signaling was reported to decrease adhesion and increase the migratory state of immune cells (253). Furthermore, a shift in cytokine profile, from pro- to anti-inflammatory, was reported in response to Nogo-A neutralization during EAE (254). A delay in EAE onset in Nogo-A receptor1 KO animals however seemed to be independent of phenotypical changes in immune cell populations (216). Apart from the role of CRMP2 in Nogo-A signaling there is a critical role for CRMP2 in T cell polarization and migration in response to CXCL12 (187). CXCL12 induces a shift in phosphorylation status of CRMP2 that promotes migration and neuroinvasion. Unpublished data demonstrate that this is also true for CCL5, CXCL10 and CCL22, chemokines involved in immune cell neuroinvasion (187). A role for CRMP2 in T cell migration during MS is even suggested.

One way to therapeutically modulate CRMP2 is the use of lanthionin ketamine, a natural metabolite that binds CRMP2. A cell permeable synthetic lathionine ketimine ester (LKE) was used to further investigate the possible neuroprotective effects of this metabolite in models of cerebral ischemia and alzheimer (255-257). LKE induces a decrease in phosphorylated CRMP2 which promotes neurogenesis,

blocks NO production by microglia and decreases neurotoxicity of microglial-conditioned medium. Administration of LKE in chow of EAE animals at the start of mild clinical symptoms reduced clinical symptoms. Further investigation showed decreased IFNγ production by T cells and less neurodegeneration. Furthermore, an increase in myelin thickness was observed (258). A direct effect of LKE on neuronal cells was shown *in vitro,* including reduced cell death in response to glutamate excitotoxicity and induction of neurogenesis (259). The effect on T cell migration was not investigated.

Other therapeutic options to target CRMP2 are available, but are currently not being tested for MS treatment. Examples are lacosamide, a small molecule like LKE that has an antagonistic effect on CRMP2 (260). Lacosamide is currently used in the treatment of epilepsy, where it blocks axonal outgrowth. Glial-derived neurotrophic factor (GDNF) and the antidepressant tianeptine are both inducers of CRMP2 expression (261, 262). GDNF however cannot pass the BBB to induce axonal extension by upregulating CRMP2, tianeptine can. Drug targeting of CRMP2 by the competitive binding of CRMP5 to CRMP2 and hetero-oligomerization, which might play an important physiological role in CRMP2 regulation (263), could also be used. Therapeutic induction or blockage of CRMP2 are thus possible, and are used in other diseases as needed. Before embarking on this, the whole range of effects of CRMP2 modulation and the involved molecular mechanisms still need to be further elucidated (174).

On top of the possible therapeutic options, the detection of specific phosphorylation forms of CRMP2 has biomarker potential. A patent application publication of P. Giraudon (264) indicates that the detection of CRMP2 Y479 phosphorylation in immune cell subsets could be indicative of inflammatory diseases of the CNS, such as MS. The patent application indicates this might help in early diagnosis, clear prognosis and monitoring of the disease. Taken together, a role for CRMP2 in neuronal and immune MS disease processes is obvious and further research on exact working mechanisms and possible interventions is well underway.

KCNMA1 as a target in MS therapy?

Blocking potassium channels with 4-AP, a general blocker of several voltage-gated potassium channels, improves neurological conduction in MS patients (265). The

use of 4-AP in MS treatment is however limited due to epileptogenic side effects (230). 4-AP does not block KCNMA1 at clinical concentrations (265). Apart from a role in neurological conduction, a functional role for potassium channels in the immune system is also plausible. In T cells, regulation of the expression of potassium channels Kv1.3 and Kca3.1 is important for T cell function during and after antigen exposure (266). In regulatory T cells of MS patients, Kv1.3 expression is reduced in comparison to healthy controls, which could be involved in the reduced function of these cells in MS patients (266). The functional role of KCNMA1 in MS pathogenesis still needs to be elucidated. KCNMA1 is known to be upregulated in activated proinflammatory microglia (168) and in activated macrophages, where this upregulation is linked to the release of inflammatory cytokines (224). Furthermore, a possible role in proliferation, cell migration, ROS production and the release of neurotrophic factors was described (168).

Given the multitude of connections KCNMA1 shows to the proteins identified in chapter 3, a further exploration of the role of KCNMA1 in different pathways and cells that are involved in MS pathogenesis is needed. Due to the nonspecific effect of paxilline seen in KCNMA1 KO cells (chapter 5), it will be necessary to use a more selective blocker to investigate cellular effects of KCNMA1 blockage. Several options, including iberiotoxin are available (225). Another option to investigate the biological and cell-specific functions of KCNMA1 is to use conditional, cell-specific KO models. These allow the conditional inactivation of KCNMA1 in a specific tissue or cell, and eliminate the systemic defects of the overall KCNMA1 KO model (221). This will also reduce the compensatory mechanisms that occur in KCNMA1 KO mice during development, which are not limited to upregulation of other potassium channels, but also include upregulation of cAMP and PKA and even changes in sympatic tone to regulate hart rate (235, 236, 267).

KCNMA1 could be a target in MS therapy, however, this potassium channel is widely expressed, which could lead to side effects when interfering with channel function. Major evidence for possible side effects of KCNMA1 interference can be found in the KCNMA1 KO mouse model. These animals show alterations is circadian rhythm, blood pressure, urination and reproduction (221, 223, 227, 234). The use of 4-AP, a potassium channel blocker used to improve neurological conduction in MS patients, is also limited due to the side-effects of potassium channel blockage (115, 230). It is therefore more plausible to investigate cell-

specific effects of these channels to elucidate disease mechanisms and identify cell-specific downstream molecules that can be targeted for therapy.

What about the other identified differentially expressed proteins?

All other proteins identified in our 2D-DIGE studies could be equally, or even more interesting targets for further research. Examples of such protein changes during EAMG are the decrease of β-enolase and the increase of CAIII. β-enolase is a glycolytic enzyme with tissue-specific isoforms that is highly expressed in fast-twitch muscle fibers. The expression increases during muscle development and changes in the expression of β-enolase are correlated to different steps in damage recovery after muscle fibre degradation (131). In EAMG/MG, the decrease of this protein could thus be linked to a compromised muscle regeneration. CAIII is also highly expressed in skeletal muscle where free radicals can rise rapidly during exercise. It's carbon dioxide hydratase functions helps to protect the muscle from oxidative stress (133). The upregulation we report, is in contradiction to the deficiency of CAIII reported in muscle biopsies (135, 268). This deficiency has been linked to weakness and fatigability in MG. The discrepancy in CAIII expression could be a result of experimental setup, and timing might be crucial as the reduction of CAIII expression is greatest immediately after denervation (122). During EAE, the decrease of GABA transaminase, succinaat-semialdehyde dehydrogenase and mitochondrial glutamate dehydrogenase (ABAT, ALDH5A1 and GLUD1) can lead to a local increase of GABA, an inhibitory neurotransmitter that has been linked to autoimmune inflammation (160). Although exogenous increases of GABA seem to aggravate EAE outcome by enhancing IL6 and TNFα production by macrophages and pushing T cells towards a Th1 response, endogenous increases of GABA are neuroprotective, which could be due to a decrease in extracellular glutamate. (160, 269). Or thimet oligopeptidase (THOP1), a protein that increased during EAE. This protein has been linked to Alzheimer's disease where increased expression of this protein was identified as a neuroprotective mechanism (270). Furthermore, THOP1 is part of the renin-angiotensin system (RAS). Another member of the RAS, angiotensin (AGT) itself is an MS-related protein from the IPA knowledge base that showed significant linkage to our data and was selected for building our focus networks (chapter 3). Several other players of the RAS are known to be elevated during MS/EAE and

antagonising this system affects Th1 and Th17 cells and decreases APC related chemokins such as CCL2 and CXCL10, causing an amelioration of EAE symptoms (163). Post-synaptic density protein 95 (DLG4) is also a central protein in the focus networks. This protein is important for clustering of post-synaptic receptors and associated with NMDA receptors in excitatory synapses. A decrease of DLG4 expression in spinal cord during active EAE was previously reported (167). This expression was partially restored during remission or after recovery and thus linked to disease activity. The decrease in DLG4 expression could be linked to an increase in NMDA receptor activity during excitotoxicity, as DLG4 blocks the calcium induced NO production when bound to the NMDA receptor (167, 271, 272). These proteins are just the beginning of the long list of proteins discovered here, but also in other proteomic studies, that could hold powerful information but need to be studied in more detail. The selection of targets for further research is driven by available literature and the data at hand, but it is a selection and remaining proteins could be the unknown major players in the disease mechanism.

Omics studies in general generate massive data sets. Often more data are created than possible to validate and follow up. Reducing data complexity by classification, clustering and identification of active pathways helps to extract biological meaning and to gain functional insights. Considering the large amount of omics data already available in literature and in public repositories, an integrated approach could even be of higher value (273) as was already shown for proteomic and metabolomics data in MS research (274). The integration of omics data could allow for a more complete characterisation of a disease featuring possible targets for further research.

7

NEDERLANDSE SAMENVATTING

Nederlandse samenvatting

Proteomica laat toe om eiwitten te identificeren die een verstoorde expressie vertonen tijdens auto-immune aandoeningen. De identificaties van deze eiwitten kunnen een startpunt betekenen voor de ontwikkeling van betere diagnostische en prognostische testen en nieuwe therapieën. Daarenboven kan deze info leiden tot een betere, meer gedetailleerde kennis van de ziektemechanismen. In dit werk bestudeerde ik de veranderingen van eiwitniveaus tijdens het ziekteverloop vertrekkend van weefsel representatief voor twee auto-immuunziektes, myasthenie en multiple sclerose (MS). Voor een aantal beloftevolle verstoorde eiwitten werd de relatie met het ziektebeeld verder onderzocht.

DEEL 1: PROTEOMICA

Bij *myasthenia gravis* (MG) binden autoantilichamen aan eiwitten van de neuromusculaire junctie. De aanwezigheid van deze autoantilichamen verhindert de signaaltransductie, wat leidt tot spierzwakte (60, 62). Hoewel dit mechanisme goed beschreven is, is het effect hiervan op de eiwitniveaus in de spieren nog grotendeels onbekend. In **hoofdstuk 2** onderzochten we het eiwitprofiel van de *tibialis anterior* spier in verschillende ziektestadia van experimentele auto-immune MG (EAMG), het diermodel voor MG. Voor tweeëntwintig eiwitten werd er een afwijking in eiwitgehalte gevonden tussen de verschillende experimentele groepen. De gevonden veranderingen wezen op een mogelijk verminderde glycolytische capaciteit in de spiercellen en het verlies van type II (fast twitch) vezels wanneer de symptomen verergeren. Gelijkaardige veranderingen werden eerder ook gerapporteerd bij andere aandoeningen die spiercontractie belemmeren (121, 122) en zijn waarschijnlijk het gevolg van de verminderde signalering tussen zenuw en spier. Verder werden er ook andere eiwitten geïdentificeerd in deze studie die interessant zijn voor verder onderzoek.

In tegenstelling tot bij MG, zijn de onderliggende ziektemechanismen bij multiple sclerose (MS) nog relatief ongekend. In **hoofdstuk 3** werden eiwitten geïdentificeerd die een veranderd eiwitniveau vertoonden bij de vorming van inflammatoire hersenletsels gedurende acute experimentele auto-immune encefalomyelitis (EAE), een diermodel voor MS. Eiwitniveaus in de hersenstam werden vergeleken voor aanvang van symptomen, wanneer de symptomen hun

hoogste peil bereikten en na herstel. Vijfenzeventig verstoorde eiwitten werden geïdentificeerd. Enkele van deze eiwitten maken deel uit van processen die actief betrokken zijn bij gekende ziekteprocessen van MS, en bevestigen daardoor de experimentele opzet en de mogelijkheid om op deze manier ziekte gerelateerde eiwitten op te sporen.

Netwerkanalyses

Proteomicastudies zoals hierboven beschreven, leveren lange lijsten met geïdentificeerde eiwitten, eventueel aangevuld met info over verschillen in eiwitniveaus tussen de stalen. Deze lijsten geven echter geen inzicht in de onderliggende biologische mechanismen. Classificatie, clustering en identificatie van actieve cellulaire mechanismen op basis van de bekomen resultaten kan de complexiteit reduceren en zo helpen om de data te interpreteren. Deze netwerkanalyses helpen bij de organisatie van de data, waardoor de moleculaire mechanismen achter de veranderde eiwitniveaus te achterhalen zijn om zo biologische en functionele inzichten te verkrijgen (242, 243). In **hoofdstuk 3** werd een netwerkanalyse uitgevoerd om verbanden tussen de geïdentificeerde eiwitten en ziekteprocessen te vinden aan de hand van Ingenuity Pathway Analysis (IPA). Hierbij werden enkele sleuteleiwitten geïdentificeerd die sterk gerelateerd waren aan onze dataset van veranderde eiwitten en dus een centrale rol kunnen spelen in de ziekteprocessen.

Verder werden de gevonden eiwitten in onze dataset vergeleken met een bestaande lijst van MS-gerelateerde eiwitten uit de IPA databank (244). Hierbij werd er weinig overlap gevonden, maar was er wel een duidelijke connectie tussen de twee datasets. Zo bleek dat onze eiwitten deel uitmaakten van de biochemische processen van de eiwitten uit de IPA-lijst. Deze IPA-lijst is gebaseerd op de literatuur en bevat vooral membraaneiwitten zoals deze aanwezig in de myelinelaag rond de axonen. Onze data zijn verkregen met een gel-gebaseerde techniek (2D-DIGE), die als nadeel heeft dat eiwitten met zeer hoge of lage moleculaire gewichten, extreem iso-elektrisch punt en hydrofobe eigenschappen minder goed op te pikken zijn (245). Hierdoor zijn 76% van de geïdentificeerde eiwitten in onze dataset cytoplasmatisch. Door gebruik te maken van de netwerkanalyse was de connectie tussen de twee datasets toch duidelijk wat de kracht van dit soort netwerkanalyses verder onderstreept. Ook één van de

sleuteleiwitten hierboven vermeld is een membraaneiwit. Buiten de reductie van complexiteit en de identificatie van biologische processen, helpt netwerkanalyse dus ook bij het omzeilen van de technische beperkingen die gepaard gaan met gebruikte technieken.

Maar ook de technieken zelf worden voortdurend geoptimaliseerd. Gel-vrije technieken om kwantitatieve proteomica studies uit te voeren zijn sterk verbeterd in de voorbije jaren. Zowel de technieken om stalen te scheiden als de technieken voor identificatie gingen vooruit door technische verbeteringen van de toestellen en betere software (246). De kwantificatie kan nu zowel met als zonder labels, en ook absolute kwantificatie is mogelijk (247). Door de recente vooruitgang van de gel-vrije technieken, zijn deze op dit moment gevoeliger en betrouwbaarder dan de gel-gebaseerde technieken.

DEEL 2: DE ROL VAN GEÏDENTIFICEERDE EIWITTEN IN ZIEKTE EN GEZONDHEID

Proteomica studies zijn een eerste stap in het vinden van ziekte gerelateerde cellulaire veranderingen. Verder onderzoek is echter nodig om de functionele rol van deze eiwitten in het ziekteproces te ontrafelen. Twee eiwitten uit de MS-studie werden geselecteerd voor verder onderzoek, namelijk CRMP2 en KCNMA1. De functie van beide eiwitten in het gezonde centraal zenuwstelsel is gekend (172, 227) en CRMP2 werd als signaalmolecule van Nogo-A al gelinkt aan MS (112). Hun functie in het immuunsysteem en de relatie hiervan met de pathogenese van MS werd echter nog niet grondig bestudeerd.

CRMP2

CRMP2 speelt een rol in de ontwikkeling van de hersenen, het is onder andere belangrijk voor de differentiatie tussen neuriet en axon. In onze studie werd CRMP2 geïdentificeerd in tien eiwitspots met een gewijzigd eiwitniveau gedurende het ziekteproces in EAE. De aanwezigheid van een eiwit in verschillende eiwitspots kan duiden op het voorkomen van verschillende isovormen, posttranslationele veranderingen (PTM) en eiwitafbraak. Verschillende fosforyleringsvormen van CRMP2 zijn gekend, en hebben elk andere functies. Zo zorgt Thr555 fosforylering voor stopzetting van neurietuitgroei en Tyr479 fosforylering voor T-celproliferatie (176, 186), functies die betrokken kunnen zijn in de progressie van MS. Verder

werd zijn neurale functie als signaalmolecule van Nogo-A gelinkt aan neurodegeneratie in MS (112). Blokkering van deze signaalcascade zorgt voor een verminderding van CRMP2 Thr555 fosforylering, verminderde axonale degeneratie en een vermindering van EAE ziekteprogressie (112). Deze associatie van CRMP2 met neurodegeneratie in MS en het feit dat CRMP2 ook betrokken is bij T-celmigratie tijdens virusgeïnduceerde neuro-inflammatie (185) hebben ervoor gezorgd dat dit eiwit geselecteerd werd voor verder onderzoek.

In **hoofdstuk 4** werd de expressie van CRMP2 in verschillende monocyt- en T-celsubsets geanalyseerd. De expressie van CRMP2 was hoger in regulatoire T-cellen (Treg) in vergelijking met conventionele T-cellen (Tconv), in geheugen T-cellen vergeleken met naïve T-cellen en in T-helper (Th)1-cellen vergeleken met Th2 en Th17 cellen. Ook in geactiveerde lymfocyten was er een verhoogde CRMP2 expressie. De expressie van CRMP2 was hoger in monocyten dan in T-cellen, met de hoogste expressie in de intermediaire pro-inflammatoire monocyten. De eiwitniveaus van CRMP2 waren hoger in T-cellen van gezonde donoren dan in die van relapsing-remitting MS patiënten. Deze resultaten laten zien dat CRMP2 niveaus variabel zijn in de verschillende T-cel- en monocytsubtypes en dat ze significant dalen in al deze celtypes bij RRMS-patiënten.

In T-cellen is CRMP2 belangrijk voor activatie van cellulaire migratie (181). Een verminderde expressie van CRMP2 in bloedafgeleide T-cellen kan dus een indicatie zijn voor een verminderde migratiecapaciteit van deze cellen. Een verminderde migratie van Treg naar het centraal zenuwstelsel kan zo leiden tot een toestand van voortdurende inflammatie. Maar ook Th1 en Th17 vertonen een verminderde CRMP2-expressie in RRMS-stalen, terwijl deze cellen sterk geassocieerd zijn met MS-hersenletsels. Een mogelijke verklaring hiervoor kan zijn dat de T-cellen met een hoge CRMP2-expressie beter migreren naar het centraal zenuwstelsel en hierdoor de cellen met een lagere CRMP2 expressie in de circulatie overblijven.

De associatie tussen CRMP2 niveaus en T-celmigratie werd al in detail bestudeerd (181, 185-187). Hieruit blijkt dat een verminderde Thr509/Thr514 fosforylering en hogere Tyr479 fosforylering van CRMP2 een belangrijke rol spelen in T-celmigratie; een rol in de MS pathogenese werd zelfs gesuggereerd. Het antilichaam dat gebruikt werd voor bepaling van CRMP2 expressie in T-cellen en monocyten kan echter geen onderscheid maken tussen de verschillende fosforyleringsvormen. Om een beter inzicht te krijgen in de rol van CRMP2

expressie in T-celmigratie gedurende de MS-pathogenese is een studie van de verschillende fosforyleringsvormen nodig. De functionele rol van CRMP2 in monocyten is nog onbekend. Het verschil in expressieniveau tussen de verschillende monocytpopulaties en de daling van het CRMP2-niveau in deze cellen gedurende RRMS kan een indicatie zijn voor een rol van CRMP2 in de migratie van deze monocyten, zoals werd aangetoond voor T-cellen. Verder onderzoek is nodig om deze hypothese te testen.

CRMP2 kan therapeutisch gemoduleerd worden met behulp van lanthionine ketamine dat CRMP2 bindt, of met de synthetische vorm hiervan, lanthionine ketimine ester (LKE) dat cellen kan binnendringen. LKE promoot neurogenese, blokkeert NO-productie door microglia en vermindert de neurotoxiciteit van geconditioneerd microglia medium (255-257). In EAE zorgt LKE voor een vermindering van de symptomen door een verlaging van de IFNγ-productie door T-cellen en een vermindering van de neurodegeneratie (258). Het effect op T-celmigratie werd niet onderzocht. Ook andere therapeutische opties om CRMP2 te moduleren zijn beschikbaar, maar deze worden momenteel niet getest voor de behandeling van MS. Voorbeelden hiervan zijn lacosamide en tianeptine, die respectievelijk gebruikt worden in de behandeling van epilepsie en depressie. Therapeutische modulatie van CRMP2 is dus mogelijk, en wordt in andere aandoeningen al gebruikt. Vooraleer hiermee verder gegaan kan worden, dient er eerst meer basisonderzoek te gebeuren naar de moleculaire mechanismen waarbij CRMP2 betrokken is in het MS ziekteproces (174).

Buiten de therapeutische opties, zou de detectie van specifieke fosforyleringsvormen van CRMP2 gebruikt kunnen worden als potentiele biomerker. In een patentaanvraag van P. Giraudon staat beschreven dat de detectie van Tyr479 fosforylering in immuuncelsubsets een indicatie kan geven van de ziekteactiviteit bij inflammatoire aandoeningen van het centraal zenuwstelsel zoals MS en dat dit kan helpen bij het stellen van een diagnose en prognose en bij de opvolging van de ziekte (264). Alles samen genomen is de rol van CRMP2 in neuronale en immunologische MS-ziekteprocessen duidelijk en is verder onderzoek naar de exacte werkingsmechanismen en mogelijke interventies momenteel aan de gang.

KCNMA1

KCNMA1 is een kaliumkanaal dat geactiveerd wordt door de aanwezigheid van calcium. Activatie zorgt ervoor dat dit kanaal open gaat, en kalium uit de cel kan. Dit resulteert in hyperpolarisatie en dus een verminderde exciteerbaarheid. KCNMA1 werd door netwerkanalyse aan onze data gelinkt, en heeft dus geen gewijzigde eiwitniveaus gedurende EAE. De centrale rol van dit eiwit in de netwerkanalyse kan dus wijzen op veranderingen in activatie en dus cel excitatie (226, 227). Andere kaliumkanalen werden eerder al onderzocht in relatie tot MS, en blokkering van dit soort kanalen is effectief voor het verminderen van de EAE-ziektescore en het verbeteren van de neurologische geleiding (228, 230). In hoofdstuk 3 toonden we aan dat KCNMA1 blokkering met paxilline zorgt voor een vermindering van myelineopname door macrofagen *in vitro*. Proinflammatiore macrofagen zijn actief betrokken bij de afbraak van myeline in MS-letsels.

Blokkering van KCNMA1 zorgde ook in primaire macrofagen voor een daling van de myelineopname (**hoofdstuk 5**). Dit effect was echter alleen te zien bij complete blokkering, er was geen dosis-afhankelijk effect. De myelineafbraak die geïnduceerd wordt door cuprizone werd vervolgens vergeleken in controle dieren en in genetisch gemanipuleerde dieren die geen KCNMA1 tot expressie brengen (KCNMA1 knock-out (KO)). Hieruit bleek dat de afbraak van myeline, die in dit model vooral op microglia berust, niet beïnvloed werd door de afwezigheid van KCNMA1. Dit kan het gevolg zijn van compensatiemechanismen, die meer uitgesproken zijn bij genetische knock-out in vergelijking met een blokkering door een chemische blokker. In verdere *in vitro* experimenten werd echter een effect gezien van paxilline op de myelineopname door KCNMA1 KO macrofagen. Dit impliceert dat de effecten die eerder geobserveerd werden met paxilline het gevolg kunnen zijn van andere mechanismen die onafhankelijk verlopen van KCNMA1.

Paxilline is bij nader inziens dus geen specifieke blokker, zoals wel beschreven is in de literatuur. Een selectieve blokker is dus nodig om de cellulaire effecten van KCNMA1 blokkering te onderzoeken. Hiervoor zijn enkele opties, waaronder iberiotoxine beschikbaar (225). Een andere optie om de biologische en cel-specifieke functie van KCNMA1 te onderzoeken is het gebruik van conditionele, cel-specifieke knock-out modellen. Hierbij kan KCNMA1 conditioneel geïnactiveerd worden in een bepaald celtype of weefsel, waardoor de systemische en

compensatoire effecten van een algemeen knock-out model kunnen voorkomen worden (221).

De exacte functionele rol van KCNMA1 in macrofagen en microglia moet nog achterhaald worden, maar enkele functies zijn al bekend. Zo gaan KCNMA1 eiwitniveaus omhoog bij de activatie van pro-inflammatoire microglia (168) en is KCNMA1 nodig voor IL-1 afhankelijke macrofaagactivatie (240) en voor TNF- α en IL-6 productie in geactiveerde type-1 macrofagen (224). Verder onderzoek naar de mogelijke functionele invloed van KCNMA1 in deze cellen tijdens ziekteprocessen gerelateerd aan MS is nodig.

CRMP2, KCNMA1,…

Zowel CRMP2 als KCNMA1 zijn eiwitten die in vele celtypes tot expressie komen. Beide werden eerder al aan celmobiliteit gekoppeld (168, 172, 173, 185, 250-252). CRMP2 stabiliseert tubuline (173) en fosforylering is verantwoordelijk voor een verminderde tubuline- en actinestabiliteit (175). Deze functie van CRMP2 wordt verantwoordelijk geacht voor de stopzetting van neuriet uitgroei (173) en T-cel migratie (187). KCNMA1 wordt verder gelinkt aan verhoogde invasiviteit van kankercellen door het verhogen van de celmigratie (250, 251). Bij mijn weten is er geen directe link tussen CRMP2 en KCNMA1, hoewel ze beiden een rol spelen bij celmotiliteit en dus beiden verantwoordelijk kunnen zijn voor immuuncelmigratie en axonale groei, processen die betrokken zijn bij MS-ziektemechanismen.

Ook andere eiwitten die geïdentificeerd werden in onze 2D-DIGE studies zijn interessante targets voor verder onderzoek. Proteomicastudies leveren in het algemeen grote datasets op. Vaak worden er meer data gecreëerd dan de hoeveelheid die gevalideerd en opgevolgd kan worden. Deze data kunnen belangrijke informatie bevatten, maar moeten meer in detail onderzocht worden. Reductie van de complexiteit van de data door middel van netwerkanalyses kan hierbij helpen omdat ze biologische en functionele inzichten verschaffen. Vele omics data zijn beschikbaar in de literatuur en een geïntegreerde aanpak om extra info uit deze data te halen kan waardevol zijn. Dit werd al gedaan voor proteomica- en metabolomicadata in MS-onderzoek (274). Dit laat een completere

karakterisering toe van een ziekte, eventueel met mogelijke targets voor verder onderzoek.

Naast de identificatie blijft een diepgaande functionele analyse noodzakelijk. De resultaten beschreven in deze thesis zijn daarom een inspanning om in eerste instantie eiwitten te identificeren die betrokken zijn bij auto-immune aandoeningen en verder, om hun specifieke rol in deze ziekten te onthullen. Van de geïdentificeerde eiwitten die betrokken zijn bij de ziektemechanismen van MG of MS werden hier twee eiwitten betrokken bij EAE-pathogenese –CRMP2 en KCNMA1- geselecteerd voor verder onderzoek naar hun functie in het immuunsysteem. De functie van CRMP2 en KCNMA1 in het immuunsysteem werd onderzocht. Vervolgonderzoek blijft evenwel noodzakelijk om de exacte functionele rol van deze eiwitten in het ziekteproces te achterhalen.

Reference list

1. Srivastava R, Aslam M, Kalluri SR, Schirmer L, Buck D, Tackenberg B, et al. Potassium channel KIR4.1 as an immune target in multiple sclerosis. N Engl J Med. 2012;367(2):115-23.
2. Slaets H, Hendriks JJ, Van den Haute C, Coun F, Baekelandt V, Stinissen P, et al. CNS-targeted LIF expression improves therapeutic efficacy and limits autoimmune-mediated demyelination in a model of multiple sclerosis. Mol Ther. 2010;18(4):684-91.
3. Han MH, Hwang SI, Roy DB, Lundgren DH, Price JV, Ousman SS, et al. Proteomic analysis of active multiple sclerosis lesions reveals therapeutic targets. Nature. 2008;451(7182):1076-81.
4. International Multiple Sclerosis Genetics C. Network-based multiple sclerosis pathway analysis with GWAS data from 15,000 cases and 30,000 controls. American journal of human genetics. 2013;92(6):854-65.
5. Bhat R, Steinman L. Innate and adaptive autoimmunity directed to the central nervous system. Neuron. 2009;64(1):123-32.
6. Kamm CP, Uitdehaag BM, Polman CH. Multiple sclerosis: current knowledge and future outlook. European neurology. 2014;72(3-4):132-41.
7. Houtchens MK, Bove R. A case for gender-based approach to multiple sclerosis therapeutics. Front Neuroendocrinol. 2018.
8. Noseworthy JH, Lucchinetti C, Rodriguez M, Weinshenker BG. Multiple sclerosis. N Engl J Med. 2000;343(13):938-52.
9. Trapp BD, Nave KA. Multiple sclerosis: an immune or neurodegenerative disorder? Annual review of neuroscience. 2008;31:247-69.
10. Hellings N, Raus J, Stinissen P. Insights into the immunopathogenesis of multiple sclerosis. Immunol Res. 2002;25(1):27-51.
11. Lassmann H. Recent neuropathological findings in MS--implications for diagnosis and therapy. J Neurol. 2004;251 Suppl 4:IV2-5.
12. Miller D, Barkhof F, Montalban X, Thompson A, Filippi M. Clinically isolated syndromes suggestive of multiple sclerosis, part 2: non-conventional MRI, recovery processes, and management. Lancet Neurol. 2005;4(6):341-8.
13. Miller DH, Chard DT, Ciccarelli O. Clinically isolated syndromes. Lancet Neurol. 2012;11(2):157-69.
14. Compston A, Coles A. Multiple sclerosis. Lancet. 2008;372(9648):1502-17.

15. McDonald WI, Compston A, Edan G, Goodkin D, Hartung HP, Lublin FD, et al. Recommended diagnostic criteria for multiple sclerosis: guidelines from the International Panel on the diagnosis of multiple sclerosis. Ann Neurol. 2001;50(1):121-7.
16. Polman CH, Reingold SC, Banwell B, Clanet M, Cohen JA, Filippi M, et al. Diagnostic criteria for multiple sclerosis: 2010 revisions to the McDonald criteria. Ann Neurol. 2011;69(2):292-302.
17. Lassmann H, Bruck W, Lucchinetti CF. The immunopathology of multiple sclerosis: an overview. Brain Pathol. 2007;17(2):210-8.
18. Hafler DA. Multiple sclerosis. J Clin Invest. 2004;113(6):788-94.
19. Lublin FD, Reingold SC, Cohen JA, Cutter GR, Sorensen PS, Thompson AJ, et al. Defining the clinical course of multiple sclerosis: the 2013 revisions. Neurology. 2014;83(3):278-86.
20. Killestein J, Rudick RA, Polman CH. Oral treatment for multiple sclerosis. Lancet Neurol. 2011;10(11):1026-34.
21. Reich DS, Lucchinetti CF, Calabresi PA. Multiple Sclerosis. N Engl J Med. 2018;378(2):169-80.
22. Ciotti JR, Cross AH. Disease-Modifying Treatment in Progressive Multiple Sclerosis. Curr Treat Options Neurol. 2018;20(5):12.
23. International Multiple Sclerosis Genetics C, Beecham AH, Patsopoulos NA, Xifara DK, Davis MF, Kemppinen A, et al. Analysis of immune-related loci identifies 48 new susceptibility variants for multiple sclerosis. Nat Genet. 2013;45(11):1353-60.
24. Lill CM. Recent advances and future challenges in the genetics of multiple sclerosis. Frontiers in neurology. 2014;5:130.
25. International Multiple Sclerosis Genetics C, Wellcome Trust Case Control C, Sawcer S, Hellenthal G, Pirinen M, Spencer CC, et al. Genetic risk and a primary role for cell-mediated immune mechanisms in multiple sclerosis. Nature. 2011;476(7359):214-9.
26. Krementsov DN, Teuscher C. Environmental factors acting during development to influence MS risk: insights from animal studies. Mult Scler. 2013;19(13):1684-9.
27. Ebers GC. Environmental factors and multiple sclerosis. Lancet Neurol. 2008;7(3):268-77.
28. Comabella M, Kakalacheva K, Rio J, Munz C, Montalban X, Lunemann JD. EBV-specific immune responses in patients with multiple sclerosis responding to IFNbeta therapy. Mult Scler. 2012;18(5):605-9.
29. Muller DN, Kleinewietfeld M, Kvakan H. Vitamin D review. Journal of the renin-angiotensin-aldosterone system : JRAAS. 2011;12(2):125-8.

30. Mouhieddine TH, Darwish H, Fawaz L, Yamout B, Tamim H, Khoury SJ. Risk factors for multiple sclerosis and associations with anti-EBV antibody titers. Clinical immunology. 2015.
31. McKay KA, Kwan V, Duggan T, Tremlett H. Risk factors associated with the onset of relapsing-remitting and primary progressive multiple sclerosis: a systematic review. Biomed Res Int. 2015;2015:817238.
32. Pantazou V, Schluep M, Du Pasquier R. Environmental factors in multiple sclerosis. Presse medicale. 2015.
33. Mameli G, Cossu D, Cocco E, Masala S, Frau J, Marrosu MG, et al. Epstein-Barr virus and Mycobacterium avium subsp. paratuberculosis peptides are cross recognized by anti-myelin basic protein antibodies in multiple sclerosis patients. J Neuroimmunol. 2014;270(1-2):51-5.
34. Vanheusden M, Stinissen P, t Hart BA, Hellings N. Cytomegalovirus: a culprit or protector in multiple sclerosis? Trends in molecular medicine. 2015;21(1):16-23.
35. Joller N, Peters A, Anderson AC, Kuchroo VK. Immune checkpoints in central nervous system autoimmunity. Immunological reviews. 2012;248(1):122-39.
36. Chastain EM, Miller SD. Molecular mimicry as an inducing trigger for CNS autoimmune demyelinating disease. Immunological reviews. 2012;245(1):227-38.
37. Stys PK, Zamponi GW, van Minnen J, Geurts JJ. Will the real multiple sclerosis please stand up? Nature reviews Neuroscience. 2012;13(7):507-14.
38. Hoglund RA, Maghazachi AA. Multiple sclerosis and the role of immune cells. World journal of experimental medicine. 2014;4(3):27-37.
39. Schneider-Hohendorf T, Stenner MP, Weidenfeller C, Zozulya AL, Simon OJ, Schwab N, et al. Regulatory T cells exhibit enhanced migratory characteristics, a feature impaired in patients with multiple sclerosis. European journal of immunology. 2010;40(12):3581-90.
40. Venken K, Hellings N, Liblau R, Stinissen P. Disturbed regulatory T cell homeostasis in multiple sclerosis. Trends in molecular medicine. 2010;16(2):58-68.
41. Broux B, Stinissen P, Hellings N. Which immune cells matter? The immunopathogenesis of multiple sclerosis. Crit Rev Immunol. 2013;33(4):283-306.
42. Hemmer B, Nessler S, Zhou D, Kieseier B, Hartung HP. Immunopathogenesis and immunotherapy of multiple sclerosis. Nature clinical practice Neurology. 2006;2(4):201-11.

43. Veldhoen M, Hocking RJ, Atkins CJ, Locksley RM, Stockinger B. TGFbeta in the context of an inflammatory cytokine milieu supports de novo differentiation of IL-17-producing T cells. Immunity. 2006;24(2):179-89.
44. Jadidi-Niaragh F, Mirshafiey A. Th17 cell, the new player of neuroinflammatory process in multiple sclerosis. Scandinavian journal of immunology. 2011;74(1):1-13.
45. Rodriguez M. Effectors of demyelination and remyelination in the CNS: implications for multiple sclerosis. Brain Pathol. 2007;17(2):219-29.
46. Hendriks JJ, Teunissen CE, de Vries HE, Dijkstra CD. Macrophages and neurodegeneration. Brain research Brain research reviews. 2005;48(2):185-95.
47. Barnett MH, Henderson AP, Prineas JW. The macrophage in MS: just a scavenger after all? Pathology and pathogenesis of the acute MS lesion. Mult Scler. 2006;12(2):121-32.
48. Fraussen J, Vrolix K, Martinez-Martinez P, Losen M, De Baets MH, Stinissen P, et al. B cell characterization and reactivity analysis in multiple sclerosis. Autoimmunity reviews. 2009;8(8):654-8.
49. de Bock L, Somers K, Fraussen J, Hendriks JJ, van Horssen J, Rouwette M, et al. Sperm-associated antigen 16 is a novel target of the humoral autoimmune response in multiple sclerosis. J Immunol. 2014;193(5):2147-56.
50. Rouwette M, Noben JP, Van Horssen J, Van Wijmeersch B, Hupperts R, Jongen PJ, et al. Identification of coronin-1a as a novel antibody target for clinically isolated syndrome and multiple sclerosis. J Neurochem. 2013;126(4):483-92.
51. Foote AK, Blakemore WF. Inflammation stimulates remyelination in areas of chronic demyelination. Brain : a journal of neurology. 2005;128(Pt 3):528-39.
52. Krishnamoorthy G, Wekerle H. EAE: an immunologist's magic eye. European journal of immunology. 2009;39(8):2031-5.
53. Matsushima GK, Morell P. The neurotoxicant, cuprizone, as a model to study demyelination and remyelination in the central nervous system. Brain Pathol. 2001;11(1):107-16.
54. Blakemore WF, Franklin RJ. Remyelination in experimental models of toxin-induced demyelination. Curr Top Microbiol Immunol. 2008;318:193-212.
55. Ransohoff RM. Animal models of multiple sclerosis: the good, the bad and the bottom line. Nat Neurosci. 2012;15(8):1074-7.

56. Procaccini C, De Rosa V, Pucino V, Formisano L, Matarese G. Animal models of Multiple Sclerosis. European Journal of Pharmacology. 2015;759:182-91.
57. Romi F, Hong Y, Gilhus NE. Pathophysiology and immunological profile of myasthenia gravis and its subgroups. Curr Opin Immunol. 2017;49:9-13.
58. Richman DP. Antibodies to low density lipoprotein receptor-related protein 4 in seronegative myasthenia gravis. Archives of neurology. 2012;69(4):434-5.
59. Silvestri NJ, Wolfe GI. Myasthenia gravis. Seminars in neurology. 2012;32(3):215-26.
60. Gomez AM, Van Den Broeck J, Vrolix K, Janssen SP, Lemmens MA, Van Der Esch E, et al. Antibody effector mechanisms in myasthenia gravis-pathogenesis at the neuromuscular junction. Autoimmunity. 2010;43(5-6):353-70.
61. Martinez-Martinez P, Losen M, Duimel H, Frederik P, Spaans F, Molenaar P, et al. Overexpression of rapsyn in rat muscle increases acetylcholine receptor levels in chronic experimental autoimmune myasthenia gravis. Am J Pathol. 2007;170(2):644-57.
62. Conti-Fine BM, Milani M, Kaminski HJ. Myasthenia gravis: past, present, and future. J Clin Invest. 2006;116(11):2843-54.
63. Zheng PP, Kros JM, Sillevis-Smitt PA, Luider TM. Proteomics in primary brain tumors. Front Biosci. 2003;8:d451-63.
64. de Sousa Abreu R, Penalva LO, Marcotte EM, Vogel C. Global signatures of protein and mRNA expression levels. Mol Biosyst. 2009;5(12):1512-26.
65. Dressaire C, Gitton C, Loubiere P, Monnet V, Queinnec I, Cocaign-Bousquet M. Transcriptome and proteome exploration to model translation efficiency and protein stability in Lactococcus lactis. PLoS computational biology. 2009;5(12):e1000606.
66. Betts JC. Transcriptomics and proteomics: tools for the identification of novel drug targets and vaccine candidates for tuberculosis. IUBMB Life. 2002;53(4-5):239-42.
67. Evans C, Corfe B. Promotion of cancer metastasis: candidate validation using an iTRAQ-based approach. Expert Rev Proteomics. 2013;10(4):321-3.
68. Evans C, Noirel J, Ow SY, Salim M, Pereira-Medrano AG, Couto N, et al. An insight into iTRAQ: where do we stand now? Anal Bioanal Chem. 2012;404(4):1011-27.

69. Werner T, Sweetman G, Savitski MF, Mathieson T, Bantscheff M, Savitski MM. Ion coalescence of neutron encoded TMT 10-plex reporter ions. Anal Chem. 2014;86(7):3594-601.
70. Werner T, Becher I, Sweetman G, Doce C, Savitski MM, Bantscheff M. High-resolution enabled TMT 8-plexing. Anal Chem. 2012;84(16):7188-94.
71. Ong SE, Mann M. Stable isotope labeling by amino acids in cell culture for quantitative proteomics. Methods Mol Biol. 2007;359:37-52.
72. Nahnsen S, Bielow C, Reinert K, Kohlbacher O. Tools for label-free peptide quantification. Mol Cell Proteomics. 2013;12(3):549-56.
73. Vidova V, Spacil Z. A review on mass spectrometry-based quantitative proteomics: Targeted and data independent acquisition. Anal Chim Acta. 2017;964:7-23.
74. Elkabes S, Li H. Proteomic strategies in multiple sclerosis and its animal models. Proteomics Clinical applications. 2007;1(11):1393-405.
75. Unlu M, Morgan ME, Minden JS. Difference gel electrophoresis: a single gel method for detecting changes in protein extracts. Electrophoresis. 1997;18(11):2071-7.
76. Alban A, David SO, Bjorkesten L, Andersson C, Sloge E, Lewis S, et al. A novel experimental design for comparative two-dimensional gel analysis: two-dimensional difference gel electrophoresis incorporating a pooled internal standard. Proteomics. 2003;3(1):36-44.
77. Karp NA, Kreil DP, Lilley KS. Determining a significant change in protein expression with DeCyder during a pair-wise comparison using two-dimensional difference gel electrophoresis. Proteomics. 2004;4(5):1421-32.
78. Bayes A, Grant SG. Neuroproteomics: understanding the molecular organization and complexity of the brain. Nature reviews Neuroscience. 2009;10(9):635-46.
79. Farias AS, Pradella F, Schmitt A, Santos LM, Martins-de-Souza D. Ten years of proteomics in multiple sclerosis. Proteomics. 2014;14(4-5):467-80.
80. Lehmensiek V, Sussmuth SD, Tauscher G, Brettschneider J, Felk S, Gillardon F, et al. Cerebrospinal fluid proteome profile in multiple sclerosis. Mult Scler. 2007;13(7):840-9.
81. Stoop MP, Singh V, Dekker LJ, Titulaer MK, Stingl C, Burgers PC, et al. Proteomics comparison of cerebrospinal fluid of relapsing remitting and primary progressive multiple sclerosis. PLoS One. 2010;5(8):e12442.

82. Farias AS, Santos LM. How can proteomics elucidate the complexity of multiple sclerosis? Proteomics Clinical applications. 2015;9(9-10):844-7.
83. Tumani H, Lehmensiek V, Rau D, Guttmann I, Tauscher G, Mogel H, et al. CSF proteome analysis in clinically isolated syndrome (CIS): candidate markers for conversion to definite multiple sclerosis. Neurosci Lett. 2009;452(2):214-7.
84. Linker RA, Brechlin P, Jesse S, Steinacker P, Lee DH, Asif AR, et al. Proteome profiling in murine models of multiple sclerosis: identification of stage specific markers and culprits for tissue damage. PLoS One. 2009;4(10):e7624.
85. Slaets H, Dumont D, Vanderlocht J, Noben JP, Leprince P, Robben J, et al. Leukemia inhibitory factor induces an antiapoptotic response in oligodendrocytes through Akt-phosphorylation and up-regulation of 14-3-3. Proteomics. 2008;8(6):1237-47.
86. Qin Z, Qin Y, Liu S. Alteration of DBP levels in CSF of patients with MS by proteomics analysis. Cell Mol Neurobiol. 2009;29(2):203-10.
87. Liu S, Bai S, Qin Z, Yang Y, Cui Y, Qin Y. Quantitative proteomic analysis of the cerebrospinal fluid of patients with multiple sclerosis. J Cell Mol Med. 2009;13(8A):1586-603.
88. Yang M, Qin Z, Zhu Y, Li Y, Qin Y, Jing Y, et al. Vitamin D-binding protein in cerebrospinal fluid is associated with multiple sclerosis progression. Molecular neurobiology. 2013;47(3):946-56.
89. Gandhi KS, McKay FC, Diefenbach E, Crossett B, Schibeci SD, Heard RN, et al. Novel approaches to detect serum biomarkers for clinical response to interferon-beta treatment in multiple sclerosis. PLoS One. 2010;5(5):e10484.
90. Liu T, Donahue KC, Hu J, Kurnellas MP, Grant JE, Li H, et al. Identification of differentially expressed proteins in experimental autoimmune encephalomyelitis (EAE) by proteomic analysis of the spinal cord. J Proteome Res. 2007;6(7):2565-75.
91. Jain MR, Bian S, Liu T, Hu J, Elkabes S, Li H. Altered proteolytic events in experimental autoimmune encephalomyelitis discovered by iTRAQ shotgun proteomics analysis of spinal cord. Proteome Sci. 2009;7:25.
92. Jain MR, Li Q, Liu T, Rinaggio J, Ketkar A, Tournier V, et al. Proteomic identification of immunoproteasome accumulation in formalin-fixed rodent spinal cords with experimental autoimmune encephalomyelitis. J Proteome Res. 2012;11(3):1791-803.
93. Stoop MP, Dekker LJ, Titulaer MK, Lamers RJ, Burgers PC, Sillevis Smitt PA, et al. Quantitative matrix-assisted laser desorption ionization-

fourier transform ion cyclotron resonance (MALDI-FT-ICR) peptide profiling and identification of multiple-sclerosis-related proteins. J Proteome Res. 2009;8(3):1404-14.
94. Rosenling T, Stoop MP, Attali A, van Aken H, Suidgeest E, Christin C, et al. Profiling and identification of cerebrospinal fluid proteins in a rat EAE model of multiple sclerosis. J Proteome Res. 2012;11(4):2048-60.
95. Stoop MP, Rosenling T, Attali A, Meesters RJ, Stingl C, Dekker LJ, et al. Minocycline effects on the cerebrospinal fluid proteome of experimental autoimmune encephalomyelitis rats. J Proteome Res. 2012;11(8):4315-25.
96. Stoop MP, Singh V, Stingl C, Martin R, Khademi M, Olsson T, et al. Effects of natalizumab treatment on the cerebrospinal fluid proteome of multiple sclerosis patients. J Proteome Res. 2013;12(3):1101-7.
97. Stoop MP, Runia TF, Stingl C, van der Vuurst de Vries RM, Luider TM, Hintzen RQ. Decreased Neuro-Axonal Proteins in CSF at First Attack of Suspected Multiple Sclerosis. Proteomics Clinical applications. 2017;11(11-12).
98. Comabella M, Fernandez M, Martin R, Rivera-Vallve S, Borras E, Chiva C, et al. Cerebrospinal fluid chitinase 3-like 1 levels are associated with conversion to multiple sclerosis. Brain : a journal of neurology. 2010;133(Pt 4):1082-93.
99. Ly L, Barnett MH, Zheng YZ, Gulati T, Prineas JW, Crossett B. Comprehensive tissue processing strategy for quantitative proteomics of formalin-fixed multiple sclerosis lesions. J Proteome Res. 2011;10(10):4855-68.
100. Kroksveen AC, Aasebo E, Vethe H, Van Pesch V, Franciotta D, Teunissen CE, et al. Discovery and initial verification of differentially abundant proteins between multiple sclerosis patients and controls using iTRAQ and SID-SRM. J Proteomics. 2013;78:312-25.
101. Kroksveen AC, Jaffe JD, Aasebo E, Barsnes H, Bjorlykke Y, Franciotta D, et al. Quantitative proteomics suggests decrease in the secretogranin-1 cerebrospinal fluid levels during the disease course of multiple sclerosis. Proteomics. 2015;15(19):3361-9.
102. Kroksveen AC, Guldbrandsen A, Vaudel M, Lereim RR, Barsnes H, Myhr KM, et al. In-Depth Cerebrospinal Fluid Quantitative Proteome and Deglycoproteome Analysis: Presenting a Comprehensive Picture of Pathways and Processes Affected by Multiple Sclerosis. J Proteome Res. 2017;16(1):179-94.
103. Raphael I, Mahesula S, Purkar A, Black D, Catala A, Gelfond JA, et al. Microwave & magnetic (M2) proteomics reveals CNS-specific protein

expression waves that precede clinical symptoms of experimental autoimmune encephalomyelitis. Sci Rep. 2014;4:6210.
104. Hinsinger G, Galeotti N, Nabholz N, Urbach S, Rigau V, Demattei C, et al. Chitinase 3-like proteins as diagnostic and prognostic biomarkers of multiple sclerosis. Mult Scler. 2015;21(10):1251-61.
105. Tremlett H, Dai DL, Hollander Z, Kapanen A, Aziz T, Wilson-McManus JE, et al. Serum proteomics in multiple sclerosis disease progression. J Proteomics. 2015;118:2-11.
106. Pavelek Z, Vysata O, Tambor V, Pimkova K, Vu DL, Kuca K, et al. Proteomic analysis of cerebrospinal fluid for relapsing-remitting multiple sclerosis and clinically isolated syndrome. Biomed Rep. 2016;5(1):35-40.
107. Opsahl JA, Vaudel M, Guldbrandsen A, Aasebo E, Van Pesch V, Franciotta D, et al. Label-free analysis of human cerebrospinal fluid addressing various normalization strategies and revealing protein groups affected by multiple sclerosis. Proteomics. 2016;16(7):1154-65.
108. Jia Y, Wu T, Jelinek CA, Bielekova B, Chang L, Newsome S, et al. Development of protein biomarkers in cerebrospinal fluid for secondary progressive multiple sclerosis using selected reaction monitoring mass spectrometry (SRM-MS). Clinical proteomics. 2012;9(1):9.
109. Dumont D, Noben JP, Raus J, Stinissen P, Robben J. Proteomic analysis of cerebrospinal fluid from multiple sclerosis patients. Proteomics. 2004;4(7):2117-24.
110. Noben JP, Dumont D, Kwasnikowska N, Verhaert P, Somers V, Hupperts R, et al. Lumbar cerebrospinal fluid proteome in multiple sclerosis: characterization by ultrafiltration, liquid chromatography, and mass spectrometry. J Proteome Res. 2006;5(7):1647-57.
111. Vanderlocht J, Hellings N, Hendriks JJ, Vandenabeele F, Moreels M, Buntinx M, et al. Leukemia inhibitory factor is produced by myelin-reactive T cells from multiple sclerosis patients and protects against tumor necrosis factor-alpha-induced oligodendrocyte apoptosis. J Neurosci Res. 2006;83(5):763-74.
112. Petratos S, Ozturk E, Azari MF, Kenny R, Lee JY, Magee KA, et al. Limiting multiple sclerosis related axonopathy by blocking Nogo receptor and CRMP-2 phosphorylation. Brain : a journal of neurology. 2012;135(Pt 6):1794-818.
113. Varrin-Doyer M, Nicolle A, Marignier R, Cavagna S, Benetollo C, Wattel E, et al. Human T lymphotropic virus type 1 increases T lymphocyte migration by recruiting the cytoskeleton organizer CRMP2. J Immunol. 2012;188(3):1222-33.

114. Hoshi T, Pantazis A, Olcese R. Transduction of voltage and Ca2+ signals by Slo1 BK channels. Physiology (Bethesda). 2013;28(3):172-89.
115. Judge SI, Lee JM, Bever CT, Jr., Hoffman PM. Voltage-gated potassium channels in multiple sclerosis: Overview and new implications for treatment of central nervous system inflammation and degeneration. J Rehabil Res Dev. 2006;43(1):111-22.
116. Lilley KS, Friedman DB. All about DIGE: quantification technology for differential-display 2D-gel proteomics. Expert Rev Proteomics. 2004;1(4):401-9.
117. Gomez AM, Vrolix K, Martinez-Martinez P, Molenaar PC, Phernambucq M, van der Esch E, et al. Proteasome inhibition with bortezomib depletes plasma cells and autoantibodies in experimental autoimmune myasthenia gravis. J Immunol. 2011;186(4):2503-13.
118. Sizova D, Charbaut E, Delalande F, Poirier F, High AA, Parker F, et al. Proteomic analysis of brain tissue from an Alzheimer's disease mouse model by two-dimensional difference gel electrophoresis. Neurobiol Aging. 2007;28(3):357-70.
119. Vanheel A, Daniels R, Plaisance S, Baeten K, Hendriks JJ, Leprince P, et al. Identification of protein networks involved in the disease course of experimental autoimmune encephalomyelitis, an animal model of multiple sclerosis. PLoS One. 2012;7(4):e35544.
120. Shevchenko A, Wilm M, Vorm O, Mann M. Mass spectrometric sequencing of proteins silver-stained polyacrylamide gels. Anal Chem. 1996;68(5):850-8.
121. Li ZB, Lehar M, Samlan R, Flint PW. Proteomic analysis of rat laryngeal muscle following denervation. Proteomics. 2005;5(18):4764-76.
122. Isfort RJ, Hinkle RT, Jones MB, Wang F, Greis KD, Sun Y, et al. Proteomic analysis of the atrophying rat soleus muscle following denervation. Electrophoresis. 2000;21(11):2228-34.
123. Parker KC, Kong SW, Walsh RJ, Salajegheh M, Moghadaszadeh B, Amato AA, et al. Fast-twitch sarcomeric and glycolytic enzyme protein loss in inclusion body myositis. Muscle Nerve. 2009;39(6):739-53.
124. Isfort RJ, Wang F, Greis KD, Sun Y, Keough TW, Bodine SC, et al. Proteomic analysis of rat soleus and tibialis anterior muscle following immobilization. J Chromatogr B Analyt Technol Biomed Life Sci. 2002;769(2):323-32.
125. Ohlendieck K. Proteomic Profiling of Fast-To-Slow Muscle Transitions during Aging. Frontiers in physiology. 2011;2:105.

126. Martignago S, Fanin M, Albertini E, Pegoraro E, Angelini C. Muscle histopathology in myasthenia gravis with antibodies against MuSK and AChR. Neuropathology and applied neurobiology. 2009;35(1):103-10.
127. Zamecnik J, Vesely D, Jakubicka B, Cibula A, Pitha J, Schutzner J, et al. Atrophy of type II fibres in myasthenia gravis muscle in thymectomized patients: steroid-induced change with prognostic impact. J Cell Mol Med. 2009;13(8B):2008-18.
128. Coers C, Telerman-Toppet N. Morphological and histochemical changes of motor units in myasthenia. Ann N Y Acad Sci. 1976;274:6-19.
129. Russell AJ, Hartman JJ, Hinken AC, Muci AR, Kawas R, Driscoll L, et al. Activation of fast skeletal muscle troponin as a potential therapeutic approach for treating neuromuscular diseases. Nat Med. 2012;18(3):452-5.
130. Keller A, Rouzeau JD, Farhadian F, Wisnewsky C, Marotte F, Lamande N, et al. Differential expression of alpha- and beta-enolase genes during rat heart development and hypertrophy. Am J Physiol. 1995;269(6 Pt 2):H1843-51.
131. Merkulova T, Dehaupas M, Nevers MC, Creminon C, Alameddine H, Keller A. Differential modulation of alpha, beta and gamma enolase isoforms in regenerating mouse skeletal muscle. Eur J Biochem. 2000;267(12):3735-43.
132. Comi GP, Fortunato F, Lucchiari S, Bordoni A, Prelle A, Jann S, et al. Beta-enolase deficiency, a new metabolic myopathy of distal glycolysis. Ann Neurol. 2001;50(2):202-7.
133. Raisanen SR, Lehenkari P, Tasanen M, Rahkila P, Harkonen PL, Vaananen HK. Carbonic anhydrase III protects cells from hydrogen peroxide-induced apoptosis. FASEB journal : official publication of the Federation of American Societies for Experimental Biology. 1999;13(3):513-22.
134. Robert-Pachot M, Desbos A, Moreira A, Becchi M, Tebib J, Bonnin M, et al. Carbonic anhydrase III: a new target for autoantibodies in autoimmune diseases. Autoimmunity. 2007;40(5):380-9.
135. Du AL, Ren HM, Lu CZ, Tu JL, Xu CF, Sun YA. Carbonic anhydrase III is insufficient in muscles of myasthenia gravis patients. Autoimmunity. 2009;42(3):209-15.
136. Guyon T, Levasseur P, Truffault F, Cottin C, Gaud C, Berrih-Aknin S. Regulation of acetylcholine receptor alpha subunit variants in human myasthenia gravis. Quantification of steady-state levels of messenger RNA in muscle biopsy using the polymerase chain reaction. J Clin Invest. 1994;94(1):16-24.

137. Asher O, Fuchs S, Zuk D, Rapaport D, Buonanno A. Changes in the expression of mRNAs for myogenic factors and other muscle-specific proteins in experimental autoimmune myasthenia gravis. FEBS Lett. 1992;299(1):15-8.
138. Santoni V, Molloy M, Rabilloud T. Membrane proteins and proteomics: un amour impossible? Electrophoresis. 2000;21(6):1054-70.
139. Tan S, Tan HT, Chung MC. Membrane proteins and membrane proteomics. Proteomics. 2008;8(19):3924-32.
140. Svejgaard A. The immunogenetics of multiple sclerosis. Immunogenetics. 2008;60(6):275-86.
141. Trapp BD, Peterson J, Ransohoff RM, Rudick R, Mork S, Bo L. Axonal transection in the lesions of multiple sclerosis. N Engl J Med. 1998;338(5):278-85.
142. Barnett MH, Prineas JW. Relapsing and remitting multiple sclerosis: pathology of the newly forming lesion. Ann Neurol. 2004;55(4):458-68.
143. Zipp F. A new window in multiple sclerosis pathology: non-conventional quantitative magnetic resonance imaging outcomes. J Neurol Sci. 2009;287 Suppl 1:S24-9.
144. Cross AH, Trotter JL, Lyons J. B cells and antibodies in CNS demyelinating disease. J Neuroimmunol. 2001;112(1-2):1-14.
145. Lau A, Tymianski M. Glutamate receptors, neurotoxicity and neurodegeneration. Pflugers Arch. 2010;460(2):525-42.
146. Pitt D, Werner P, Raine CS. Glutamate excitotoxicity in a model of multiple sclerosis. Nat Med. 2000;6(1):67-70.
147. Fountoulakis M, Tsangaris GT, Maris A, Lubec G. The rat brain hippocampus proteome. J Chromatogr B Analyt Technol Biomed Life Sci. 2005;819(1):115-29.
148. Dasgupta B, Yi Y, Hegedus B, Weber JD, Gutmann DH. Cerebrospinal fluid proteomic analysis reveals dysregulation of methionine aminopeptidase-2 expression in human and mouse neurofibromatosis 1-associated glioma. Cancer Res. 2005;65(21):9843-50.
149. Lafon-Cazal M, Adjali O, Galeotti N, Poncet J, Jouin P, Homburger V, et al. Proteomic analysis of astrocytic secretion in the mouse. Comparison with the cerebrospinal fluid proteome. J Biol Chem. 2003;278(27):24438-48.
150. Siman R, McIntosh TK, Soltesz KM, Chen Z, Neumar RW, Roberts VL. Proteins released from degenerating neurons are surrogate markers for acute brain damage. Neurobiol Dis. 2004;16(2):311-20.
151. Sironi L, Guerrini U, Tremoli E, Miller I, Gelosa P, Lascialfari A, et al. Analysis of pathological events at the onset of brain damage in stroke-

prone rats: a proteomics and magnetic resonance imaging approach. J Neurosci Res. 2004;78(1):115-22.
152. Alt C, Duvefelt K, Franzen B, Yang Y, Engelhardt B. Gene and protein expression profiling of the microvascular compartment in experimental autoimmune encephalomyelitis in C57Bl/6 and SJL mice. Brain Pathol. 2005;15(1):1-16.
153. Duzhak T, Emerson MR, Chakrabarty A, Alterman MA, Levine SM. Analysis of protein induction in the CNS of SJL mice with experimental allergic encephalomyelitis by proteomic screening and immunohistochemistry. Cell Mol Biol (Noisy-le-grand). 2003;49(5):723-32.
154. Tumani H, Lehmensiek V, Lehnert S, Otto M, Brettschneider J. 2D DIGE of the cerebrospinal fluid proteome in neurological diseases. Expert Rev Proteomics. 2010;7(1):29-38.
155. Mikkat S, Lorenz P, Scharf C, Yu X, Glocker MO, Ibrahim SM. MS characterization of qualitative protein polymorphisms in the spinal cords of inbred mouse strains. Proteomics. 2010;10(5):1050-62.
156. Baeten K, Hendriks JJ, Hellings N, Theunissen E, Vanderlocht J, Ryck LD, et al. Visualisation of the kinetics of macrophage infiltration during experimental autoimmune encephalomyelitis by magnetic resonance imaging. J Neuroimmunol. 2008;195(1-2):1-6.
157. Zellner M, Babeluk R, Diestinger M, Pirchegger P, Skeledzic S, Oehler R. Fluorescence-based Western blotting for quantitation of protein biomarkers in clinical samples. Electrophoresis. 2008;29(17):3621-7.
158. Bogie JF, Stinissen P, Hellings N, Hendriks JJ. Myelin-phagocytosing macrophages modulate autoreactive T cell proliferation. J Neuroinflammation. 2011;8:85.
159. Imlach WL, Finch SC, Dunlop J, Meredith AL, Aldrich RW, Dalziel JE. The molecular mechanism of "ryegrass staggers," a neurological disorder of K+ channels. J Pharmacol Exp Ther. 2008;327(3):657-64.
160. Bhat R, Axtell R, Mitra A, Miranda M, Lock C, Tsien RW, et al. Inhibitory role for GABA in autoimmune inflammation. Proc Natl Acad Sci U S A. 2010;107(6):2580-5.
161. Banati RB, Gehrmann J, Lannes-Vieira J, Wekerle H, Kreutzberg GW. Inflammatory reaction in experimental autoimmune encephalomyelitis (EAE) is accompanied by a microglial expression of the beta A4-amyloid precursor protein (APP). Glia. 1995;14(3):209-15.
162. Stornetta RL, Hawelu-Johnson CL, Guyenet PG, Lynch KR. Astrocytes synthesize angiotensinogen in brain. Science. 1988;242(4884):1444-6.

163. Luhder F, Lee DH, Gold R, Stegbauer J, Linker RA. Small but powerful: short peptide hormones and their role in autoimmune inflammation. J Neuroimmunol. 2009;217(1-2):1-7.
164. Tuller T, Atar S, Ruppin E, Gurevich M, Achiron A. Global map of physical interactions among differentially expressed genes in multiple sclerosis relapses and remissions. Hum Mol Genet. 2011.
165. Szewczyk A, Jarmuszkiewicz W, Kunz WS. Mitochondrial potassium channels. IUBMB Life. 2009;61(2):134-43.
166. van Horssen J, Drexhage JA, Flor T, Gerritsen W, van der Valk P, de Vries HE. Nrf2 and DJ1 are consistently upregulated in inflammatory multiple sclerosis lesions. Free Radic Biol Med. 2010;49(8):1283-9.
167. Zhu B, Luo L, Moore GR, Paty DW, Cynader MS. Dendritic and synaptic pathology in experimental autoimmune encephalomyelitis. Am J Pathol. 2003;162(5):1639-50.
168. Schilling T, Eder C. Microglial K(+) channel expression in young adult and aged mice. Glia. 2015;63(4):664-72.
169. Marouga R, David S, Hawkins E. The development of the DIGE system: 2D fluorescence difference gel analysis technology. Anal Bioanal Chem. 2005;382(3):669-78.
170. Viswanathan S, Unlu M, Minden JS. Two-dimensional difference gel electrophoresis. Nat Protoc. 2006;1(3):1351-8.
171. Schmidt EF, Strittmatter SM. The CRMP family of proteins and their role in Sema3A signaling. Advances in experimental medicine and biology. 2007;600:1-11.
172. Arimura N, Menager C, Fukata Y, Kaibuchi K. Role of CRMP-2 in neuronal polarity. J Neurobiol. 2004;58(1):34-47.
173. Rogemond V, Auger C, Giraudon P, Becchi M, Auvergnon N, Belin MF, et al. Processing and nuclear localization of CRMP2 during brain development induce neurite outgrowth inhibition. J Biol Chem. 2008;283(21):14751-61.
174. Hensley K, Venkova K, Christov A, Gunning W, Park J. Collapsin response mediator protein-2: an emerging pathologic feature and therapeutic target for neurodisease indications. Molecular neurobiology. 2011;43(3):180-91.
175. Arimura N, Menager C, Kawano Y, Yoshimura T, Kawabata S, Hattori A, et al. Phosphorylation by Rho kinase regulates CRMP-2 activity in growth cones. Mol Cell Biol. 2005;25(22):9973-84.
176. Arimura N, Inagaki N, Chihara K, Menager C, Nakamura N, Amano M, et al. Phosphorylation of collapsin response mediator protein-2 by Rho-kinase. Evidence for two separate signaling pathways for growth cone collapse. J Biol Chem. 2000;275(31):23973-80.

177. Yoshimura T, Kawano Y, Arimura N, Kawabata S, Kikuchi A, Kaibuchi K. GSK-3beta regulates phosphorylation of CRMP-2 and neuronal polarity. Cell. 2005;120(1):137-49.
178. Cole AR, Soutar MP, Rembutsu M, van Aalten L, Hastie CJ, McLauchlan H, et al. Relative resistance of Cdk5-phosphorylated CRMP2 to dephosphorylation. J Biol Chem. 2008;283(26):18227-37.
179. Deo RC, Schmidt EF, Elhabazi A, Togashi H, Burley SK, Strittmatter SM. Structural bases for CRMP function in plexin-dependent semaphorin3A signaling. EMBO J. 2004;23(1):9-22.
180. Kimura T, Watanabe H, Iwamatsu A, Kaibuchi K. Tubulin and CRMP-2 complex is transported via Kinesin-1. J Neurochem. 2005;93(6):1371-82.
181. Vincent P, Collette Y, Marignier R, Vuaillat C, Rogemond V, Davoust N, et al. A role for the neuronal protein collapsin response mediator protein 2 in T lymphocyte polarization and migration. J Immunol. 2005;175(11):7650-60.
182. Kawano Y, Yoshimura T, Tsuboi D, Kawabata S, Kaneko-Kawano T, Shirataki H, et al. CRMP-2 is involved in kinesin-1-dependent transport of the Sra-1/WAVE1 complex and axon formation. Mol Cell Biol. 2005;25(22):9920-35.
183. Ryan KA, Pimplikar SW. Activation of GSK-3 and phosphorylation of CRMP2 in transgenic mice expressing APP intracellular domain. J Cell Biol. 2005;171(2):327-35.
184. Ito Y, Oinuma I, Katoh H, Kaibuchi K, Negishi M. Sema4D/plexin-B1 activates GSK-3beta through R-Ras GAP activity, inducing growth cone collapse. EMBO reports. 2006;7(7):704-9.
185. Vuaillat C, Varrin-Doyer M, Bernard A, Sagardoy I, Cavagna S, Chounlamountri I, et al. High CRMP2 expression in peripheral T lymphocytes is associated with recruitment to the brain during virus-induced neuroinflammation. J Neuroimmunol. 2008;193(1-2):38-51.
186. Varrin-Doyer M, Vincent P, Cavagna S, Auvergnon N, Noraz N, Rogemond V, et al. Phosphorylation of collapsin response mediator protein 2 on Tyr-479 regulates CXCL12-induced T lymphocyte migration. J Biol Chem. 2009;284(19):13265-76.
187. Giraudon P, Nicolle A, Cavagna S, Benetollo C, Marignier R, Varrin-Doyer M. Insight into the role of CRMP2 (collapsin response mediator protein 2) in T lymphocyte migration: the particular context of virus infection. Cell adhesion & migration. 2013;7(1):38-43.
188. Calderon TM, Eugenin EA, Lopez L, Kumar SS, Hesselgesser J, Raine CS, et al. A role for CXCL12 (SDF-1alpha) in the pathogenesis of

multiple sclerosis: regulation of CXCL12 expression in astrocytes by soluble myelin basic protein. J Neuroimmunol. 2006;177(1-2):27-39.
189. McCandless EE, Piccio L, Woerner BM, Schmidt RE, Rubin JB, Cross AH, et al. Pathological expression of CXCL12 at the blood-brain barrier correlates with severity of multiple sclerosis. Am J Pathol. 2008;172(3):799-808.
190. Krumbholz M, Theil D, Cepok S, Hemmer B, Kivisakk P, Ransohoff RM, et al. Chemokines in multiple sclerosis: CXCL12 and CXCL13 up-regulation is differentially linked to CNS immune cell recruitment. Brain : a journal of neurology. 2006;129(Pt 1):200-11.
191. Claes N, Dhaeze T, Fraussen J, Broux B, Van Wijmeersch B, Stinissen P, et al. Compositional changes of B and T cell subtypes during fingolimod treatment in multiple sclerosis patients: a 12-month follow-up study. PLoS One. 2014;9(10):e111115.
192. Venken K, Hellings N, Broekmans T, Hensen K, Rummens JL, Stinissen P. Natural naive CD4+CD25+CD127low regulatory T cell (Treg) development and function are disturbed in multiple sclerosis patients: recovery of memory Treg homeostasis during disease progression. J Immunol. 2008;180(9):6411-20.
193. Zuniga LA, Jain R, Haines C, Cua DJ. Th17 cell development: from the cradle to the grave. Immunological reviews. 2013;252(1):78-88.
194. Crome SQ, Clive B, Wang AY, Kang CY, Chow V, Yu J, et al. Inflammatory effects of ex vivo human Th17 cells are suppressed by regulatory T cells. J Immunol. 2010;185(6):3199-208.
195. Morita R, Schmitt N, Bentebibel SE, Ranganathan R, Bourdery L, Zurawski G, et al. Human blood CXCR5(+)CD4(+) T cells are counterparts of T follicular cells and contain specific subsets that differentially support antibody secretion. Immunity. 2011;34(1):108-21.
196. Cohen CJ, Crome SQ, MacDonald KG, Dai EL, Mager DL, Levings MK. Human Th1 and Th17 cells exhibit epigenetic stability at signature cytokine and transcription factor loci. J Immunol. 2011;187(11):5615-26.
197. Noster R, Riedel R, Mashreghi MF, Radbruch H, Harms L, Haftmann C, et al. IL-17 and GM-CSF expression are antagonistically regulated by human T helper cells. Science translational medicine. 2014;6(241):241ra80.
198. Eyerich S, Zielinski CE. Defining Th-cell subsets in a classical and tissue-specific manner: Examples from the skin. European journal of immunology. 2014;44(12):3475-83.

199. Deenick EK, Tangye SG. Autoimmunity: IL-21: a new player in Th17-cell differentiation. Immunology and cell biology. 2007;85(7):503-5.
200. Dong C. TH17 cells in development: an updated view of their molecular identity and genetic programming. Nature reviews Immunology. 2008;8(5):337-48.
201. Then Bergh F, Dayyani F, Ziegler-Heitbrock L. Impact of type-I-interferon on monocyte subsets and their differentiation to dendritic cells. An in vivo and ex vivo study in multiple sclerosis patients treated with interferon-beta. J Neuroimmunol. 2004;146(1-2):176-88.
202. Tang Y, Hua SC, Qin GX, Xu LJ, Jiang YF. Different subsets of macrophages in patients with new onset tuberculous pleural effusion. PLoS One. 2014;9(2):e88343.
203. Bogie JF, Stinissen P, Hendriks JJ. Macrophage subsets and microglia in multiple sclerosis. Acta neuropathologica. 2014;128(2):191-213.
204. Tallone T, Turconi G, Soldati G, Pedrazzini G, Moccetti T, Vassalli G. Heterogeneity of human monocytes: an optimized four-color flow cytometry protocol for analysis of monocyte subsets. Journal of cardiovascular translational research. 2011;4(2):211-9.
205. Movahedi K, Laoui D, Gysemans C, Baeten M, Stange G, Van den Bossche J, et al. Different tumor microenvironments contain functionally distinct subsets of macrophages derived from Ly6C(high) monocytes. Cancer Res. 2010;70(14):5728-39.
206. Abeles RD, McPhail MJ, Sowter D, Antoniades CG, Vergis N, Vijay GK, et al. CD14, CD16 and HLA-DR reliably identifies human monocytes and their subsets in the context of pathologically reduced HLA-DR expression by CD14(hi) /CD16(neg) monocytes: Expansion of CD14(hi) /CD16(pos) and contraction of CD14(lo) /CD16(pos) monocytes in acute liver failure. Cytometry Part A : the journal of the International Society for Analytical Cytology. 2012;81(10):823-34.
207. Fadini GP, Cappellari R, Mazzucato M, Agostini C, Vigili de Kreutzenberg S, Avogaro A. Monocyte-macrophage polarization balance in pre-diabetic individuals. Acta diabetologica. 2013;50(6):977-82.
208. Neumann H, Medana IM, Bauer J, Lassmann H. Cytotoxic T lymphocytes in autoimmune and degenerative CNS diseases. Trends in neurosciences. 2002;25(6):313-9.
209. Sun D, Whitaker JN, Huang Z, Liu D, Coleclough C, Wekerle H, et al. Myelin antigen-specific CD8+ T cells are encephalitogenic and produce severe disease in C57BL/6 mice. J Immunol. 2001;166(12):7579-87.

210. Huseby ES, Liggitt D, Brabb T, Schnabel B, Ohlen C, Goverman J. A pathogenic role for myelin-specific CD8(+) T cells in a model for multiple sclerosis. J Exp Med. 2001;194(5):669-76.
211. Killestein J, Eikelenboom MJ, Izeboud T, Kalkers NF, Ader HJ, Barkhof F, et al. Cytokine producing CD8+ T cells are correlated to MRI features of tissue destruction in MS. J Neuroimmunol. 2003;142(1-2):141-8.
212. El-behi M, Rostami A, Ciric B. Current views on the roles of Th1 and Th17 cells in experimental autoimmune encephalomyelitis. Journal of neuroimmune pharmacology : the official journal of the Society on NeuroImmune Pharmacology. 2010;5(2):189-97.
213. Fletcher JM, Lonergan R, Costelloe L, Kinsella K, Moran B, O'Farrelly C, et al. CD39+Foxp3+ regulatory T Cells suppress pathogenic Th17 cells and are impaired in multiple sclerosis. J Immunol. 2009;183(11):7602-10.
214. Viglietta V, Baecher-Allan C, Weiner HL, Hafler DA. Loss of functional suppression by CD4+CD25+ regulatory T cells in patients with multiple sclerosis. J Exp Med. 2004;199(7):971-9.
215. Jiang Z, Jiang JX, Zhang GX. Macrophages: a double-edged sword in experimental autoimmune encephalomyelitis. Immunology letters. 2014;160(1):17-22.
216. Litwak SA, Payne NL, Campanale N, Ozturk E, Lee JY, Petratos S, et al. Nogo-receptor 1 deficiency has no influence on immune cell repertoire or function during experimental autoimmune encephalomyelitis. PLoS One. 2013;8(12):e82101.
217. Baecher-Allan C, Wolf E, Hafler DA. MHC class II expression identifies functionally distinct human regulatory T cells. J Immunol. 2006;176(8):4622-31.
218. Cruz-Orengo L, Holman DW, Dorsey D, Zhou L, Zhang P, Wright M, et al. CXCR7 influences leukocyte entry into the CNS parenchyma by controlling abluminal CXCL12 abundance during autoimmunity. J Exp Med. 2011;208(2):327-39.
219. Chuluundorj D, Harding SA, Abernethy D, La Flamme AC. Expansion and preferential activation of the CD14(+)CD16(+) monocyte subset during multiple sclerosis. Immunology and cell biology. 2014;92(6):509-17.
220. Tacke F, Randolph GJ. Migratory fate and differentiation of blood monocyte subsets. Immunobiology. 2006;211(6-8):609-18.
221. Zemen BG, Lai MH, Whitt JP, Khan Z, Zhao G, Meredith AL. Generation of Kcnma1fl-tdTomato, a conditional deletion of the BK channel alpha subunit in mouse. Physiol Rep. 2015;3(11).

222. Martinez-Espinosa PL, Yang C, Gonzalez-Perez V, Xia XM, Lingle CJ. Knockout of the BK beta2 subunit abolishes inactivation of BK currents in mouse adrenal chromaffin cells and results in slow-wave burst activity. J Gen Physiol. 2014;144(4):275-95.
223. Meredith AL, Thorneloe KS, Werner ME, Nelson MT, Aldrich RW. Overactive bladder and incontinence in the absence of the BK large conductance Ca2+-activated K+ channel. J Biol Chem. 2004;279(35):36746-52.
224. Papavlassopoulos M, Stamme C, Thon L, Adam D, Hillemann D, Seydel U, et al. MaxiK blockade selectively inhibits the lipopolysaccharide-induced I kappa B-alpha /NF-kappa B signaling pathway in macrophages. J Immunol. 2006;177(6):4086-93.
225. Yu M, Liu SL, Sun PB, Pan H, Tian CL, Zhang LH. Peptide toxins and small-molecule blockers of BK channels. Acta Pharmacol Sin. 2016;37(1):56-66.
226. Hermann A, Sitdikova GF, Weiger TM. Oxidative Stress and Maxi Calcium-Activated Potassium (BK) Channels. Biomolecules. 2015;5(3):1870-911.
227. Sausbier M, Hu H, Arntz C, Feil S, Kamm S, Adelsberger H, et al. Cerebellar ataxia and Purkinje cell dysfunction caused by Ca2+-activated K+ channel deficiency. Proc Natl Acad Sci U S A. 2004;101(25):9474-8.
228. Reich EP, Cui L, Yang L, Pugliese-Sivo C, Golovko A, Petro M, et al. Blocking ion channel KCNN4 alleviates the symptoms of experimental autoimmune encephalomyelitis in mice. European journal of immunology. 2005;35(4):1027-36.
229. Kieseier BC, Hartung HP. Targeting two-pore domain potassium channels - a promising strategy for treating T cell mediated autoimmunity. Exp Neurol. 2013;247:286-8.
230. Bever CT, Jr., Young D, Anderson PA, Krumholz A, Conway K, Leslie J, et al. The effects of 4-aminopyridine in multiple sclerosis patients: results of a randomized, placebo-controlled, double-blind, concentration-controlled, crossover trial. Neurology. 1994;44(6):1054-9.
231. Rawji KS, Yong VW. The benefits and detriments of macrophages/microglia in models of multiple sclerosis. Clin Dev Immunol. 2013;2013:948976.
232. Gudi V, Gingele S, Skripuletz T, Stangel M. Glial response during cuprizone-induced de- and remyelination in the CNS: lessons learned. Front Cell Neurosci. 2014;8:73.

233. Hiremath MM, Saito Y, Knapp GW, Ting JP, Suzuki K, Matsushima GK. Microglial/macrophage accumulation during cuprizone-induced demyelination in C57BL/6 mice. J Neuroimmunol. 1998;92(1-2):38-49.
234. Imlach WL, Finch SC, Miller JH, Meredith AL, Dalziel JE. A role for BK channels in heart rate regulation in rodents. PLoS One. 2010;5(1):e8698.
235. Sprossmann F, Pankert P, Sausbier U, Wirth A, Zhou XB, Madlung J, et al. Inducible knockout mutagenesis reveals compensatory mechanisms elicited by constitutive BK channel deficiency in overactive murine bladder. FEBS J. 2009;276(6):1680-97.
236. Rieg T, Vallon V, Sausbier M, Sausbier U, Kaissling B, Ruth P, et al. The role of the BK channel in potassium homeostasis and flow-induced renal potassium excretion. Kidney Int. 2007;72(5):566-73.
237. Eder C. Ion channels in microglia (brain macrophages). Am J Physiol. 1998;275(2 Pt 1):C327-42.
238. Wogram E, Wendt S, Matyash M, Pivneva T, Draguhn A, Kettenmann H. Satellite microglia show spontaneous electrical activity that is uncorrelated with activity of the attached neuron. Eur J Neurosci. 2016;43(11):1523-34.
239. Bilmen JG, Wootton LL, Michelangeli F. The mechanism of inhibition of the sarco/endoplasmic reticulum Ca2+ ATPase by paxilline. Arch Biochem Biophys. 2002;406(1):55-64.
240. Scheel O, Papavlassopoulos M, Blunck R, Gebert A, Hartung T, Zahringer U, et al. Cell activation by ligands of the toll-like receptor and interleukin-1 receptor family depends on the function of the large-conductance potassium channel MaxiK in human macrophages. Infect Immun. 2006;74(7):4354-6.
241. Ren JD, Fan L, Tian FZ, Fan KH, Yu BT, Jin WH, et al. Involvement of a membrane potassium channel in heparan sulphate-induced activation of macrophages. Immunology. 2014;141(3):345-52.
242. Khatri P, Sirota M, Butte AJ. Ten years of pathway analysis: current approaches and outstanding challenges. PLoS Comput Biol. 2012;8(2):e1002375.
243. Karimpour-Fard A, Epperson LE, Hunter LE. A survey of computational tools for downstream analysis of proteomic and other omic datasets. Hum Genomics. 2015;9:28.
244. [Available from: https://www.qiagenbioinformatics.com/products/ingenuity-pathway-analysis/.

245. Baggerman G, Vierstraete E, De Loof A, Schoofs L. Gel-based versus gel-free proteomics: a review. Comb Chem High Throughput Screen. 2005;8(8):669-77.
246. Iwamoto N, Shimada T. Recent advances in mass spectrometry-based approaches for proteomics and biologics: Great contribution for developing therapeutic antibodies. Pharmacol Ther. 2018;185:147-54.
247. Chahrour O, Cobice D, Malone J. Stable isotope labelling methods in mass spectrometry-based quantitative proteomics. J Pharm Biomed Anal. 2015;113:2-20.
248. Aleshin S, Strokin M, Sergeeva M, Reiser G. Peroxisome proliferator-activated receptor (PPAR)beta/delta, a possible nexus of PPARalpha- and PPARgamma-dependent molecular pathways in neurodegenerative diseases: Review and novel hypotheses. Neurochem Int. 2013;63(4):322-30.
249. Ferret-Sena V, Capela C, Sena A. Metabolic Dysfunction and Peroxisome Proliferator-Activated Receptors (PPAR) in Multiple Sclerosis. Int J Mol Sci. 2018;19(6).
250. Cheng YY, Wright CM, Kirschner MB, Williams M, Sarun KH, Sytnyk V, et al. KCa1.1, a calcium-activated potassium channel subunit alpha 1, is targeted by miR-17-5p and modulates cell migration in malignant pleural mesothelioma. Mol Cancer. 2016;15(1):44.
251. Khaitan D, Sankpal UT, Weksler B, Meister EA, Romero IA, Couraud PO, et al. Role of KCNMA1 gene in breast cancer invasion and metastasis to brain. BMC Cancer. 2009;9:258.
252. Fukata Y, Itoh TJ, Kimura T, Menager C, Nishimura T, Shiromizu T, et al. CRMP-2 binds to tubulin heterodimers to promote microtubule assembly. Nat Cell Biol. 2002;4(8):583-91.
253. Pool M, Niino M, Rambaldi I, Robson K, Bar-Or A, Fournier AE. Myelin regulates immune cell adhesion and motility. Exp Neurol. 2009;217(2):371-7.
254. Karnezis T, Mandemakers W, McQualter JL, Zheng B, Ho PP, Jordan KA, et al. The neurite outgrowth inhibitor Nogo A is involved in autoimmune-mediated demyelination. Nat Neurosci. 2004;7(7):736-44.
255. Nada SE, Tulsulkar J, Raghavan A, Hensley K, Shah ZA. A derivative of the CRMP2 binding compound lanthionine ketimine provides neuroprotection in a mouse model of cerebral ischemia. Neurochem Int. 2012;61(8):1357-63.
256. Hubbard C, Benda E, Hardin T, Baxter T, St John E, O'Brien S, et al. Lanthionine ketimine ethyl ester partially rescues neurodevelopmental defects in unc-33 (DPYSL2/CRMP2) mutants. J Neurosci Res. 2013;91(9):1183-90.

257. Hensley K, Gabbita SP, Venkova K, Hristov A, Johnson MF, Eslami P, et al. A derivative of the brain metabolite lanthionine ketimine improves cognition and diminishes pathology in the 3 x Tg-AD mouse model of Alzheimer disease. J Neuropathol Exp Neurol. 2013;72(10):955-69.
258. Dupree JL, Polak PE, Hensley K, Pelligrino D, Feinstein DL. Lanthionine ketimine ester provides benefit in a mouse model of multiple sclerosis. J Neurochem. 2015;134(2):302-14.
259. Marangoni N, Kowal K, Deliu Z, Hensley K, Feinstein DL. Neuroprotective and neurotrophic effects of Lanthionine Ketimine Ester. Neurosci Lett. 2017;664:28-33.
260. Beyreuther BK, Freitag J, Heers C, Krebsfanger N, Scharfenecker U, Stohr T. Lacosamide: a review of preclinical properties. CNS Drug Rev. 2007;13(1):21-42.
261. Chu CC, Wang JJ, Chen KT, Shieh JP, Wang LK, Shui HA, et al. Neurotrophic effects of tianeptine on hippocampal neurons: a proteomic approach. J Proteome Res. 2010;9(2):936-44.
262. Kodama Y, Murakumo Y, Ichihara M, Kawai K, Shimono Y, Takahashi M. Induction of CRMP-2 by GDNF and analysis of the CRMP-2 promoter region. Biochem Biophys Res Commun. 2004;320(1):108-15.
263. Petratos S, Lee JY. Stop CRMPing my style: a new competitive model of CRMP oligomerization. J Neurochem. 2013;125(6):800-2.
264. Giraudon P, inventor Cleaved and phosphorylated CRMP2 as blood marker of inflammatory diseases of the central nervous system. US 2012/0135009 A1 2012 May 31.
265. Judge SI, Bever CT, Jr. Potassium channel blockers in multiple sclerosis: neuronal Kv channels and effects of symptomatic treatment. Pharmacol Ther. 2006;111(1):224-59.
266. Varga Z, Csepany T, Papp F, Fabian A, Gogolak P, Toth A, et al. Potassium channel expression in human CD4+ regulatory and naive T cells from healthy subjects and multiple sclerosis patients. Immunol Lett. 2009;124(2):95-101.
267. Lai MH, Wu Y, Gao Z, Anderson ME, Dalziel JE, Meredith AL. BK channels regulate sinoatrial node firing rate and cardiac pacing in vivo. Am J Physiol Heart Circ Physiol. 2014;307(9):H1327-38.
268. Huang H, Ren HM, Shang XL, Liu XY. Detection of the phosphatase activity of carbonic anhydrase III on a nitrocellulose membrane following 2D gel electrophoresis. Mol Med Rep. 2014;10(4):1887-92.
269. Carmans S, Hendriks JJ, Slaets H, Thewissen K, Stinissen P, Rigo JM, et al. Systemic treatment with the inhibitory neurotransmitter gamma-aminobutyric acid aggravates experimental autoimmune

encephalomyelitis by affecting proinflammatory immune responses. J Neuroimmunol. 2013;255(1-2):45-53.
270. Pollio G, Hoozemans JJ, Andersen CA, Roncarati R, Rosi MC, van Haastert ES, et al. Increased expression of the oligopeptidase THOP1 is a neuroprotective response to Abeta toxicity. Neurobiol Dis. 2008;31(1):145-58.
271. Lu X, Rong Y, Baudry M. Calpain-mediated degradation of PSD-95 in developing and adult rat brain. Neurosci Lett. 2000;286(2):149-53.
272. Sattler R, Xiong Z, Lu WY, Hafner M, MacDonald JF, Tymianski M. Specific coupling of NMDA receptor activation to nitric oxide neurotoxicity by PSD-95 protein. Science. 1999;284(5421):1845-8.
273. Vaudel M, Verheggen K, Csordas A, Raeder H, Berven FS, Martens L, et al. Exploring the potential of public proteomics data. Proteomics. 2016;16(2):214-25.
274. Del Boccio P, Rossi C, di Ioia M, Cicalini I, Sacchetta P, Pieragostino D. Integration of metabolomics and proteomics in multiple sclerosis: From biomarkers discovery to personalized medicine. Proteomics Clinical applications. 2016;10(4):470-84.

Curriculum Vitae

Annelies Vanheel werd geboren op 8 januari 1985 te Genk. In 2003 behaalde ze haar diploma Algemeen Secundair Onderwijs (ASO) in de afstudeerrichting Wetenschappen-Wiskunde aan het Virga Jessecollege te Hasselt. Vervolgens starte ze haar opleiding Biomedische Wetenschappen aan de Universiteit Hasselt/transnationale Universiteit Limburg, waar ze in 2006 haar diploma Bachelor in de Biomedische Wetenschappen behaalde. Aansluitend behaalde ze haar diploma Master in de Biomedische Wetenschappen met onderscheiding. Haar masterstage, getiteld "The role of rat cytomegalovirus R78 gene in viral assembly" voerde ze uit aan het academisch ziekenhuis Maastricht in de onderzoeksgroep Medische Microbiologie onder leiding van dr. Patrick Beisser. In september 2007 starte ze als onderzoeksmedewerker aan de Universiteit Maastricht, op de afdeling neurowetenschappen van de School for Mental Health and Neuroscience. In januari 2008 behaalde ze in diezelfde onderzoeksgroep een Kootstra Talent Fellowship beurs voor basis immunologieonderzoek in myasthenia gravis. In 2009 startte ze haar doctoraat/assistentsschap aan het Biomedisch Onderzoeksinstituut van de Universiteit Hasselt in de groep van Prof. Dr. Niels Hellings. Haar doctoraatsonderzoek was gericht op de identificatie van eiwitten betrokken bij de auto-immune ziekteprocessen van multiple sclerose en myasthenia gravis. Daarnaast was ze lid van het onderwijsteam in de opleidingen Biomedische wetenschappen en Geneeskunde, begeleidde stagestudenten uit de bachelor en master opleiding, en volgde zelf cursussen Proefdierkunde II (FELASA C) (UHasselt), Project Management (True Colours), Good scientific conduct and Lab book taking (UHasselt), Bioveiligheid (UHasselt en Perseus), qPCR experiment design and data-analysis (Biogazelle), Effective Scientific Communication (Principiae) and Effective writing for life sciences research (VIB) . Ze was betrokken bij de organisatie van het PhD symposium "Cytokines and Cell Trafficking in Immunological Disorders" in 2012 te Diepenbeek, en nam zelf deel aan verscheidene nationale en internationale symposia waar ze haar onderzoeksresultaten presenteerde aan wetenschappers van over heel de wereld.

Bibliography

Publications

Identification of protein networks in the disease course of experimental autoimmune encephalomyelitis, an animal model of multiple sclerosis
A. Vanheel*, R. Daniels*, S. Plaisance, K. Baeten, JJA. Hendriks, P. Leprince, D. Dumont, J. Robben, B. Brône, P. Stinissen, JP. Noben and N. Hellings
Plos One 2012; 7(4):e35544.
* These authors contributes equally to this work

Proteomic analysis of rat tibialis anterior muscles at different stages of experimental autoimmune myasthenia gravis
AM. Gomez*, **A. Vanheel***, M. Losen, PC. Molenaar, MH. De Baets, JP. Noben, N. Hellings, P. Martinez-Martinez
J. Neuroimmunol. 2013 Aug 15;261(1-2):141-5.
* These authors contributes equally to this work

Oral Presentations

Is there a role for KCNMA1 in MS?
A. Vanheel, B. Brône, P. Stinissen, JP. Noben and N. Hellings
EURON PhD days 2012, Maastricht, The Netherlands

Identification of putative protein networks involved in the disease course of experimental autoimune encephalitis, an animal model of multiple sclerosis.
A. Vanheel, R. Daniels, S. Plaisance, K. Baeten, JJA. Hendriks, P. Leprince, D. Dumont, J. Robben, P. Stinissen, JP. Noben and N. Hellings
4th NUBIN symposium 2012, Amsterdam, The Netherlands

Identification of proteins involved in the disease course of EAE, an animal model of multiple sclerosis. **A. Vanheel**, R. Daniels, S. Plaisance, K. Baeten, JJA. Hendriks, P. Leprince, D. Dumont, J. Robben, P. Stinissen, JP. Noben and N. Hellings
Mini-symposium on neuro-immunology 2011, Brussel, Belgium

Identification of putative networks involved in brain inflammation during EAE: DLG4 and KCNMA1 as candidate regulatory proteins.
A. Vanheel, R. Daniels, S. Plaisance, K. Baeten, JJA. Hendriks, P. Leprince, D. Dumont, J. Robben, P. Stinissen, JP. Noben and N. Hellings
MS Research days 2010, Alphen aan den rijn, The Netherlands

Detection of differentially expressed phosphorylated brain proteins in an animal model of multiple sclerosis.
A. Vanheel, R. Daniels, S. Plaisance, K. Baeten, JJA. Hendriks, P. Leprince, D. Dumont, J. Robben, P. Stinissen, JP. Noben and N. Hellings
14th EURON PhD days 2010, Hasselt, Belgium

Differentially expressed phosphorylated proteins in an animal model of MS.
A. Vanheel, R. Daniels, S. Plaisance, K. Baeten, JJA. Hendriks, P. Leprince, D. Dumont, J. Robben, P. Stinissen, JP. Noben and N. Hellings
MS Research days 2009, Groningen, The Netherlands

Quantitative analysis of differentially expressed brain proteins in the EAE-model for multiple sclerosis.
A. Vanheel, R. Daniels, S. Plaisance, K. Baeten, JJA. Hendriks, P. Leprince, D. Dumont, J. Robben, P. Stinissen, JP. Noben and N. Hellings
MS Research days 2008, Oegstgeest, The Netherlands

Poster Presentations

Is there a role for KCNMA1 in MS?
A. Vanheel, B. Brône, P. Stinissen, JP. Noben and N. Hellings
ECTRIMS 2012, Lyons, France

Identification of putative protein networks involved in the development of inflammatory brain lesions.
A. Vanheel, R. Daniels, S. Plaisance, K. Baeten, JJA. Hendriks, P. Leprince, D. Dumont, J. Robben, P. Stinissen, JP. Noben and N. Hellings
ACTRIMS/ECTRIMS 2011, Amsterdam, The Netherlands

Detection of differentially expressed phosphorylated brain proteins in an animal model of multiple sclerosis.
A. Vanheel, R. Daniels, S. Plaisance, K. Baeten, JJA. Hendriks, P. Leprince, D. Dumont, J. Robben, P. Stinissen, JP. Noben and N. Hellings
KVCV Proteomics 2010, Antwerp, Belgium

Alterations in phosphorylation status of brain proteins in an animal model of multiple sclerosis.
A. Vanheel, R. Daniels, S. Plaisance, K. Baeten, JJA. Hendriks, P. Leprince, D. Dumont, J. Robben, P. Stinissen, JP. Noben and N. Hellings
International congress of Neuroimmunology 2010, Sitges, Spain

Detection of phosphorylated brainstem proteins that are differentially expressed over the disease course of experimental autoimmune encephalomyelitis (EAE).
A. Vanheel, R. Daniels, S. Plaisance, K. Baeten, JJA. Hendriks, P. Leprince, D. Dumont, J. Robben, P. Stinissen, JP. Noben and N. Hellings
Autumn meeting BSCDB 2010, Hasselt, Belgium

Identification of differentially expressed phosphorylated proteins in an animal model of multiple sclerosis.
A. Vanheel, R. Daniels, S. Plaisance, K. Baeten, JJA. Hendriks, P. Leprince, D. Dumont, J. Robben, P. Stinissen, JP. Noben and N. Hellings
BSCDB 2010, Luik, Belgium

Quantitative study of phosphorylated brain proteins in a model of multiple sclerosis.
A. Vanheel, R. Daniels, S. Plaisance, K. Baeten, JJA. Hendriks, P. Leprince, D. Dumont, J. Robben, P. Stinissen, JP. Noben and N. Hellings
Biomedica 2010, Aachen, Germany

Quantitative analysis of differentially expressed phosphorylated brain proteins in experimental autoimmune encephalomyelitis.
A. Vanheel, R. Daniels, S. Plaisance, K. Baeten, JJA. Hendriks, P. Leprince, D. Dumont, J. Robben, P. Stinissen, JP. Noben and N. Hellings
Protein modifications in developmental signaling and disease 2009, Sart-Tilman, Belgium

Quantitative analysis of differentially expressed phosphorylated brain proteins in experimental autoimmune encephalomyelitis.
A. Vanheel, R. Daniels, S. Plaisance, K. Baeten, JJA. Hendriks, P. Leprince, D. Dumont, J. Robben, P. Stinissen, JP. Noben and N. Hellings
HUPO 2009, Toronto, Canada

Quantitative analysis of differentially expressed phosphorylated brain proteins in experimental autoimmune encephalomyelitis.
A. Vanheel, R. Daniels, S. Plaisance, K. Baeten, JJA. Hendriks, P. Leprince, D. Dumont, J. Robben, P. Stinissen, JP. Noben and N. Hellings
17th European congress of immunology 2009, Berlin, Germany

Quantitative analysis of differentially expressed brain proteins in the EAE-model for multiple sclerosis.
A. Vanheel, R. Daniels, S. Plaisance, K. Baeten, JJA. Hendriks, P. Leprince, D. Dumont, J. Robben, P. Stinissen, JP. Noben and N. Hellings
Biomedica 2009, Luik, Belgium

Dankwoord

Het is zover… ik ben op het punt gekomen dat ik een dankwoord mag schrijven. Het heeft bloed, zweet, tranen en geduld gekost om hier te staan vandaag en zonder jullie was dat niet gelukt! Ik weet dat de meerderheid van 'mijn lezers' snel naar deze pagina zal zoeken, en dat het lezen van deze thesis voor velen stopt na dit dankwoord. Maar ik moet jullie teleurstellen, ik ga het echt kort houden.

Niels, bedankt voor de begeleiding en de sturing die je me gaf, ik heb ontzettend veel geleerd van jou. Bedankt dat je deur altijd open stond, dat ik altijd bij jou terecht kon met vragen en bezorgdheden. Niet alleen je wetenschappelijke input, maar ook je relativeringsvermogen en positivisme hebben me vooruitgeholpen en soms vooruit gesleept in moeilijke periodes. Je wist steeds hoe je me opnieuw moest motiveren bij een dipje, of welke mensen je daarvoor kon inschakelen. Al kon je ook de oorzaak zijn van de tranen ;-). Bedankt! Ik kan me geen betere promotor voorstellen.

Jean-Paul, of mag ik nu JP zeggen? Jouw kritische ingesteldheid en diepgaande proteomics kennis hebben me enorm geholpen en gestimuleerd om zelf dieper te graven in de literatuur. Hoe je over massa spectrometers kan praten, zoals kleine jongens over lego…het heeft lang geduurd, maar misschien ben ik nu toch overgestapt naar de gel-free proteomics kant. Jean-Paul, bedankt dat je mijn copromotor wilde zijn.

Piet, tijdens onze meetings wist je altijd alles terug in perspectief te plaatsen. Jij had altijd het grote geheel voor ogen. Met je wetenschappelijke input wist je me steeds weer te motiveren om er tegenaan te gaan.

Bedankt aan alle juryleden en de juryvoorzitter voor jullie kritische blik en opbouwende suggesties, en de tijd die jullie willen vrijmaken voor de evaluatie en verdediging van mijn thesis. Ook de Universiteit Hasselt en Maastricht University wil ik bedanken voor de financiële ondersteuning van mijn project.

Beste collega's, bedankt! Bedankt dat jullie me onmiddellijk een 'thuisgevoel' gaven op BIOMED, voor de fantastische sfeer, de leuke lunches samen, de toffe babbels en opbeurende woorden wanneer dat nodig was. Bedankt voor de ontspannende uitjes, maar ook de stimulerende werksfeer, voor de discussies over resultaten, de hulp in het labo, en ook voor jullie bloed ☺. Bedankt ook voor

de logistieke en administratieve ondersteuning. Zoals ik zei, ik hou het kort, maar ik ben jullie allemaal enorm dankbaar.

Ik kan het natuurlijk niet laten om enkele mensen toch nog een beetje extra in de bloemetjes te zetten. Al mijn bureaugenootjes, en dat zijn er wel een paar, verdeeld over verschillende bureauruimtes (en gebouwen). Mijn bureau was altijd een beetje mijn thuis, en jullie hebben daar alles mee te maken!

Veronique, je geduld bij het stofvrij maken van de DIGE platen, onze leuke babbels, je administratieve hulp nu het einde in zicht is,…. Je bent van onschatbare waarde! Bedankt.

Mijn studenten, enkelen ondertussen collega's, die toch steeds weer nieuwe/andere energie brachten.

Liesbeth, ik weet niet waar ik moet beginnen… Bedankt om er te zijn voor mij, onze vriendschap betekent zo veel voor me. Je beste vriendin als collega hebben, ik kan het iedereen aanraden! Ontspannende babbels, besprekingen over experimenteel opzet, wetenschappelijke discussies, troost, onvoorwaardelijke steun! Ik mis je elke dag op de UHasselt. Gelukkig zijn er de weekends! Ik kan niet beschrijven hoe dankbaar ik ben, merci!

Ook alle vriendinnen die buiten het werk voor ontspanning zorgen, tijdens onze gezellige etentjes, bedankt. Bedankt Bram, voor het geduld. Bedankt mama, papa, Pieter en Iris, voor de liefde, steun, de vriendschap, de ontspanning en de interesse. Bedankt voor ons warme nest waar alles kan en alles mogelijk is.

Jonas en Eline, zonder het te weten zorgen jullie voor ALLES wat ik nodig heb. Ik krijg tranen in mijn ogen van puur geluk als ik aan jullie denk. Bedank voor jullie liefde, knuffels, enthousiasme, ondeugendheden, …. Jullie zijn perfect!

"'Impossible' is not a scientific term."

-Vanna Bonta